White Paper: Research and Development Efforts towards the Production of the Leatt-Brace® Moto GPX Unrestrained Torso Neck Brace

by

Dr. Chris Leatt

Mr. Cornel de Jongh

Mr. Pieter André Keevy

prepared for / by

Leatt Corporation®

Research and Development Department – Biomedical Engineering Division

Last Draft April 2009

PUBLIC RELEASE MAY 2012

Draft Reviewed by

Prof. Kit Vaughan

(Hyman Goldberg Professor of Biomedical Engineering, University of Cape Town)

Dr. Steffen Peldschus

(Dr. rer. biol. hum. Dipl.-Ing., Group Leader Biomechanics, Munich University)

Declaration by Independent Reviewers

We, the undersigned, hereby acknowledge the credibility of the work conducted in this document and declare that the work contained in this white paper is the authors' own original work.

Signature: . . . . . .

Prof. Kit Vaughan - Deputy Dean for Research, Faculty of Health Sciences, Hyman Goldberg Professor of Biomedical Engineering, University of Cape Town, South Africa.

Signature:  . . . . . .

Dr. Steffen Peldschus – Group Leader Biomechanics, Ludwig Maximilians-Universität, Munich, Germany.

Date: 28 ***October 2009***

Declaration

We, the undersigned, hereby declare that the scientific work described in this white paper is our own original work.

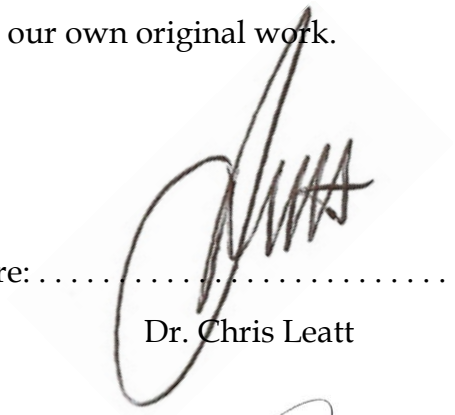

Signature: . . . . . .

Dr. Chris Leatt

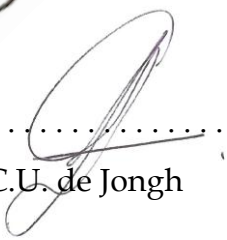

Signature: . . . . . .

C.U. de Jongh

Signature: . . . . . .

P.A. Keevy

Date: ***1 April 2009***

Abstract

White Paper: Research and Development Efforts towards the Production of the Leatt-Brace® Moto GPX Unrestrained Torso Neck Brace

Dr. C.J. Leatt; C.U. de Jongh; P.A. Keevy

Leatt Corporation R&D Department
Biomedical Division

Neck injuries are relatively common in active sports and may have a high incidence in particular categories and disciplines. Cervical spine injuries may cause pain, paralysis or death. Until the advent of the Leatt-Brace® there was no effective device to mitigate this injury risk in the unrestrained torso (motorcycle) accident.

This White Paper summarizes research, development, and performance verification activities conducted by Leatt Corporation. Individuals involved in the work include Dr. Chris Leatt, biomedical engineers Cornel de Jongh and Pieter Keevy, and industrial designer Mark Hopkins. BMW Motorrad and KTM Motorrad also participated in testing, simulations, or field trials to help develop and assess the Leatt-Brace® Moto GPX Unrestrained Torso Neck Brace.

Extensive background research provided information on cervical and thoracic spine trauma, cervical and thoracic spine dynamics, and the coupled forces and motions involved in dynamic events. A model to simulate various impulse scenarios used Adams LifeMOD™ software to compensate for scarce physical testing in the motorcycle environment. The computer model in turn was correlated with testing performed with a Hybrid III 50TH percentile male ATD (Anthropomorphic Test Device). Initial correlation testing used pendulum tests developed by and conducted at BMW Motorrad. With the model pre-validated,

pendulum tests and other dynamic testing at Leatt Corporation further assessed product performance.

Crash simulations reconstructed the well documented crash of a SuperCross rider, James Marshall[1], to compare impact dynamics with the modalities of neck and brain injury. Simulations also assessed specific features, including the breakaway thoracic strut, clavicle protection, and platform height. For these simulations, a detailed spine model was developed that incorporated the non-linear behavioral effects of the intervertebral (IV) discs.

Lastly, recent work by Leatt Corporation on an unrestrained torso neck protection device test protocol is presented.

The validated simulation models described in this document are being used as a tool in the ongoing development and refinement of the Leatt-Brace® as well as for the simulation and reconstruction of real accident events.

This document is intended to answer common questions asked by users, institutions and the public. In AMA (American Motorcycle Association) sanctioned MotoCross and SuperCross events, the total number of spinal injuries may be as high as 7% of all injuries [Table 2-6]. Neck protection should lower the incidence and severity of neck injuries. Encouraging is the fact that, over a five-year period ending in 2005 (before the introduction of the Leatt-Brace®) at Motorsport South Africa "all class head and neck injury rates" in competitive off-road motorcycle sporting events were significantly higher than in the following years as riders began wearing the Leatt-Brace®.

[1] Marshall suffered catastrophic spinal injury in 2006 that left him a paraplegic.

Acknowledgements

We would like to express our sincere thanks to the following people and organizations, who have contributed to this project and helped make this work possible:

- Delphi Test Centre, Vandalia, Ohio
- BMW Motorrad
- Land Mobility Technologies/SABS
- Dr. Steve Augustine, AMA
- Dr. John Boden, MSA, RSA
- Various professional riders
- KTM Motorrad and riders
- Dr. Steffen Peldschus, Munich University, Munich, Germany
- Prof. Kit Vaughan, Hyman Goldberg Professor of Biomedical Engineering, UCT Biomedical Engineering Department, Cape Town
- MSC.ADAMS LifeMOD™, SimOffice™

Dedications

To all of those who have shown a keen interest and belief in what Leatt Corporation stands for: "Their ability to incorporate pure science, engineering and passion into the development of motorsport safety products."

Contents

List of Figures

List of Tables

Nomenclature

Variables

a(t)	acceleration in time
a_x, a_y, a_z	acceleration components
B_f	brain factor
D	distance between the axis of the load cell and the axis of the condyle
E	modulus of elasticity
F_z	axial force
F_x	shear force
F_{zc}	critical axial force
Hz	hertz
kHz	kilohertz
M_{ROM}	maximum Hybrid III range of motion
M_y	bending moment
M_{ocy}	occipital condyle bending moment
M_{yc}	critical bending moment
N_{TE}	tension-extension
N_{TF}	tension-flexion
N_{CE}	compression-extension
N_{CF}	compression-flexion
N	newton
Nm	newton-meter
Nm/deg	newton-meter per degree
t	time
ρ	density

Abbreviations

ALL	Anterior Longitudinal Ligament
ALPT	Alternative Load Path Technology ™
ATD	Anthropomorphic Test Device
AMA	American Motorcycle Association
ATV	All-Terrain Vehicle
COR	Center of Rotation
CT	Computed Tomography
CAD	Computer-Aided Design
CSF	Cerebrospinal Fluid
DAI	Diffuse Axonal Injury
ECE	Economic Commission for Europe
FSU	Functional Spinal Unit
FMVSS	Federal Motor Vehicle Safety
FEM	Finite Element Modeling
GRN	Glass-Reinforced Nylon
GSI	Gadd Severity Index
HIC	Head Injury Criteria
H-III	Hybrid-III
ILL	Interspinous Ligament
IV	Intervertebral
IAR	Instantaneous Axis of Rotation
LF	Ligamentum Flavum
MTBI	Mild Traumatic Brain Injury
N_{ij}	Neck Injury Criteria
NHTSA	National Highway Traffic Safety Administration
pCSA	physiological Cross-Sectional Area

PLL	Posterior Longitudinal Ligament
R&D	Research and Development
ROM	Range Of Motion
SCI	Spinal Cord Injury
SDH	Subdural Hematoma
SABS	South African Bureau of Standards
UTS	Ultimate Tensile Stress
WSTC	Wayne State Tolerance Curve

Chapter 1

Introduction

1.1 Background

The human neck is constantly exposed to the physical demands of sport and recreational activities and their inherent risks. Accidents involving motorcycles, ATVs, snowmobiles, and other wheeled sports where the rider/driver is unrestrained demonstrate the need for effective safety equipment. Neck protection has, to a large degree, not kept pace with other facets of safety equipment development. Whiplash injuries affect the lives of over 1 000 000 people in the U.S. every year, and it is estimated that between 25% and 40% of those affected will have chronic symptoms [1].

In crashes in which the rider's/driver's torso is unrestrained, injuries occur during hyper-flexion, but most are hyper-extension injuries in the form of Jefferson fractures (typically a four-part first cervical vertebra fracture), lower to mid-cervical facet region fractures, dislocated or locked facets, anterior vertebral body fractures with kyphosis, unilateral or bilateral facet dislocation, fractured spinous processes or lamina injuries. During falls on the superior aspect (top) of the skull, compressive burst fractures and complete ligamentous disruption may occur [2].

The design rationale (Chapter 3) for a device to help protect the cervical spine from sustaining injuries during impact should include the use of biofidelic constraints in the basic design and construct. Our objectives were to prevent/limit catastrophic injury, thereby minimizing the chance of a neurological deficit. It is vital to consider design aspects such as helmet-device-body absorption and subsequent material choice, clavicle relief, thoracic strut break away, device removal, and

anterior access to facilitate airway management. Significant testing was conducted on components of the device, as well as on the device as a whole, using various applied load and impact scenarios typical of real-life accident situations.

The Moto GPX has been designed by a team of specialized professionals to optimize its performance for neck protection in helmeted sports. The design includes input from neurosurgery, spinal surgery, biomedical engineering and mechanical engineering, and from competitive sporting professionals. This, in conjunction with software (LifeMOD™) capable of simulating the human reaction to various impacts and quasi-static loading scenarios, ensured that the device design was optimized through multiple design and simulation iterations.

1.2 Motivation

Arguably the most significant injuries in motorcycle and other extreme sports occur in the cervical spine (neck) region. Injuries in this area may often cause paralysis or even death. Therefore, it was deemed imperative that a device be designed to help protect people from the aforementioned cervical spine injuries.

1.3 Objectives

The research, design, and simulation underlying the Moto GPX focused on overall efficacy in creating an effective and reliable product. The Moto GPX Research and Development (R&D) rationale "chain" is presented in Figure 1-1, and the objective of this paper is to elaborate on each of the "links" in the chain. Natural questions regarding various aspects of the Leatt-Brace® Moto GPX, such as injury mechanisms and the product's ability to prevent them from occurring, are addressed.

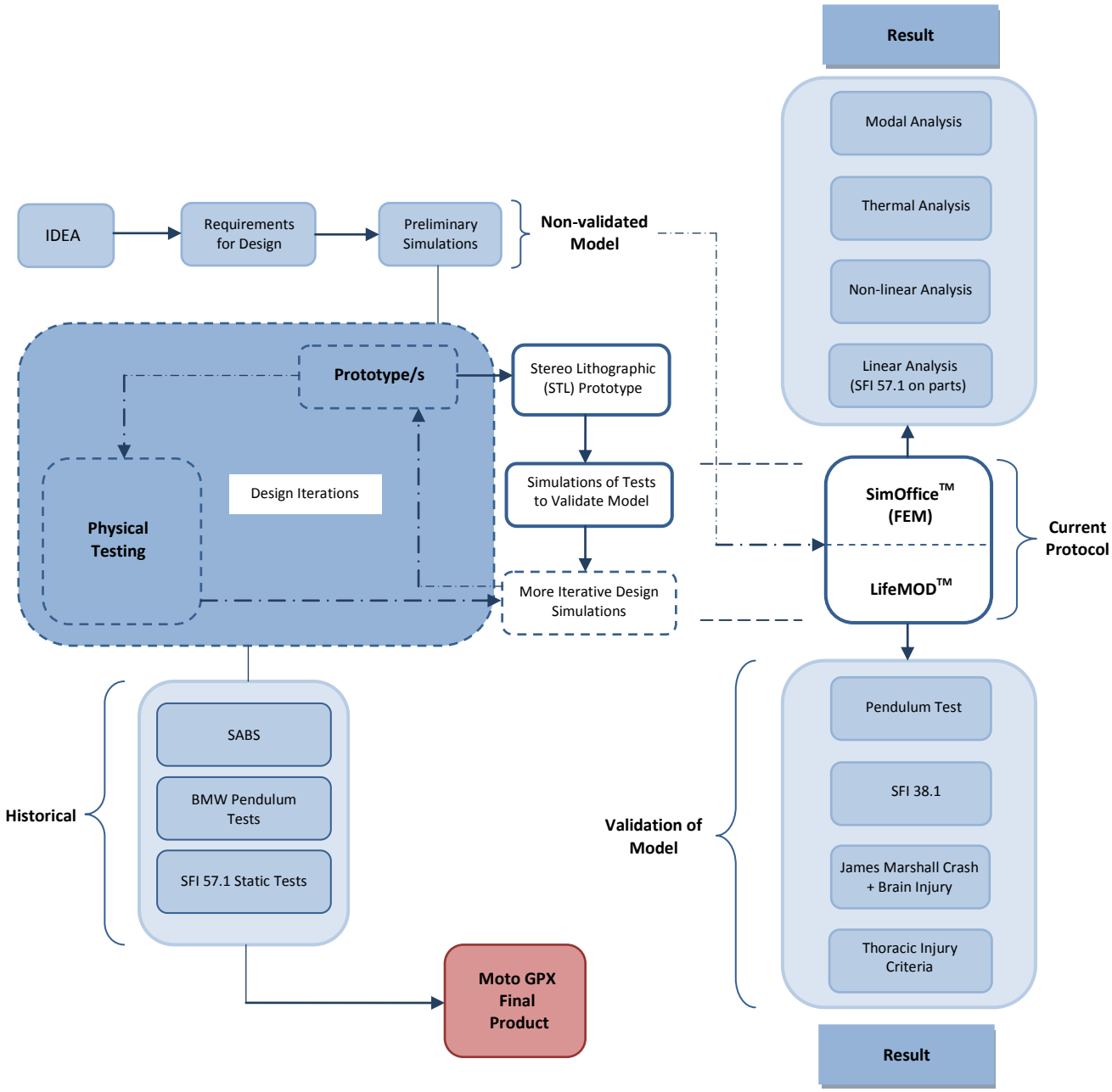

Figure 1-1: Design chain for the Moto GPX

The specific objectives for this study can be summarized as:

- The identification of relevant knowledge in the fields of cervical spine anatophysiology, kinematics, impact mechanics and injury mechanisms through an extensive literature review.

- The presentation of the Moto GPX design rationale.
- The presentation of representative tests conducted on the Moto GPX and discussion of their results.
- The presentation of a validated simulation model as an extension to the physical tests, as an aid in further design iterations and performance.
- The development of a detailed spinal model, incorporating non-linear IV disc stiffness characteristics derived from cadaver tests and validated through *in vivo* intradiscal pressure measurements. This model helped validate the design of the thoracic strut on the Moto GPX brace.
- A presentation of ongoing research on and development regarding the establishment of a test protocol, by the U.S.-based SFI Foundation, for unrestrained torso head and neck safety devices.

1.4 Outline

Chapter 2 discusses some of the relevant literature for this study, including literature on the anatomy and physiology of the cervical spine. Cervical spine kinematics, specifically the range of motion (ROM) of the cervical spine and whiplash theory are discussed. IV disc dynamics are discussed, along with the injury modalities associated with the cervical spine. Options for the protection of the cervical spine and associated challenges are also described. Simulation of the cervical spine in the form of dynamic and quasi-static simulation is discussed, including the parameters and methods used for the determination of the various forces and coupled motions in neck mechanics, bending moments, axial forces, shear forces, and brain movement in the cranium.

In Chapter 3 the general and specific rationales for the design of the Moto GPX are discussed. The general rationale includes considerations such as the allowable device ROM and the "fulcrum effect" hypothesis, material considerations, release clip design, and brace removal options. The discussion of specific design

considerations includes factors such as the clavicle relief area and the thoracic strut. Additional emphasis is placed on the high probability of clavicle injury during impact with or without the device, and the interrelation between clavicle injury and alternate load path theory.

Chapter 4 forms the body of the document and offers a presentation of the testing and simulations conducted on the Moto GPX. These range from early sled tests at the SABS, the pendulum tests conducted at BMW's test facility in Munich, Germany, and the subsequent pre-validation and validation simulations using SFI 38.1 restrained torso head and neck safety device test. Further simulations are presented in the form of an investigation of the video documented James Marshall crash and the effect of whiplash-type and head-first (lawn-dart) crashes on brain dynamics, with and without the use of the Moto GPX. A detailed spine model is presented, which was developed, amongst other uses, as a method to evaluate the injury potential to the thoracic spine as a result of the energy absorption and load-transferring strut on the Moto GPX. Lastly, the FEM analysis of two important strength-dependent components is discussed.

Finally, Chapter 5 concludes with a discussion of more recent work being done and further developments being planned by Leatt Corporation regarding the Moto GPX. This includes work on the development of an SFI specification to evaluate the performance of any unrestrained torso head and neck protection device, as well as a proposal to revise the Nij calculation, specifically pertaining to unrestrained torso head and neck protection.

Chapter 2

Literature Review

This chapter discusses the field of spinal biomechanics, focusing on the cervical spine. A short introduction to cervical spine anatomy is presented, followed by a discussion of the kinematics and the ROM of the cervical spine. IV disc dynamics and spinal injury modalities are discussed, along with cervical spine protection options and their challenges. Lastly, the simulation of spinal behavior is discussed.

2.1 Anatophysiology of the Cervical Spine

2.1.1 Anatomy of the Skeletal Cervical Unit

The cervical spine consists of seven bony cervical vertebrae and seven fibro-cartilaginous intervertebral discs (Figure 2-1 and Figure 2-3). The cervical spine forms the top section of the entire spine and is connected to the head. The shape of the cervical spine is somewhat lordotic (backwards curved). The reason for this is so that the weight of the head can be transmitted through a straight line, connecting to the line with which the thoracic and lumbar sections of the spine transmit the weight of the body towards the pelvis [3], [4]. The lordotic curve also assists in energy management and absorption following impact to the head or upper torso.

Cervical vertebrae are shaped in such a way that they can be stacked on top of one another by means of interlocking processes, so that the small relative motion of each vertebra can produce an extensive combined smooth ROM for the entire unit [5], [6].

Each vertebra consists of an oval-shaped section of solid bone, called the vertebral body; a ring of bone consisting of two pedicles and two lamina bones, which protects

the spinal cord; the transverse processes; and the spinous process at the back (posterior) end of the structure (Figure 2-2).

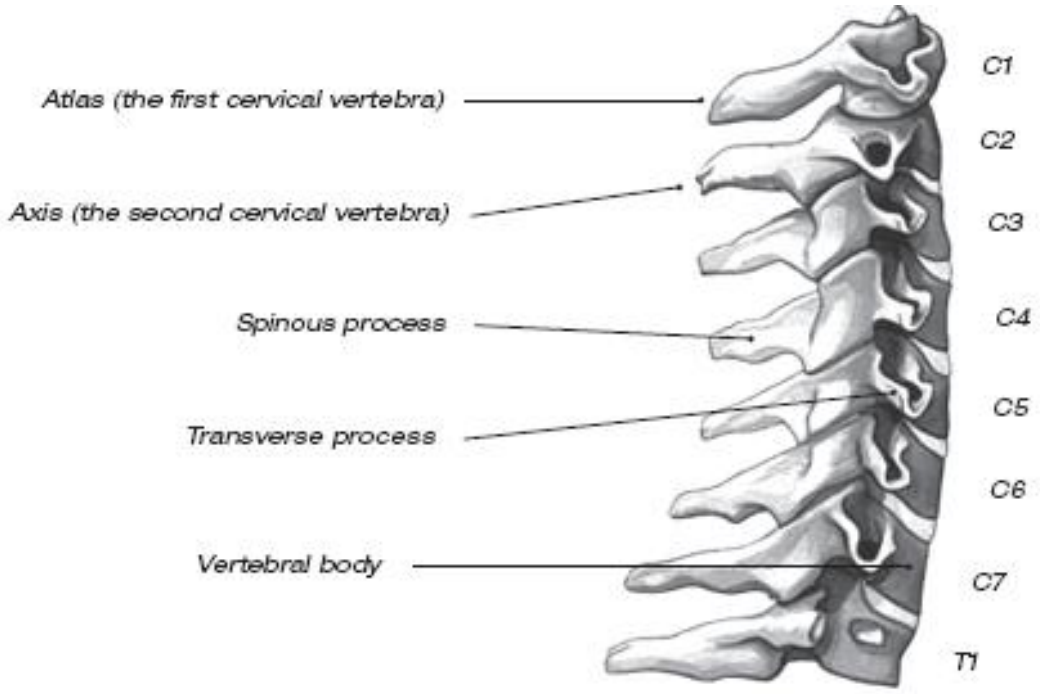

Figure 2-1: Lateral view of the cervical spine

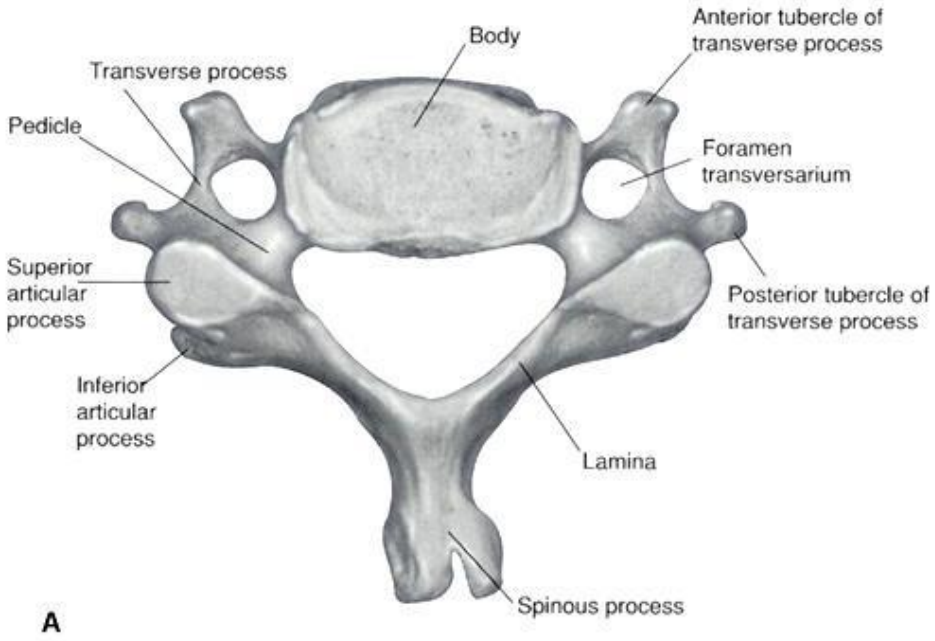

Figure 2-2: Transverse plane view of cervical vertebra

2.1.2 Cervical Spine Kinematics

In the cervical spine, flexion (forward bending), extension (rearward bending), lateral (sideways) motion, rotation (as in indicating "no" with the head) and superior/inferior (up and down) motion can occur. Flexion and extension are the predominant types of motion. This movement is due to the alignment of the superior and inferior articular processes forming the zygapophyseal joints (as shown in Figure 2-2) between two adjacent vertebrae, and the protruding "lips" (uncinate processes) on the outside (lateral) edges of the vertebral body. Although rotation and lateral motion are important kinematic factors in the cervical spine, this study will focus mostly on flexion, extension, and axial (superior and inferior) motion. The reason for this is that the main parameters to consider during the design of a head and neck safety device are the axial forces and the bending moments relating to flexion and extension (which will be explained in Section 2.3).

2.1.2.1 ROM in the Functional Spinal Unit

The range of motion (ROM) is used as a measuring tool to understand motion and is often measured in degrees. Methods include measurement of the anterior plane from one vertebral body to the next (viewed laterally), or the ROM of the total cervical spine, from the anterior body of C1 to C7.

According to a study conducted by Christelis [7], the largest flexion and extension ROM in the cervical spine, apart from the atlanto-occipital joint, occurs from C4 to C6. A general tendency is that the ROM in the cervical spine in flexion is significantly larger than that in extension; therefore, the stiffness of the cervical spinal unit in extension is higher than in flexion. This is due to the fact that the intervertebral (IV) disc anatomy allows for more motion towards the anterior (frontal) part of the disc and that the spinous processes stack together during extension, limiting motion. This is important to take into consideration when modeling spinal behavior (as will be discussed in Sections 2.3 and 4.4) and is also incorporated into the allowable bending moments during impact, as part of the injury criteria for safety, where the allowable bending moment in flexion is higher than that in extension. Ligaments provide an additional stabilizing factor, giving the cervical spine integral strength in controlling flexion, extension, rotation and lateral flexion. The three main ligaments providing this stabilization are called the interspinous longitudinal ligament (ILL), the anterior longitudinal ligament (ALL) and the posterior longitudinal ligament (PLL). They are referred to as the three pillars of spinal integral strength. Secondary to these, the ligamentum flavum (LF) assists in rotational stability.

The ROM for an individual can be seen as degrees of variation and not as a discrete number. An individual's ROM can be influenced by such variables as the sequence of motion, i.e., whether motion is executed from flexion to extension or vice versa. This can result in significant differences of up to 5^{o} to 15^{o} per segment (vertebrae pair), which in turn can be limited by age, spondylosis or other factors. The ROM can also vary significantly depending on the time of day it is measured

(this is influenced by water retention by the IV discs). Therefore, different ROM studies should be viewed in context in terms of the variability that may exist between data capturing, assumptions and methodologies.

Less research has been done on the ROM of the cervical functional spinal unit compared to research on the lumbar spine. Studies to define ROM were reviewed by Panjabi and Meyers [8] and included radiographic studies of flexion and extension in volunteers, CT (computed tomography) scans, cadaver sled and drop tests, cadaver whole cervical spine ROM, trauma studies, physical surrogates and mathematical surrogates. Panjabi and Meyers's [8] findings are summarized in Table 2-1 below, together with the findings of Christelis [7]. Christelis deduced that, in general, range of motion is lowest for the C2/C3 and C6/C7 levels and greatest for the C4/C5 and C5/C6 levels.

TABLE 2-1: CERVICAL ROM STUDY

CERVICAL LEVEL	MOVEMENT	APPROXIMATE ANGLE	COMMENTS
		PANJABI [8]/CHRISTELIS [7]	
C0 – C2	FLEXION	$25^{o}/17^{o}$	
C0 – C2	EXTENSION	$40^{o}/25^{o}$	
C0 – C7	FLEXION AND EXTENSION	$119.6^{o}/125^{o}$	RECOMMENDED MAXIMUM RANGE OF MOTION BEFORE IDENTIFIABLE INJURY - MEAN SD
C0 – C7	LATERAL FLEXION	86.4^{o}	
C0 – C7	ROTATION	91.4^{o}	

If allowed to flex and extend fully, as demonstrated by a sled test, the helmeted dummy head will achieve a ROM of approximately 175° at a sudden deceleration velocity of 50 km/h (high-speed camera capture of Leatt® Corporation tests – non-braced control run with helmeted dummy conducted with modified SABS - South African Bureau of Standards protocols, thorax secured and sled speed of 49.7 km/h, June 2004 [9]). This extreme ROM (above 125°) shows that a non-braced individual will sustain injury, even at such a relatively low speed, and

therefore the need for a device to restrict ROM to below 125° is apparent. Injury modalities will be discussed in further detail from Section 2.3.7 onwards.

2.1.3 Cervical Intervertebral Disc Physiology and Dynamics

The intervertebral discs are located between two adjacent vertebrae (Figure 2-3). An intervertebral disc consists of a fibrous outer ring, called the annulus fibrosus and made up of lamellae, which are concentric sheets of collagen fibers connected to the vertebral endplates. The annulus fibrosus surrounds the core, or nucleus pulposus. The nucleus pulposus consists of a hydrated gel that resists compressive forces [3] [10], [11].

The intervertebral discs act as dampers, absorbing shock impulses transmitted through the spine. They also allow relative movement between adjacent vertebrae, i.e. flexion (forward rotation) and extension (backward rotation), lateral (side to side) movement and rotation [11].

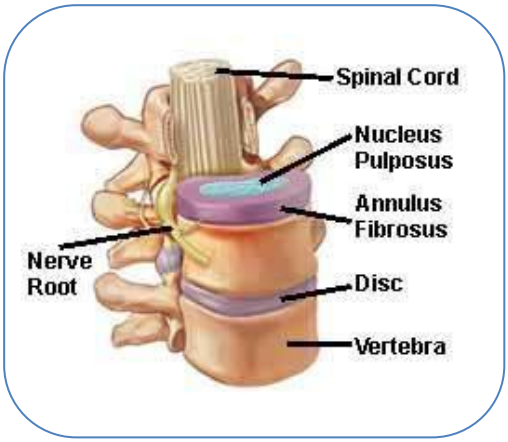

Figure 2-3 : Cervical IV disc anatomy [12]

The IV discs have a unique property in that they are stiffer in compression than in tension and, as the degree of translational or rotational motion applied to a IV disc through its two attached vertebrae is increased, the stiffness in the disc increases in a non-linear fashion. The discs also become stiffer as the velocity of the applied motion is increased. According to the authors, therefore, there is more than one stiffness graph for each vertebra and this makes it challenging to design appropriate protection for the spine, as there are a multitude of impact scenarios that need to be considered, each resulting in a different reaction in terms of forces and coupled motions transmitted through the spine. This will be discussed in finer detail in later sections.

2.2 Cervical Spine Injury Modalities

To develop a neck protection device, it is necessary to understand the mechanisms of neck injury and major injury vectors. The design rationale behind the Moto GPX has been modeled on common classification systems (Table 2-2, Table 2-3 and Table 2-4) of cervical spine injury mechanisms in use worldwide by spinal surgeons, and on common motor vehicle and motorcycle-induced cervical spine injuries, as detailed below.

Table 2-5 below indicates the highest level of neurological lesion in 396 patients with traumatic spinal cord injuries (SCI) at discharge. Generally, the most common area for cervical spine injury is in the upper cervical spine or at the base of the skull (referred to as a supra-cervical injury by the authors), arising when the head strikes an object in flexion and is forced into hyper-extension (extreme backwards rotation of the head), and in the lower cervical spine (C6/C7), arising when the head is forced into hyper-flexion (extreme forwards rotation of the head). These phenomena typically occur during whiplash-related incidents (as will be discussed below). Between 1971 and 1975, only 13% of reported accidents in the USA resulting in cervical quadriplegia occurred in hyper-flexion (10%) and hyper-

extension (3%), while 52% were attributed to axial loading [1] However, this may vary somewhat in different motorcycle racing disciplines, such as MotoCross or SuperCross. Axial loading refers to the loading in the longitudinal direction (parallel) to the spine. This type of injury often occurs when contact is made with the top of the head when the cervical spine is in a straight-segmented position, i.e., the normal lordotic (backwards curved) shape of the cervical spine is straightened, subsequently losing its ability to absorb the impact energy effectively and hence damaging the internal structures (such as the vertebral bodies, IV discs, ligaments and even muscles). Excessive lateral bending may also place traction or compressive forces on the nerve roots (Figure 2-3) protruding from the foramen transversarium (opening in the side of the vertebrae). Lateral bending of the cervical spine is accompanied by rotation due to the oblique orientation of the facets. During right rotation of C0 (atlas), the left transverse foramen of the atlas moves anteriorly while the right transverse foramen moves posteriorly relative to those of the subjacent C1 (axis). This rotation causes an increased distance between the adjacent transverse foramen, potentially resulting in increased tensile loading on the vertebral artery and nerve.

It should be taken into consideration, however, that muscle tone at the time of impact can have a significant effect on the impact required to effect an injury to the cervical spine or its surrounding structures. Allowable parameter limits in the form of maximum forces and moments at the C0/C1 joint (atlanto-occipital joint), before life-threatening injury becomes highly likely, have been developed through extensive cadaveric tests. These allowable parameters have been combined into a Nij parameter (discussed in Section 2.3.7), which must typically have a value below 1.0 to ensure a safe device. A discussion of the tolerable cervical spine forces and the Nij parameter will follow in Section 2.3.7 and Chapter 5.

It should be noted that a Nij below 1.0 does not guarantee a clinically non-injurious scenario. An example of this could include a significant hyper-extension combined with a small axial force component. Since the Nij has a heavily weighted

axial component, the large bending moment (because of hyper-extension) may not have a major effect on the outcome of this parameter, even though a fracture or other clinical injury is likely. Published data on intradiscal bending moments to fracture indicate that, in pure hyper-extension, clinical injuries may in fact occur without the presence of an axial force. It therefore is important that an "apples with apples" scenario is always used to indicate the relative changes in the Nij.

TABLE 2-2: LOWER CERVICAL SPINE INJURY MODALITIES [C3-C7] [2]

MAJOR LOADING FORCE	ACTING ALONE	WITH COMPRESSION	WITH DISTRACTION
Flexion	▪ Unilateral or bilateral facet dislocation	▪ Anterior vertebral body fracture with kyphosis ▪ Disruption of the interspinous ligament ▪ Teardrop fracture	▪ Torn posterior ligaments (may be occult) ▪ Dislocated or locked facets
Extension	▪ Fractured spinous process and possible lamina injury	▪ Fracture through facet region	▪ Disruption of ALL with retrolisthesis of superior vertebrae on inferior one
Neutral position		▪ Burst fracture	▪ Complete ligamentous disruption (very unstable)

TABLE 2-3: LOWER CERVICAL SPINE INJURIES [C3-C7] [13]

Compression Injuries

- Anterior Compression
- Comminuted Fracture
- Teardrop Fracture

Flexion-Extension-Distraction Injuries

- Moderated Sprain/Dislocation
- Severe Sprain
- Bilateral Fracture

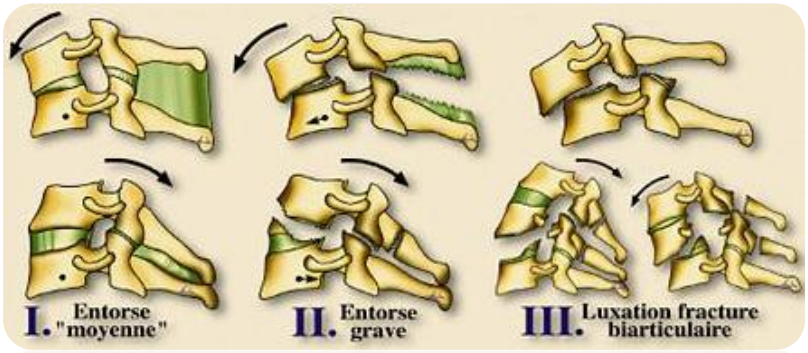

Rotational Injuries

- Unifacet Fracture
- Fracture Separation of the Articular Pillar
- Unilateral Dislocation

TABLE 2-4: UPPER CERVICAL SPINE INJURIES [C0-C2]

Injury Mechanisms

- Flexion
- Extension
- Distraction
- Rotation
- Compression

Types of Injury

- Atlanto-Occipital Dislocation
- Condylar Fractures
- Atlantico-Axial Dislocations
- Atlas Fractures
- Odontoid Fractures
- Hangman's Fractures
- Base of Skull Fractures

TABLE 2-5: DISTRIBUTION OF NEUROLOGICAL LESIONS AT DISCHARGE IN 396 PATIENTS WITH TRAUMATIC SCIS FROM MOTORCYCLE ACCIDENTS, OCCURRING FROM JULY 1992 TO JUNE 1996, TAIWAN, ROC [14]

LEVEL	% INJURIES
C1	7.57
C2	14.36
C3	17.2
C4	11.99
C5	***26.35***
C6	11.99
C7	1.58

TABLE 2-6: AMA MOTOCROSS ACCIDENT STATISTICS 2001 TO 2005 (NO BRACES) IN APPROXIMATELY 834 RIDER EVENTS, 142 ACCIDENTS (17%), ONE DEATH*

- 31% Upper Extremity
- 25% Head Injuries
- 20% Lower Extremities
- 16% Miscellaneous (burns, dehydration, etc.)
- 6% Torso
- 2% Spine – 10 Vertebral: 5 x Cervical
  4 x Thoracic
  1 x Coccygeal
- 1.4% SCI – 2 Accidents: 1 x Paraplegic
  1 x Quadriplegic
- 7% of accidents with spinal fractures

*Unpublished data provided privately to authors

2.3 Simulation of the Coupled Forces and Dynamics in the Cervical Spine

To fully understand the reaction of the spine during impact, both physical testing and simulations with validated models are required. Therefore, it is difficult enough to design a device to protect the spine but even more so if the complex behavior of the spine is not taken into account. Accordingly, many assumptions and simplifications must be made to model the behavior of the spine. For example, using cadavers to evaluate a spinal protection device might result in certain insights, but other factors such as the absence of reaction forces in terms of muscle pre-tension and contraction or the loss of ligament pre-tension can obscure the results and lead to misinterpretation.

In order to successfully evaluate a spinal protection device, the positive attributes of testing and simulations need to be combined, i.e., basic testing can be performed (either using H-III ATDs or another form of detailed surrogate spine),

and then simulations can be developed to mimic the tests. A validated model can then be constituted, producing the same results as those in the physical tests for the identical setup, load or impact inputs and design parameters. After this, the ideal would be to further develop the model with validated data, such as validated IV disc stiffnesses (physically obtained from either cadaveric studies or from *in vivo* intradiscal pressure measurements) and muscle and ligament biomechanics (available in the literature from physical studies conducted on humans *in vivo* and cadaveric studies). The accurate simulation model can then be used to test real-life accident scenarios that are impossible or impractical to create in a physical test. Accident reconstruction data also can be used to recreate the accident kinematics of a typical injury-inducing scenario in a given sport.

2.3.1 Introduction

Dynamic simulation of the cervical spine entails inputting various parameters, such as IV disc, ligament, muscle and brain properties (when modeling head/neck dynamics) in order to acquire specific parameter outputs, such as axial forces in the spine, bending moments, shear forces, vertebral angles (for comparison with allowable ROMs according to the literature and injury criterion) and combinations of these parameters, such as Nij and HIC (neck and head injury criterion).

It should be noted, however, that modeling fast dynamic simulations (where the model can expect any impact at any time and is therefore "ready" for the impact) requires specific joint properties (active joints), whilst modeling slow dynamic or quasi-static simulations requires passive joints that are in effect "trained" to behave in a specific way according to predetermining stiffness and motion parameters and according to muscle and ligament properties. The modeling of impact mechanics is therefore not ideal using passive joints, since these joints are designed to react (linearly or non-linearly) to a user-defined applied load and motion (or combination thereof), although accurate and validated modeling for simulation can be achieved if

the exact resultant motions of the various parts (vertebrae, head, etc.) are known. (This can be achieved partially through motion capturing of dummy impacts, although the motion will not be ideally representative because of a lack of biofidelity). H-III ATD models are used for many high-impact simulations, as they incorporate active joints representing muscle and IV disc dynamics. These joints are usually situated at the atlanto-occipital (C0/C1) joint and at the C7/T1 IV disc level and therefore are easy to model, and simplify validation of the model.

Only with the advent of finite element method (FEM) analysis and anatomical modeling was it possible to produce a neck model for testing that has the necessary biofidelity to represent the human neck in impact, including all elements of IV discs, bone, ligament, muscle, including muscle response, and other soft tissues, and that can be applied in all likely impact scenarios.

2.3.2 Axial Force

The axial force is the force (measured in Newton or N) in the longitudinal direction of the spine, i.e., parallel to the spine (Figure 2-4). This force is usually transmitted via the head or via excessive bending of the spine and transmitted from a vertebra, directed through the IV discs and transmitted to the next vertebrae. This force, when excessive, can damage the IV discs, causing them to rupture or, in extreme cases, can cause the vertebra/e to crack or fracture, which in its turn may lead to paralysis or even death. It is important to be able to monitor this force vector through the entire duration of an impact or quasi-static motion, in order to be able to assess the potential of the safety device to moderate excessive axial force. So-called "pure" axial force is not effectively moderated by any current technology.

Another closely related parameter to the axial force is the intradiscal pressure (axial force over the vertebral endplate area). McGuan and Friedrichs [15] reported intradiscal pressures obtained from a model of the cervical spine developed in ADAMS™ and, in another study, De Jongh [16] and De Jongh *et al.* [17] reported this

parameter from a simulation model developed in ADAMS LifeMOD™. Since the vertebral endplate areas for the cervical spine are very small (up to six times smaller than lumbar vertebrae, as determined with MIMICS™ software from CT scan data by De Jongh [16] in Figure 2-5) when compared to the rest of the spine (thoracic and lumbar), it was hypothesized by De Jongh [16] that intradiscal pressures can reach high values (up to 3 MPa) quicker than other areas of the spine, once again showing why cervical spinal injuries are highly prevalent in spinal injuries and why it is so important to address axial forces in this area (also see Table 2-6).

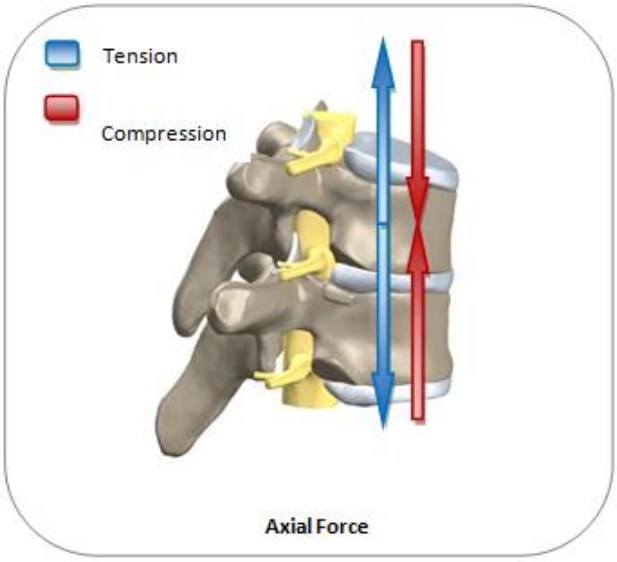

Figure 2-4: Axial force measured in N

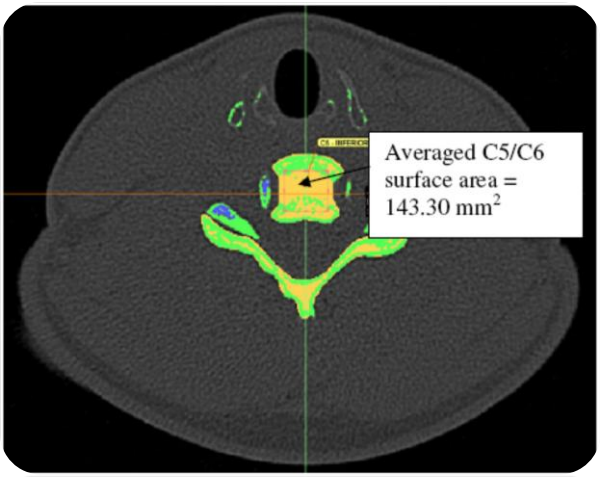

Figure 2-5: Cross-sectional area in the transverse plane of vertebral bodies in a CT scan using MIMICS™ [15]

2.3.3 Bending Moments

The bending moments present in the spine (Figure 2-6) at the time of impact are arguably one of the most important parameters to consider when evaluating the efficacy of a protective device. This parameter can combine with axial force to effect devastating injuries to the cervical spine in terms of fractures and other disruptions, as summarized in Table 2-2, Table 2-3 and Table 2-4. The bending moment is calculated in simulation models as the force applied (N) to a vertebrae pair, multiplied (through a mathematical method termed a "dot" or "cross" product) by the distance from where it is applied to the center of rotation (COR or instantaneous axis of rotation (or IAR)) around which the bending moment is measured (typically in mm in spinal applications), giving a torque measured in Nmm.

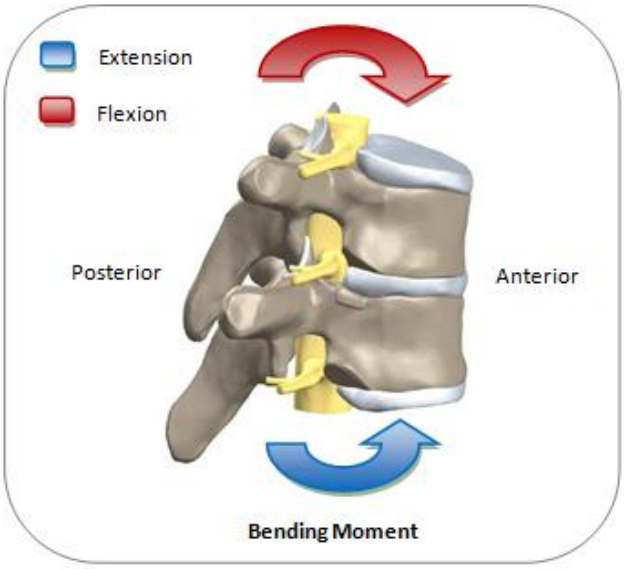

Figure 2-6: Bending moment measured in Nmm

2.3.4 Shear Force

The shear force (measured in N) is the force applied to a vertebrae pair from two opposing directions (Figure 2-7), causing the IV disc or facet joint to "shear" or tear apart if the force is high enough. This force, combined with the distance from which it is applied to the COR or IAR of a vertebrae pair, yields a bending moment that is applied (specifically at the C0/C1 junction or atlanto-occipital joint) in the calculation of the Nij injury criterion.

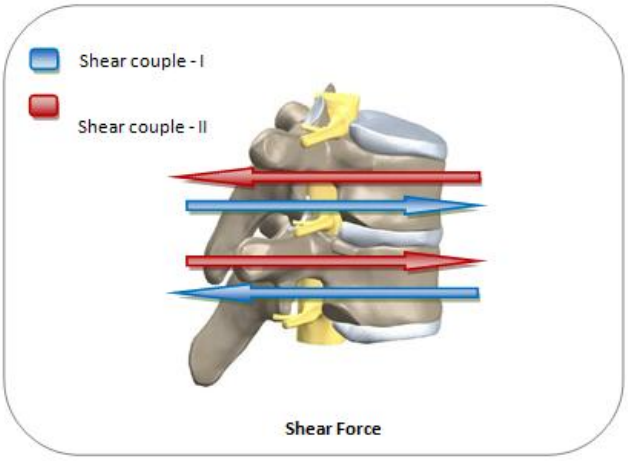

Figure 2-7: Shear force measured in N

2.3.5 Head/Brain Dynamics

In the process of protecting the cervical spine, brain dynamics should also be considered. The brain is at its most vulnerable during rotational trauma, i.e., when the brain is accelerated (or decelerated) relative to the skull in an angular fashion 0. If excessive motion of the cervical spine is limited by a protection device through a sudden, short-timed (non-absorbed) stop in cervical spine motion by whatever means, the brain may be subjected to high relative angular velocities and accelerations. It therefore is vital to look at the subsequent effects on brain dynamics, in addition to considering pure spinal biomechanics.

There is an important interrelation between limiting motion in the cervical spine and controlling the duration of relative angular deceleration during impact. If the duration of relative angular deceleration is too long (through excessive absorption of the cervical motion), mild traumatic brain injuries (MTBI) may occur at the peak of the relative acceleration. An important consideration to account for is "catching the head early" in extension (after initial flexion), thereby effectively allowing the brain (which is in delayed recoil from flexion) to "catch up" with the skull, subsequently decreasing the terminal deceleration magnitude and duration, as

well as the relative (skull/brain) rotational velocity and displacement. On the other hand, if the duration of angular deceleration is too short (through an abrupt stop of the cervical motion by means of zero absorption), the relative displacements and subsequent velocities and accelerations may be too large, and serious injuries to the brain may occur. This phenomenon was parameterized through the establishment of the well-known Wayne State Tolerance Curve (discussed in Section 2.3.8, Figure 2-15). Two additional curves, indicating the acceleration/velocity/time injury criterion interactions, are presented in Figure 2-8 and Figure 2-9 0. Injuries may include shearing (tearing) of the bridging veins between the skull and brain because of excessive tissue strain (Figure 2-10), leading to subdural hematoma or SDH (Figure 2-8). Diffuse axonal injuries (DAI) may also occur (Figure 2-9) 0. SDH refers to bleeding within the inner meningeal layer of the dura (the outer protective covering of the brain) (Figure 2-14), whilst DAI causes extensive, widespread lesions in white matter tracts because of shearing in this area. It was postulated by Kleiven 0 that bridging vein rupture may occur when the peak angular acceleration and peak change in velocity exceed 4 500 rad/s^2 and 50 rad/s respectively. It should also be considered that the helmet plays a role in the absorption and deceleration of the skull upon impact. It therefore is important that a good understanding of the abovementioned factors be obtained in order to assess brain dynamics and the subsequent injury potential of the brain.

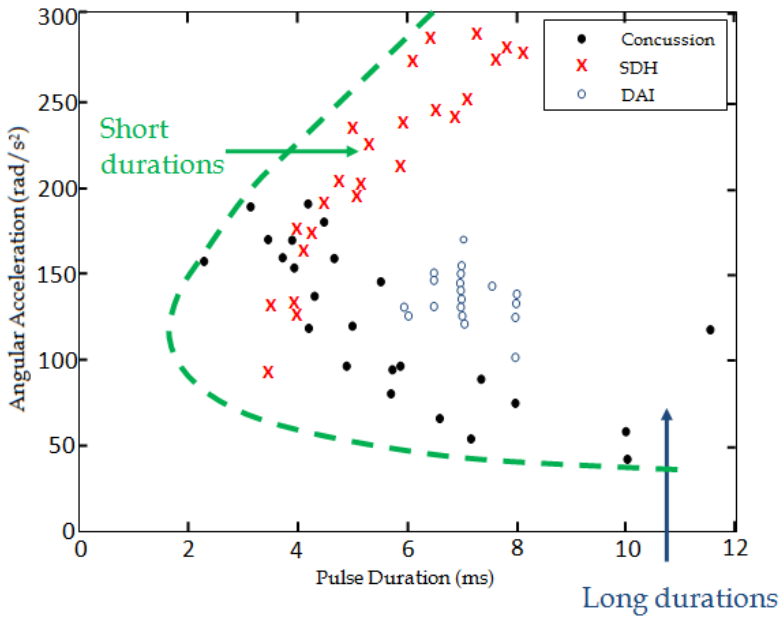

Figure 2-8: Acceleration vs. time injury tolerance curve 0

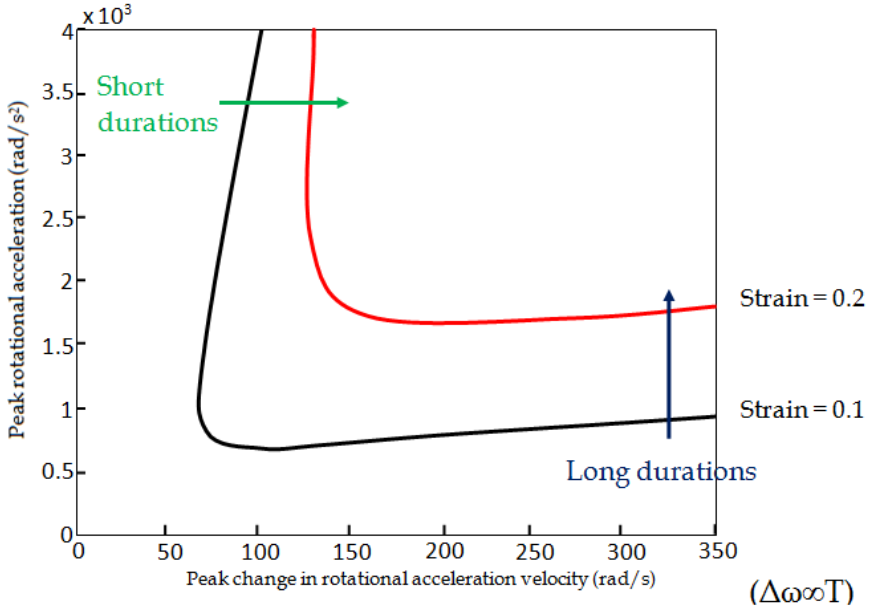

Figure 2-9: Acceleration vs. time injury tolerance curve 0

It is virtually impossible to physically test brain dynamics using either physical surrogates (for obvious reasons) or cadavers (because of post-mortem proteolysis and preconditioning). The mechanical properties of brain tissue are compromised after death 0. Simulations, using brain properties from the literature, therefore yield the best opportunity for understanding brain dynamics. Using iterative simulation runs may help to find the correct combination of the abovementioned absorption and relative angular acceleration factors. Further discussion of brain dynamics and its application in the design of the Moto GPX follow in Section 4.3.

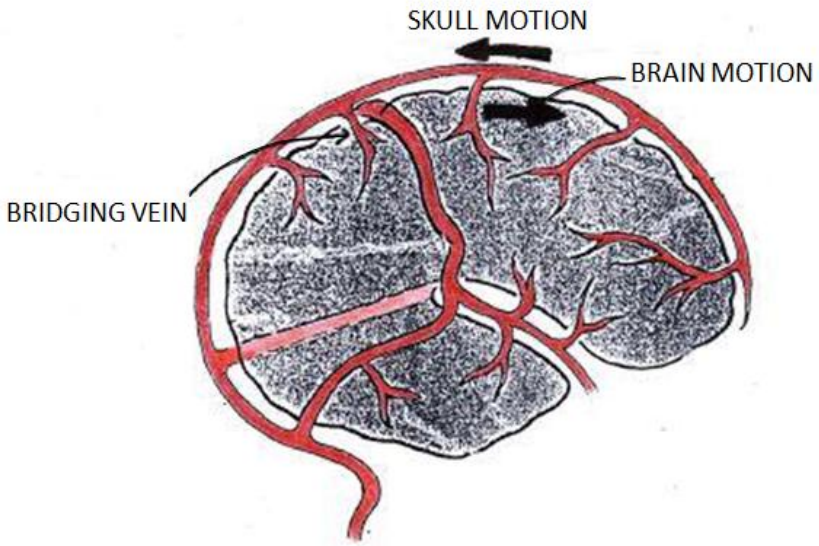

Figure 2-10: Bridging vein shear with relative brain/skull motion 0

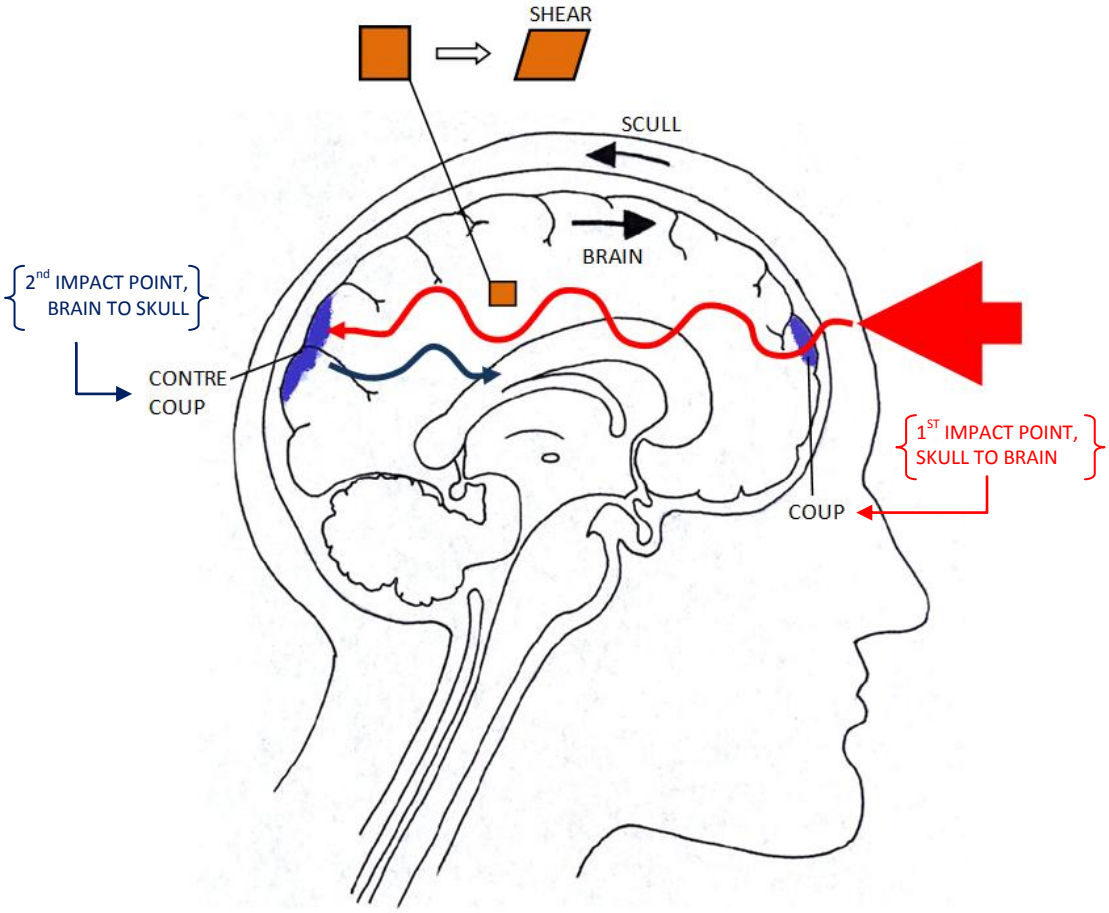

Figure 2-11: DAI biomechanics 0

2.3.6 Vertebral Angles

Vertebral angles in simulation models used for the design of the Moto GPX can be measured either through the change in the angle of the joints at C0/C1 and C7/T1, or through the change in the rotation of the COR or IAR of the passive joint elements representing the IV discs during rotation. The software used here (MSC.ADAMS LifeMOD™) employs the latter.

One of the typical methods used to measure vertebral rotations is from radiographic images, using the angles of the anterior bodies of the vertebrae (viewed laterally). However, according to the authors of this paper it makes more sense to measure vertebral rotations from the COR or IAR between each vertebrae pair

(which is easily achievable through simulation), although it is acknowledged that this is not possible *in vivo*, since the IAR is not precisely known, even with X-ray technology. More on the IAR will be presented in Section 4.4.

2.3.7 Nij

The majority of neck injuries are caused by indirect loading produced by inertial loads being transferred from the torso to the head following head impact, or from the head to the torso following torso impact or high acceleration [19]. The reaction of the head during impact is a combination of multidirectional rotations and translations. The type of impact also greatly affects the reaction of the head. It is thus important to study the combined effects of these multifaceted inputs to the spine in order to calculate a resultant injury factor. Therefore, the neck injury criteria (Nij) were developed and are now widely used as a measure of the severity of injury during crash scenarios with ATDs and computer human surrogate models.

The Nij is made up of different load types, which are measured at the upper neck load cell of the H-III ATD for the duration of the crash or impact. This is typically the weakest part of the cervical spine (because of the thin cross-section area of the axis of C2) and is made up of the upper two cervical vertebrae, namely the atlas (C1) and axis (C2), and is joined to the lower part of the cranium (on the head) via the atlanto-occipital joint. A combination of the following forces (Figure 2-12) is used to calculate the Nij:

Upper Neck Axial Forces

- Tension (pull) or compression (push)

Upper Neck Bending Moments

- Flexion (head forward) or extension (head backward), $BM = Force.distance$

Upper Neck Shear Forces

- Positive or negative shear

The combination of axial forces and bending moment results in four possible loading conditions, as stated in the Federal Motor Vehicle Safety Standard (FMVSS) §571.208 [20]. These are tension-extension (N_{TE}), tension-flexion (N_{TF}), compression-extension (N_{CE}), and compression-flexion (N_{CF}). Only one of these four loading conditions can exist at any point in time and the corresponding Nij is calculated with the other three values at zero (Table 2-7).

The FMVSS §571.208 [20] states that the expression for the calculation of the Nij is given by:

$$N_{ij} = \frac{F_z}{F_{zc}} + \frac{M_{ocy}}{M_{yc}} \tag{2-1}$$

where F_z is the upper neck load cell force output in the z-direction (axial force), M_{ocy} is the bending moment about the occipital condyle, and *Fzc* and *Myc* are critical values which are individually defined for each type of test dummy (Table 2-8). These values also vary according to the test type (in-position or out-of-position). The out-of-position cases are limited to the small female and child dummies. The expression for the calculation of the M_{ocy} is given by:

$$M_{ocy} = M_y - (D \times F_x) \quad (2\text{-}2)$$

where M_y is the upper neck load cell moment output about the y-axis (bending moment), F_x is the upper neck load cell force output in the x-direction (shear force), and D is the distance between the axis of the load cell and the axis of the condyle. The upper neck load cell is installed through the hole in the base of the skull for the H-III ATD (95th percentile, 50th percentile, 5th percentile, and six-year-old) and therefore the value used for D is 17.78 mm.

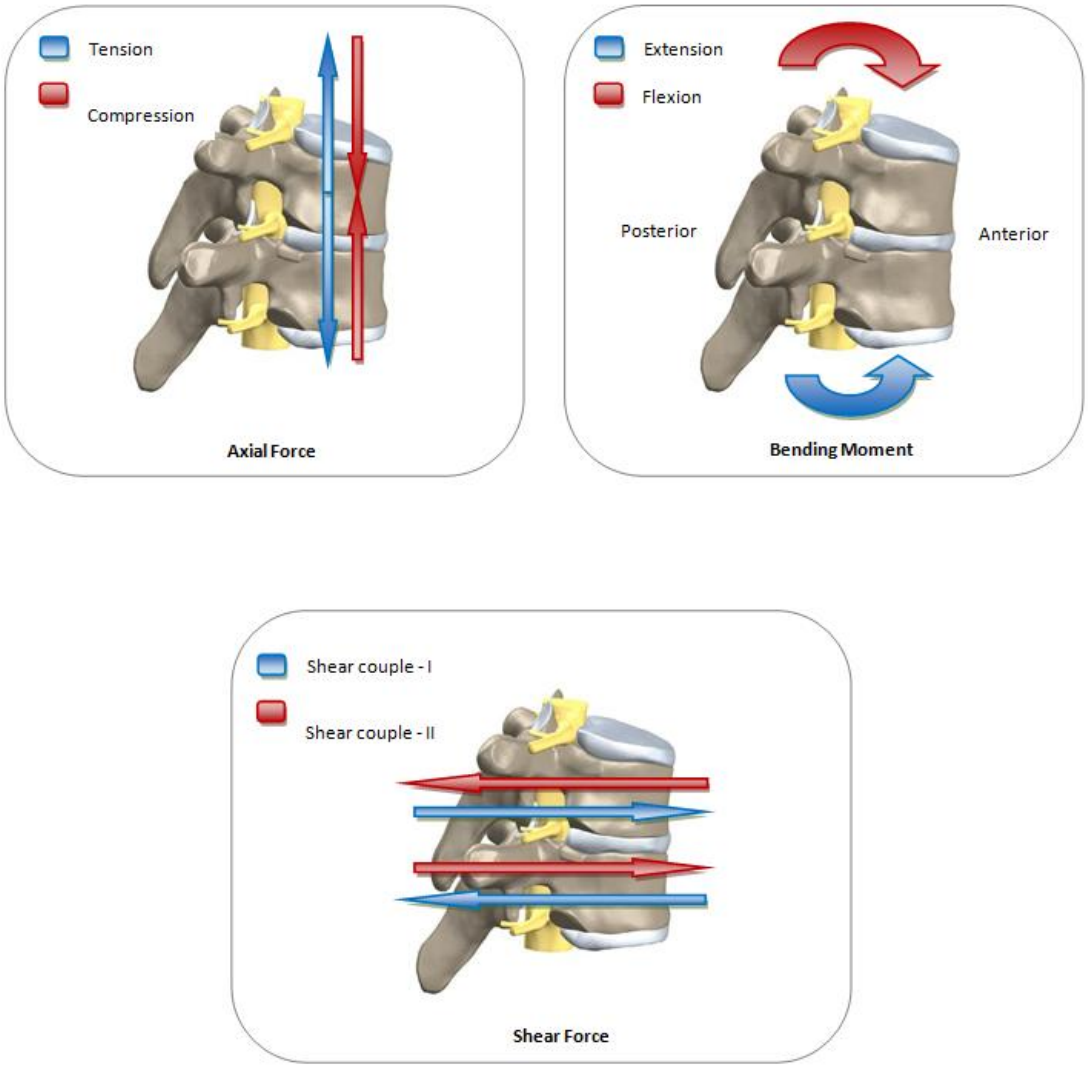

Figure 2-12: Coupled force vectors used in Nij calculation

The axial force (F_z), bending moment (M_y) and shear force (F_x) must be filtered for the calculation of the Nij. This must be done in accordance with SAE J211/1 rev. Mar 95 Channel Frequency Class 600 (Table 2-9). None of the Nij values may ever exceed 1.0 at any time during the crash/impact event (Figure 2-13).

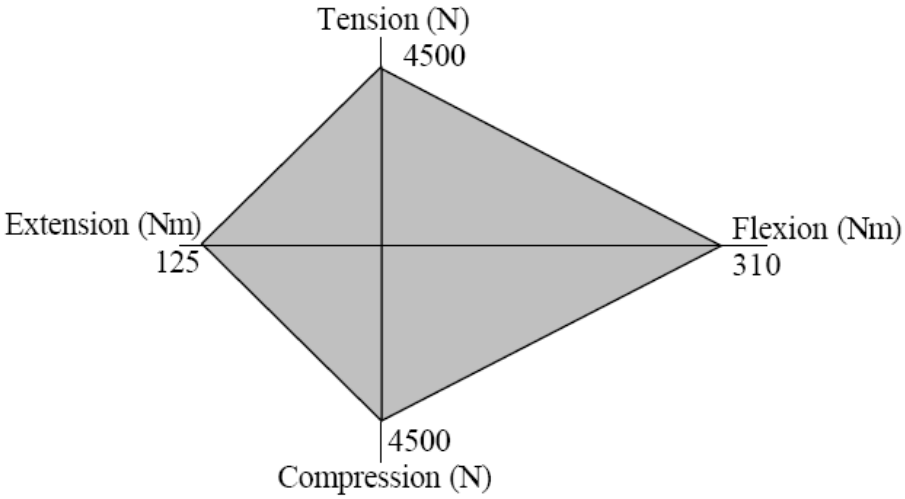

Figure 2-13: Neck injury criteria for the 50th percentile male dummy [21]

TABLE 2-7: NIJ FORCES AND MOMENTS [22]

Nij	Forces	Moments
N_{CF}	Compression (force of pressure) F < 0	Flexion (forwards bending) M > 0
N_{CE}		Extension (backwards extension) M < 0
N_{TF}	Tension (tensile force) F > 0	Flexion (forwards bending) M > 0
N_{TE}		Extension (backwards extension) M < 0

TABLE 2-8: CRITICAL VALUES FOR COMPUTING NIJ

ATD	Test Type	Critical Value / Condition			
Hybrid III		F_{zc} [N] Tension	F_{zc} [N] Compression	M_{yc} [NM] Flexion	M_{yc} [NM] Extension
Male 50th	In Position	6806	6160	310	135
Female 5th	In Position	4287	3880	155	67
	Out of Position	3880	3880	155	61
6 yr old	Out of Position	2800	2800	93	37
3 yr old	Out of Position	2120	2120	68	27
12 mnth old	In Position	1460	1460	43	17

TABLE 2-9: CFC FILTER TYPES [22]

Filter Type	Filter Parameters	
CFC60	3dB limit frequency	100 Hz
	Stop damping	-30 dB
	Sampling frequency	at least 600 Hz
CFC180	3dB limit frequency	300 Hz
	Stop damping	-30 dB
	Sampling frequency	at least 1800 Hz
CFC600	3dB limit frequency	1000 Hz
	Stop damping	-40 dB
	Sampling frequency	at least 6 kHz
CFC1000	3dB limit frequency	1650 Hz
	Stop damping	-40 dB
	Sampling frequency	at least 10 kHz

2.3.8 HIC

Due to the complexity of the human head, it is necessary to define and describe certain areas pertaining to the head in order to explain the head injury criteria (HIC). The head can be divided into three distinct components, namely:

Skull

- Skeleton of the head (spherical in shape)
- Made up of two bony parts, which are fused [23]
- Facial skeleton - made up of orbits (eye sockets), nasal cavities, maxilla (upper jaw), mandible (lower jaw)

Skin and Soft Tissue

- Known as the SCALP, consisting of skin, connective tissue, aponeurosis, loose connective tissue and the pericranium

Skull Contents

- Brain
- Cranial meninges
- Cranial nerves and blood vessels
- Neorocranium – houses and protects the brain, cranial meninges, cranial nerves and blood vessels, attaches to neck at occipital condyles
- Durae (mater, pia, arachnoidea)
- Cerebrospinal fluid (CSF)

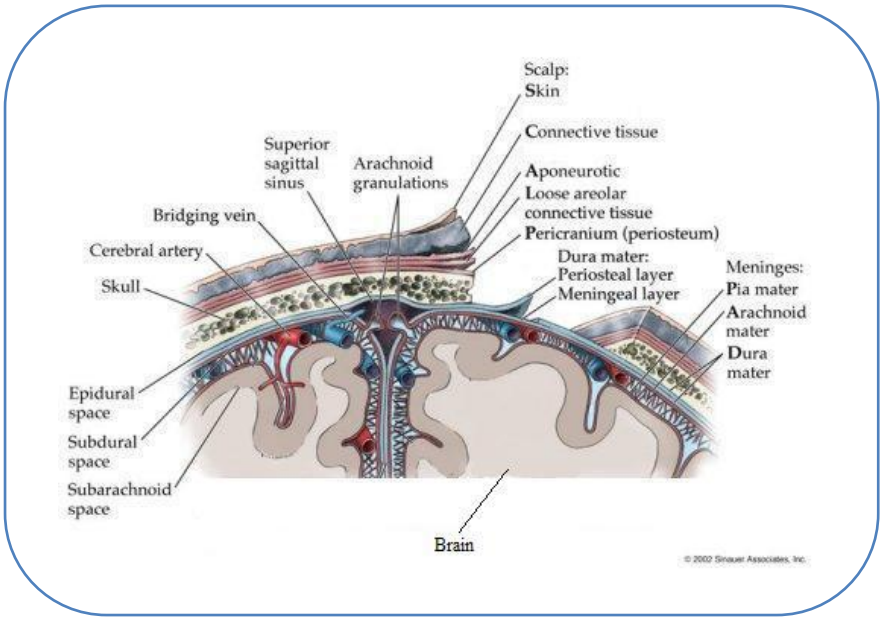

Figure 2-14: Coronal section of human head [24]

The brain controls motion, both voluntary and involuntary, and is also the center of consciousness [3]. Brain injuries can be fatal or have major debilitating consequences, as brain tissue does not regenerate.

Brain injury modalities were discussed briefly in Section 2.3.5. Brain injuries can be divided into two categories dependent on the injury mechanism: diffuse and focal injuries [3]. Diffuse (distributed) brain injuries are normally associated with impacts to rigid surfaces, abrupt head deceleration (rotational in particular) or a combination of the two. This type of impact causes high brain accelerations, resulting in injuries that can range from mild concussion to a fatality. Focal (localized) brain injuries occur due to a direct impact on a specific area of the brain. This results in injuries ranging from bruising to direct brain penetration. Brain damage is caused by reduced blood flow to the brain or internal brain rupturing, tearing of tracts or hemorrhaging (bleeding), which is a direct result of these two types of brain injuries. Depending on its extent and severity, brain damage can be permanent.

It is important to have a tool or guideline that can be used to prove and improve the quality of head protection devices and thereby to decrease the likelihood of brain damage. The relationship between head acceleration and impulse duration was discussed in Section 2.3.5 and was first depicted by the Wayne State Tolerance Curve (WSTC) [25] (Figure 2-15). Since then, this has become the relationship on which currently accepted head-injury criteria are based. The initial WSTC was approximated by a straight line function by C.W. Gadd [26] in 1961 for a weighted impulse criterion. This was as a result of limited data points, lack of documentation, uncertainty about accelerations levels, etc., as well as a lack of biomechanically proven theories.

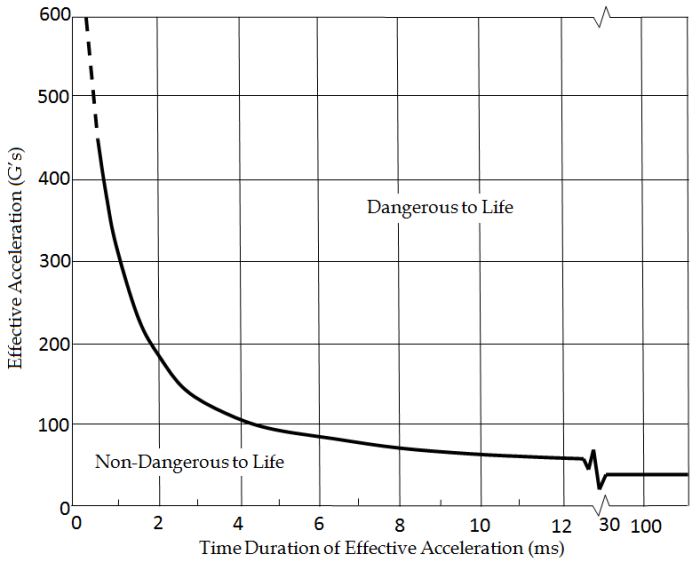

Figure 2-15: Wayne State Tolerance Curve

The criterion of Gadd [26] became known as the Gadd Severity Index (GSI) and is defined by the following expression:

$$\mathrm{GSI} = \int [\mathrm{a(t)}]^{2.5}\,\mathrm{dt} \tag{2-1}$$

where *a(t)* is the acceleration at any given point in time and is integrated as a function of time. In 1972, the current head injury criteria (HIC) were defined by the National Highway Traffic Safety Administration (NHTSA), in response to the WSTC and Gadd Severity Indexes. The main difference is that the resultant translational acceleration is used as a base, as opposed to the frontal axis acceleration as initially defined by the WSTC. The HIC can be defined by the following expression:

$$\mathrm{HIC} = \left[\frac{1}{t_2 - t_1}\int_1^2 a\,dt\right]^{2.5}(t_2 - t_1) \tag{2-2}$$

where t_1 and t_2 are the points in time during the crash/event at which the HIC is at maximum, and *a* is the resultant acceleration of the center of gravity of the head. This acceleration is given in units of gravity (G's). The resultant acceleration can be calculated using the following expression:

$$a = \sqrt{a_x{}^2 + a_y{}^2 + a_z{}^2} \tag{2-3}$$

where a_x, a_y and a_z is the acceleration of the head at its center of gravity in the *x, y* and *z*-directions. The measured accelerations must be filtered for the calculation of the HIC. This must be done in accordance with SAE J211/1 rev. Mar 95 Channel Frequency Class 1000 (Table 2-9).

The possibility of brain injury and skull fractures increases with an increase in the severity of the impact. The HIC is used as a measure and certain threshold values are used to indicate the limit of the probability of serious injury.

The HIC for the Hybrid III 50th percentile ATD used in FMVSS 208 [20] is calculated over two distinct interval periods, 36 ms and 15 ms. The HIC limit or injury threshold for the 36 ms time interval calculation is set at 1 000. This corresponds to a constant head acceleration of ± 60 G. The HIC limit for the 15 ms time interval calculation is set at 700. This corresponds to a constant head acceleration of ± 74 G. The difference between the two HIC calculations is shown in Figure 2-16.

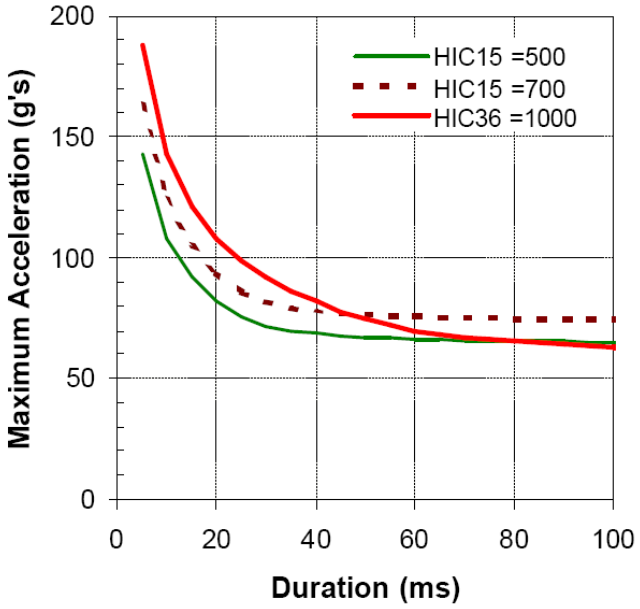

Figure 2-16: HIC comparison [21]

2.3.9 Whiplash-associated Disorders [27]

2.3.9.1 Definition

Whiplash is an injury that occurs when the neck and head experience a sudden, sharp motion. The injury often affects the muscles, soft tissue, ligaments, nerves, IV discs and bones of the neck.

2.3.9.2 Description

About one million whiplash injuries occur in the United States every year. Most occur during car accidents or sporting events. In these cases, an unexpected force jerks the head backward and then, almost immediately, forward, causing the vertebrae of the cervical spine to misalign. Nerves in the neck may be pinched, resulting in damage and possible neurological deficit.

2.3.9.3 Causes

Whiplash in motor vehicle accidents is likely to occur when a person's muscles are in a relaxed state. This is typically the case when an impact is unexpected. In the case of both cars and motorcycles, however, a person's muscles may contract prior to impact, if the accident is expected. Studies have been conducted to quantify the differences in injury potential between these two scenarios, but great discrepancies have been found because of the significant variations in a variety of factors, such as impact parameters (impact modalities, contact, contact geometries, etc.), protection used, etc. In both cases, however, the chance of damage to the neck is high.

2.3.9.4 Injuries [1]

Co-morbid injuriy that may be sustained in the whiplash scenarios include:

- Injuries to the head and neck
- Brain injuries (generally minor brain injuries or concussions)
- Spinal and clavicle fractures
- Herniations of the spinal IV discs
- Soft tissue injuries
- Lower back injuries
- Internal injuries - sometimes caused by lap belts
- Bruises
- Abrasions (scrapes) - sometimes caused by shoulder restraints
- Jaw injuries
- Chest injuries

2.4 Proposed Test Protocols for the Evaluation of Cervical Spine Protection Devices for Unrestrained Torsos

At present there are no test protocols in any country approved for assessing the efficacy of cervical spine protection devices for the *unrestrained torso*; however, one of the approved test protocols for *restrained torso* protection devices (SFI 38.1) tests these devices using a sled test. With the protection device in place on a H-III 50th percentile (median sized) anthropomorphic test device (ATD), the sled is accelerated to 68 G, then stopped, simulating a frontal impact of 70 G. This is done at angles of 0^{o} and 30^{o} from the front. Various cervical spine parameters, such as axial force (tension and compression), bending moments, shear forces and the Nij (measured at the C0/C1 and C7/T1 dummy joints), are evaluated against the allowable limits and the efficacy of the device is gauged.

We believe that evaluation of the efficacy of an unrestrained torso protection device should repetitively measure the reduction in the force and motion parameters present in the spine. Based on an idea first employed elsewhere, the authors propose a pendulum dummy swing with head impact incorporating front, rear and

side impacts. The protocol would evaluate the three main directions of cervical spine motion and their associated parameters via H-III ATD testing and simulations. In addition, static and quasi-static tests and simulations can be conducted using a detailed spine model to evaluate various components of the protection device. A combination of these evaluation methods should prove valuable in assessing an unrestrained torso protection device. Leatt Corporation's work on such a protocol, and cooperation with the SFI foundation, are presented in Chapter 5.

2.5 Anthropomorphic Test Devices (ATD)

Hybrid III 50th Percentile Male ATD

The H-III 50th Percentile Male ATD (Figure 2-17) is one of the most commonly used test devices in the world and is used for the evaluation of automotive safety restraint systems in frontal impact crash scenarios. It was developed by General Motors Corporation under an NHTSA contract beginning in 1973. These dummies were designed utilizing a wide range of materials, which included rubber, foam, vinyl, aluminum and steel, to create a device aimed at some form of biofidelity. Using biomechanical data, and combining more than thirty years of testing and development to make the impact response of the test dummy closely approximate that of humans, the Hybrid III 50th Percentile Male ATD can accommodate a wide range of instrumentation--accelerometers, load cells, and transducers from the head to toe, making it a versatile device for compliance testing and research and development. The H-III 50th Percentile Male ATD represents a 50th percentile (median) male occupant in mass and inertia (

Table 2-10) and is the preferred test device for FMVSS 208 [20] testing. It is regulated by the U.S. Code of Federal Regulations Part 572, Subpart E, as well as the European ECE Regulations.

Shear force, compression/tension (axial) forces, and directional bending moments are commonly measured using a six-axis upper or lower neck load cell in an H-III ATD. Although the H-III ATD neck fidelity was initially designed for sled testing and the evaluation of airbag deployment, it nevertheless became the "gold standard" neck biofidelity model in impact tests. Due to the limited biofidelity of the H-III neck, however, impact results must be interpreted with caution in any other impact test scenario, including pendulum, drop and other tests [ISO 13232 – 5(E) page 5, 4.4]

Figure 2-17: Hybrid III 50th Percentile Male ATD [28]

TABLE 2-10: HYBRID III 50TH PERCENTILE MALE ATD WEIGHTS [29]

WEIGHTS	POUNDS	KILOGRAMS
Head	10.0	4.54
Neck	3.4	1.54
Upper Torso	37.9	17.19
Lower Torso	50.8	23.04
Upper Arm	4.4	2.00
Lower Arm	3.75	1.70
Hand	1.25	0.57
Upper Leg	13.2	5.99
Lower Leg & Foot	12.0	5.44
Total Weight	**171.3**	**77.70**

TABLE 2-11: HYBRID III 50TH PERCENTILE MALE ATD DIMENSIONS [29]

DIMENSIONS	INCHES	CENTIMETERS
Head Circumference	22.5	57.15
Head Breadth	6.1	15.49
Head Depth	7.7	19.56
Buttock to Knee Pivot	23.3	59.2
Knee Pivot Height	19.4	49.3
Hip Pivot from Backline	5.4	13.7
Hip Pivot Height	3.4	8.6
Sitting Height	**34.8**	**88.4**

Limitations of the Hybrid III ATD

Specific limitations of the H-III ATD are that it is not ideally suited to large, side- or rear-impact crash pulses (typically above 40 G). However, it is commonly used for the SFI 38.1 test specification at 30 degree frontal impact under a 68 G pulse. Side and rear impact dummies (SID and RID) were developed with these limitations of the H-III ATD in mind and are used for large, side and rear impact crash scenarios respectively.

Another variation of the H-III ATD, specifically pertaining to motorcycle applications, is the promising but not yet common Motorcycle Anthropomorphic Test Dummy (MATD). The significant differences between these two dummies are the unique posture and multi-directional biofidelity ability of the MATD neck. This allows the MATD to be adjusted for a wide range of inclined upper torso and neck angles that are typical of the large variety of riding postures in motorcyclists. There are no differences in the instrumentation setup of the necks of the two dummies.

Leatt Corporation is presently using both the ATD and MATD versions of the Hybrid III.

Chapter 3

Rationale for the Design of the Moto GPX Neck Brace

3.1 Introduction

The design rationale of the Moto GPX is based on common neck injury classification systems as presented in Section 2.2 and as used by spinal surgeons and biomedical engineers.

The design criteria used in the development of the Moto GPX are as follows:

- To decrease the number and severity of significant neck injuries through injury prevention or the reduction of the grade of injury to reduce neurological deficit.
- To find the best compromise between decreasing dangerous ranges of motion, neck forces and impulse momentum relationships, whilst maintaining driver/rider usability.
- To design a system similar to the automotive racing "D-Cell" head and neck restraint, so as to prevent extremes of movement by providing an alternative load path deceleration surface adjacent to a crash helmet in such a way that it travels with the rider/driver and therefore always will be positioned correctly.
- To prevent extreme ranges of motion producing / associated injury [8].
- To maintain ROM to the extent that overly restricted ROM would result in high axial forces, i.e., to preserve the head's ability to move out of the way of the impact force.

- To transfer lateral compression-flexion forces to the device with a laterally flexed neck.
- To transfer extension-compression forces to the device.
- To allow the neck to continue to move in order to reduce compression injuries, but to prevent the extreme movement that can produce injury.
- To transfer forces from one spinal motion segment to a greater number of motion segments, as well as to the chest, paraspinal muscles and shoulders.
- To create a dynamic device that allows for a controlled deceleration of the head and neck with a built-in ability to collapse, thereby preserving the recommended range of safe movement without collateral injuries.
- To ensure controlled head deceleration that helps prevent traumatic brain injury.
- To decrease the anterior exposure of the neck to intrusion from potentially harmful objects such as vegetation, fences, and other obstacles.
- To decrease lateral neck exposure to penetrating trauma.
- To reduce neck fatigue from long-distance riding.
- To ensure that the device accommodates a wide range of body types while still preventing helmet projection over the device and fulcrum risks.

The Moto GPX, designed with these parameters in mind, fulfills these design criteria.

3.2 Allowable ROM

The Moto GPX has an optimum height (calculated through repetitive simulations to be at 15 mm to 85 mm), that is the distance from the underside of the helmet to the device. A device that rides too high means the neck cannot move out of the path of a force directed to the helmet, with resultant high axial forces; a device that rides too low and becomes ineffective. In order to prevent injury, the Moto GPX restricts extreme ranges of movement that cause injury but allows sufficient freedom of movement so as not to transmit excessive forces to the helmet or to limit vision below that required for safe and competitive operation. These extreme ranges of movement (Figure 3-1) are:

- Hyper-flexion (a & e)
- Hyper-extension (b & f)
- Posterior hyper-translation – head moving backwards on the neck
- Lateral hyper-flexion (c, d, g & h)
- Axial loading – initially compressive force acting on the spine but converted to the movements illustrated in e to h below.

Figure 3-1: Extreme head movement without and with the Moto GPX

The Moto GPX was designed to be compatible with most motorcycle types and allows riders an adequate range of head and neck movement. Moto GPX prototypes were tested extensively by BMW and KTM works riders under racing conditions, and the test riders reported a good range of movement and comfort. Over long distances on motorcycles with no wind protection, the brace also can also offer some relief from neck fatigue.

Another important design consideration ensures that the device has the correct size and shape to prevent helmet projection over its edges. An incorrect size or shape of the upper surface of the brace can result in a "fulcrum effect". This is where the helmet projects over the outer edge of the device and pivots around the contact point, causing a potentially devastating bending moment or torque on the neck of the rider.

3.3 Alternative Load Path Technology (ALPT)™

Alternative Load Path Technology (ALPT)™ refers to the ability of the Moto-GX to redirect to other structures the forces applied to the neck in crashes or collisions. The design rationale of the Moto GPX is to bring the head to a *controlled* halt and to act as an *alternative load path*. In the unrestrained torso, the helmeted head comes into contact with a surface during an impact, e.g. the ground. Force is transmitted from the ground to the helmet, the skull, the base of the skull and the neck, and then to the thoracic spine and torso. With the Moto GPX, the force is transmitted from the ground to the helmet and then, as the helmet contacts the brace, the force is transmitted through the brace to the torso, thereby reducing neck loads by creating an alternative load path. This is assisted by the construct of the Moto GPX, as the helmet rim comes into contact with the brace and creates an additional load path. The alternative load path is also is designed to yield at pre-determined anatomical loading forces to reduce further injuries. Specifics on loading parameters and force reductions will be presented in Chapter 4.

3.4 Material/Absorption Considerations

The Moto GPX is designed to decelerate the head in a controlled way without imposing a sudden deceleration force on the brain. In terms of the pure injury-prevention capacity, the biomechanics are complex; however, the material from which the device is manufactured, as well as the physical proportions of the device, is both important.

The chosen solution is to steer away from having a platform that is too rigid, subsequently rendering very high-impact acceleration in a short time or, on the other hand, having a platform that is too flexible or soft and subsequently having lower acceleration over a longer time. According to the WSTC (Figure 2-15), both these extremes tend to result in life-threatening scenarios. The ideal thus would be to combine the two abovementioned factors and have an optimized combination of

rigid motion limitation and deceleration through absorption. However, the device is designed to yield well before anatomical structures yield so as not to cause injuries to the sternum or the thoracic spine.

The Moto GPX Club is constructed from conditioned glass reinforced nylon (GRN) or polycarbonate (PC) in both its upper and lower sections and weighs approximately 850 g. The Moto GPX Sport is constructed from a conditioned GRN lower section and a carbon fiber/Kevlar® upper section and weighs about 780 g. Physical testing was used to determine the correct type of GRN (15% glass filled) and PC. The device has to be somewhat stiff but also needs the ability to flex and break during an extreme impact or load. A GRN of 15% and PC were chosen due to its good combination of these two factors (see datasheet, Appendix A). The conditioning of the GRN ensures that the parts will not fracture catastrophically. The upper section of the Moto GPX Sport was designed using carbon fiber due to its high strength and low weight. Weight is an important factor to consider because safety devices perceived to be uncomfortable or, worse yet, a handicap to performance will not be worn.

The entire surface of the device that could possibly interact with human skin during normal use is covered by padding. This is to protect the soft tissue of the rider's neck structures. The padding that is used in the Moto GPX is made up of two outer layers of Lycra, with EVA foam in the core. The density of the EVA was chosen to give maximum effectiveness to the *Alternative Load Path Technology (ALPT)* ™. The padding has a minimum thickness of 5 mm over covered surfaces and is fixed to the device using hook and loop fastener. This ensures that the controlled fracture surfaces are adequately contained. Brace parts have been designed to fail after high impact and it therefore is essential that the padding contains these parts to ensure the absolute safety of the rider. In addition, the front and back top components of the device were designed with a cup shape to ensure that the lower parts of the device are contained in the event of the device fracturing after impact.

The same reasoning was used in the design of the carbon fiber parts. A layer of Kevlar® is used at the center of the carbon fiber layup to ensure that the carbon parts are kept intact during impact or failure. This eliminates the possibility of catastrophic fracture, which will result in sharp inward protrusions that could cause injuries to the rider. The padding also cushions the chin so as not to cause soft tissue trauma to the chin or other body structures during an impact.

3.5 Clip/Hinge Design

The Moto GPX is designed with hinge points lateral to the neck, one on either side of the neck. This allows the device to be unlocked and hinged open on the left side (Figure 3-2a) or the right side, or for the anterior (front) part being completely removed from the posterior (back) part of the device (Figure 3-2b). This allows easy access to the throat area after a rider has suffered an injurious crash. It can be critical to access an injured rider's airway or throat without excessive movement of the rider's neck or body in case CPR (cardiopulmonary resuscitation) or if airway protection is required.

Figure 3-2: Hinge mechanism

The hinge is an over-center lock mechanism, which is designed to lock securely and not open during normal use or during a crash. The mechanism includes a pivoting shoe on the anterior part of the brace and a fixed jaw comprising a complementary C-shaped section in a different plane, molded into the posterior part of the device. Engagement of the hinge mechanism connects the anterior and posterior parts of the brace and locks it securely (Figure 3-3).

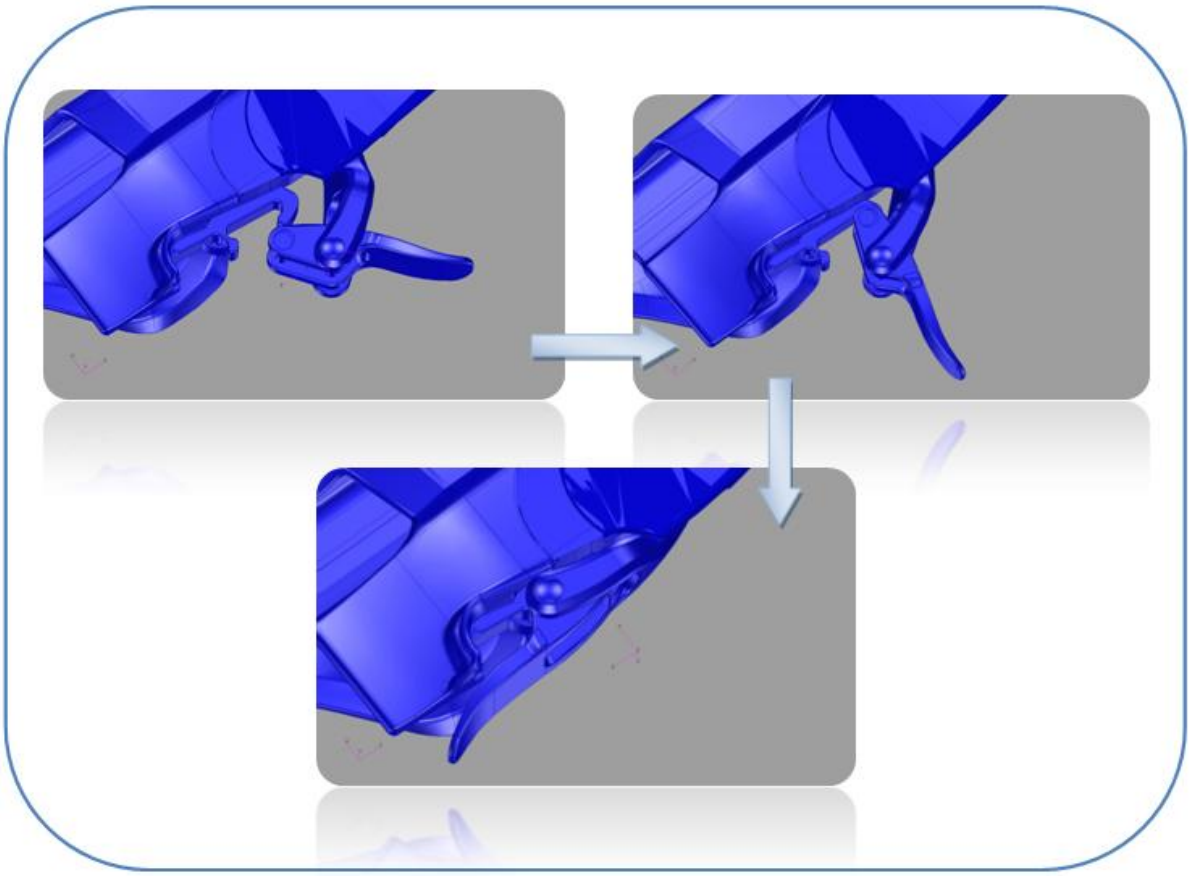

Figure 3-3: Hinge locking mechanism

3.6 Designed for Adjustability

The Moto GPX is designed to fit the body types of most of the motorcycling population. Multi-dimensional adjustability allows the device to be customized to suit the specific rider's body configuration and, within limits, comfort level. The anterior and posterior impact platforms can be adjusted to raise (decreasing the vertical distance between the helmet rim and the device upper surface) or lower (increasing the vertical distance between the helmet rim and the device upper surface). The pivot point for these adjustments is a virtual rotational axis situated at the height of the shoulder joint, as illustrated in Figure 3-4. This point was chosen to ensure that the impact platforms are always adjusted in the same concentric plane of motion as the head.

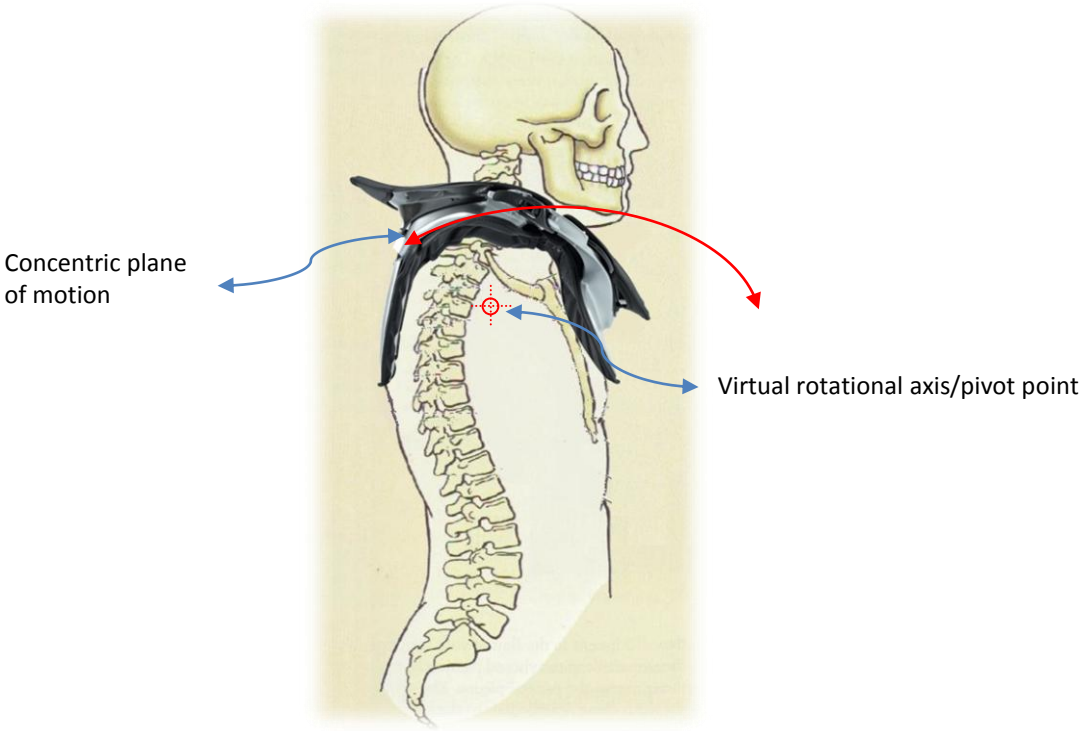

Figure 3-4: Illustration of virtual pivot point

For price economy, the ADVenture™ brace employs non-adjustable, one-piece, front and back platforms, but the platform heights are identical to the adjustable parts set in the "mid" position.

The anterior/posterior internal size of the device (distance between the anterior and the posterior parts of the brace) can be adjusted by changing out specially designed pins available in a range of sizes. This adjustability is augmented by the thoracic strut box design which incorporates a number of internal shims. The shims allow the thoracic strut to be inserted at varying distances from the rider's back, and struts of differing angles provide even more adjustability.

Because the device employs a modular design, various parts can be replaced as needed.

3.7 Clavicle Relief Area

In the experience of motocross and Supercross riders, clavicle fractures (collarbone injuries) are approximately 50 times more likely than cervical spine fractures.

Clavicle fractures usually occur in one of three ways:

1. A fall onto an outstretched arm, transmitting the force up the arm to the clavicle.
2. A direct fall onto the shoulder, transmitting force to the clavicle.
3. The helmet rim striking the clavicle in a fall.

The Moto GPX is designed to limit this third type of clavicle fracture by protecting the clavicle from the helmet rim via the "clavicle relief area" on the underside of the Moto GPX (Figure 3-5). The device was designed to allow the arm/shoulder to be abducted (lifted up) all the way without the clavicle coming into contact with the underside of the device. This prevents the occurrence of a bending moment acting on the clavicle. Because the upper brace surface adjacent to the clavicle relief area has contact with the helmet rim, a reduction in the third type of

clavicle fracture described above is anticipated and the overall incidence of clavicle fractures could be reduced.

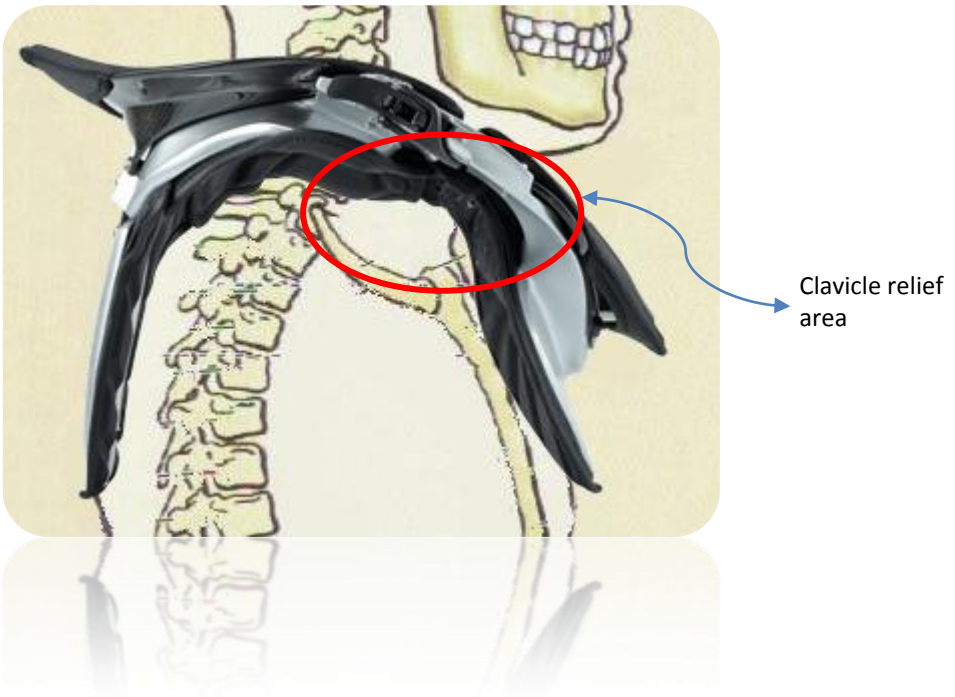

Figure 3-5: Clavicle relief area

3.8 Thoracic Strut Design

The thoracic member and strut of the Moto GPX were designed to prevent the upper platform of the Moto GPX from rotating when helmet strike forces are present, and to prevent the brace from rotating around the thorax. The carbon fiber strut was engineered with specific tolerances to ensure failure during extreme helmet impact events. The strut is designed to break at relatively low loads compared to high forces needed to fracture a thoracic vertebra.

The thoracic member allows for easy brace fitment (self-locating), and allows for the transmission of hyper-extension and hyper-translation forces from one spinal segment to approximately eleven segments. It was designed to be completely safe, even in the event of a direct fall onto the back while using the device. The energy is applied to the muscles that run on either side of the spine, especially since the thoracic strut is enclosed in padding. An in-depth discussion of the strut design is presented in Section 4.4.

3.9 Zip Relief Area

The lower front part of the Moto GPX was designed with a zip relief area. This groove allows comfort when the device is worn with jackets, etc. with a zip running down the front by bridging this area. The relief "groove" also ensures that the zip does not penetrate the sternal area during a hard helmet impact with the brace, by ensuring that the force is transmitted to the areas adjacent to the zip.

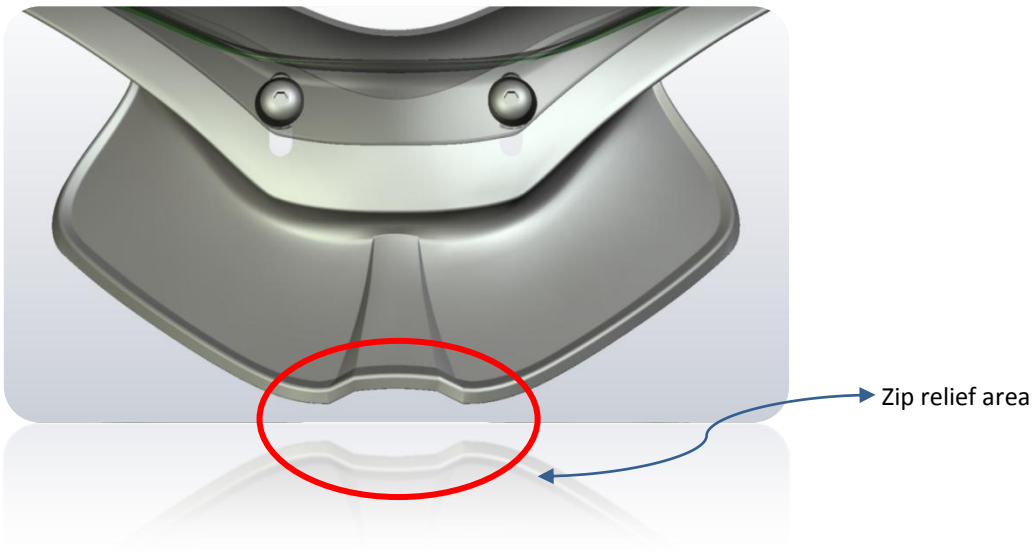

Figure 3-6: Zip relief area

Chapter 4

Testing and Simulation of the Leatt-Brace® Moto GPX® Neck Brace

4.1 Pendulum Tests

4.1.1 Introduction

As explained elsewhere, pendulum tests on Moto GPX prototypes were first conducted at BMW's test facilities in Munich, Germany. *See,* Neck Brace System: An Insight Into Research Activities, Geisinger, et al., 6th International Safety-Environment-Future Conference, October 2006, Cologne, Germany. The results obtained with these tests correlated well with, and were used to validate, a LifeMOD™ computer simulation model also using a 50th percentile H-III ATD. The joints at which the forces and motions were measured were located at the same positions on the actual dummy as in the model (Figure 4-1). Correlating the modeling data with the physical tests helped validate the model for use in future simulations and design iterations.

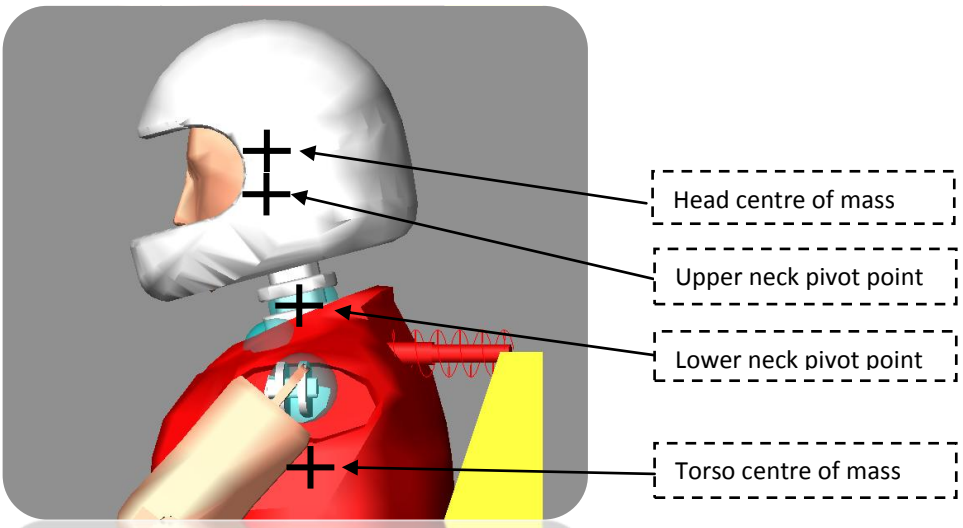

Figure 4-1: Dummy joint positioning

4.1.2 Model Setup

The model was set up to represent exactly the test setup (Figure 4-2). A fixed 72 kg steel block was used as the impact body for the swinging dummy torso, striking on the helmet head, to produce hyper-flexion, hyper-extension, and lateral hyper-flexion. Swinging the dummy from a constant height using fixed rotational joint constituted a very repeatable test setup.

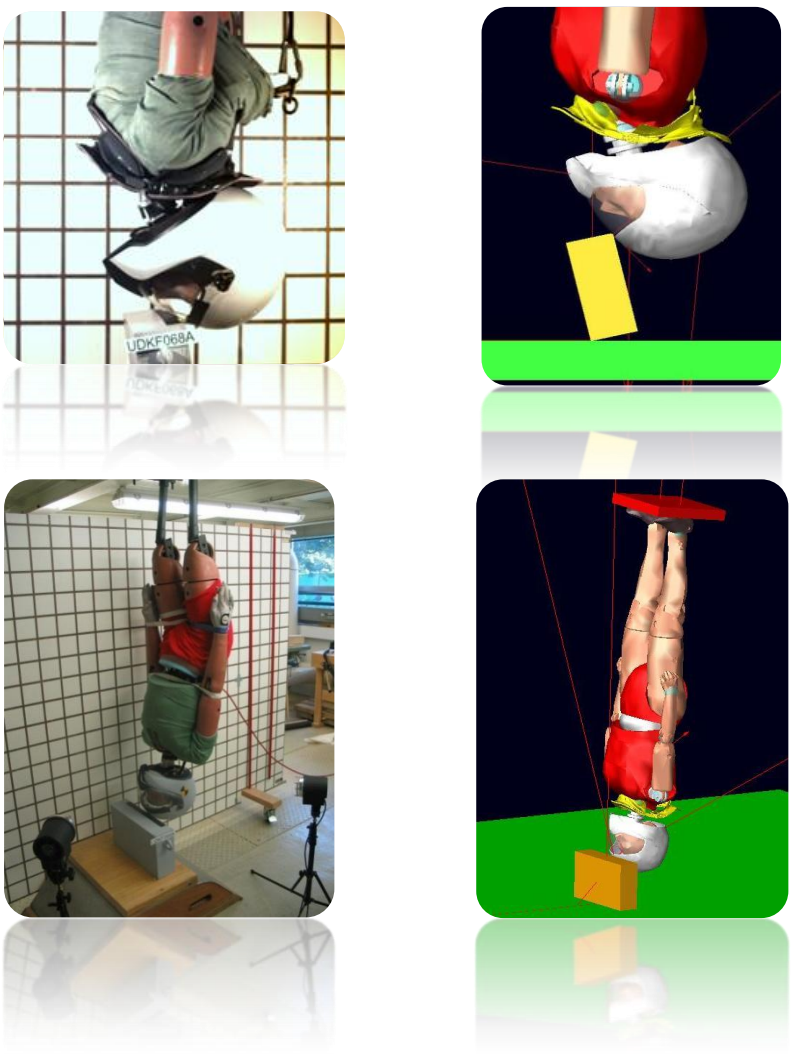

Figure 4-2: Pendulum test and simulation setup

4.1.3 Limitations and Challenges of the Model

A challenge and possible limitation of this specific simulation was ensuring the correct combinations of material and contact properties (helmet/block; helmet/device; block/floor), taking into account variables such as friction coefficients, contact stiffnesses and contact damping. Although all of these values are inputted automatically in LifeMOD™ following the specification of the material, the

authors felt that some of the model's reactions were not realistic or correlated significantly enough with those of the physical test. Since these values are also not well documented in the literature, because of the multitude of different materials interacting with one another, acceptable values were determined iteratively by comparing physical test footage and data and comparing the end-points and test results of physical and surrogate tests. Another challenge was the reaction properties between the helmet and the head and the device and the torso. These properties were determined through many iterations by studying the inter-reactions of the helmet and the device from the physical test footage, and modeled through the use of bushings providing six degrees of inputs (*x* direction, *y* direction, *z* direction and rotation around all these axes) for stiffness and damping.

The values ultimately used are summarized in Table 4-1 and Table 4-2 below:

TABLE 4-1: PENDULUM SIMULATION CONTACT PARAMETERS

	IMPACT FORCE PARAMETERS				COULOMB FRICTION PARAMETERS			
	STIFFNESS [N/MM]	DAMPING [N-SEC/MM]	EXPONENT	DMAX [MM]	MU STATIC	MU DYNAMIC	STICTION TRANSITION VELOCITY [MM/SEC]	FRICTION TRANSITION VELOCITY [MM/SEC]
GPX - Helmet	50	150	2.2	0.1	0.3	0.1	100	1000
Helmet - Chest	1.00E+05	10	2.2	0.1	0.3	0.1	100	1000
Helmet - BMW Block	100	150	2.2	0.1	0.3	0.1	100	1000
Helmet - Floor	1.00E+05	20	2.2	0.1	0.3	0.1	100	1000
BMW Block - Floor	1000	10	2.2	0.1	0.3	0.1	100	1000

TABLE 4-2: PENDULUM SIMULATION BUSHING PARAMETERS

BUSHING PARAMETERS

	STIFFNESS [N/MM]	DAMPING [N-SEC/MM]	TSTIFFNESS [N-MM/DEG]	TDAMPING [N-MM-SEC/DEG]
GPX - Torso	1e4, 1e4, 1e4	1e5, 1e5, 1e5	1e7,1e7,1e7	1e8,1e8,1e8
Helmet - Head	2e3,2e3,2e3	20,20,20	2e3,2e3,2e2	20,20,10

One of the challenges of modeling impacts in LifeMOD™ is the unrealistic contact "spike" observed in the results. This "spike" constitutes a discontinuity in the calculation of the applicable parameter. Methods to partially alleviate this effect include increasing the time steps (sampling rate), decreasing the calculation error or "Hmax" (iteration error), or increasing the force exponent parameter above the value of 1.0. Although these techniques proved helpful, this did not solve the problem in its entirety. The results should be interpreted by the eye as a smooth "interpolated" polynomial, in effect ignoring the "spike". Very low frequency filters could be used to remove this spike, but may subsequently alter the validity of the results.

4.1.4 Pre-validation of the Model Using the Physical Test Results

By obtaining results in the same order of magnitude as those of the physical tests, the model could be pre-validated ahead of further simulations being done using the same model.

4.1.5 Results

Selected pendulum test results provided by BMW are presented, followed by the result of the accompanying LifeMOD™ simulation for each parameter at the C7/T1 dummy joint or IV disc (Figure 4-3 through Figure 4-7). The bending moments, axial forces and Nij were compared. The simulation results were filtered using a digital Butterworth low-pass filter at 600 Hz. The physical test results were filtered using a CFC Class 1000 filter (600 Hz Low-Pass). Validation of the model allowed

simulations utilizing rear and side impacts in addition to frontal impacts, with high confidence in the results.

The results of these tests validated the behavior of the H-III 50th percentile ATD used in the simulation software. It is worthwhile noting that, whilst the device was being used, the Nij was reduced from a baseline value of 0.3 to approximately 0.1, a 67% reduction, as indicated in Figure 4-7. Subsequent simulations with differing setups could therefore be run and produce realistic results in terms of spinal forces and moments. More physical tests were simulated with LifeMOD™ using the SFI 38.1 test protocol described in Section 4.2.

Bending Moments

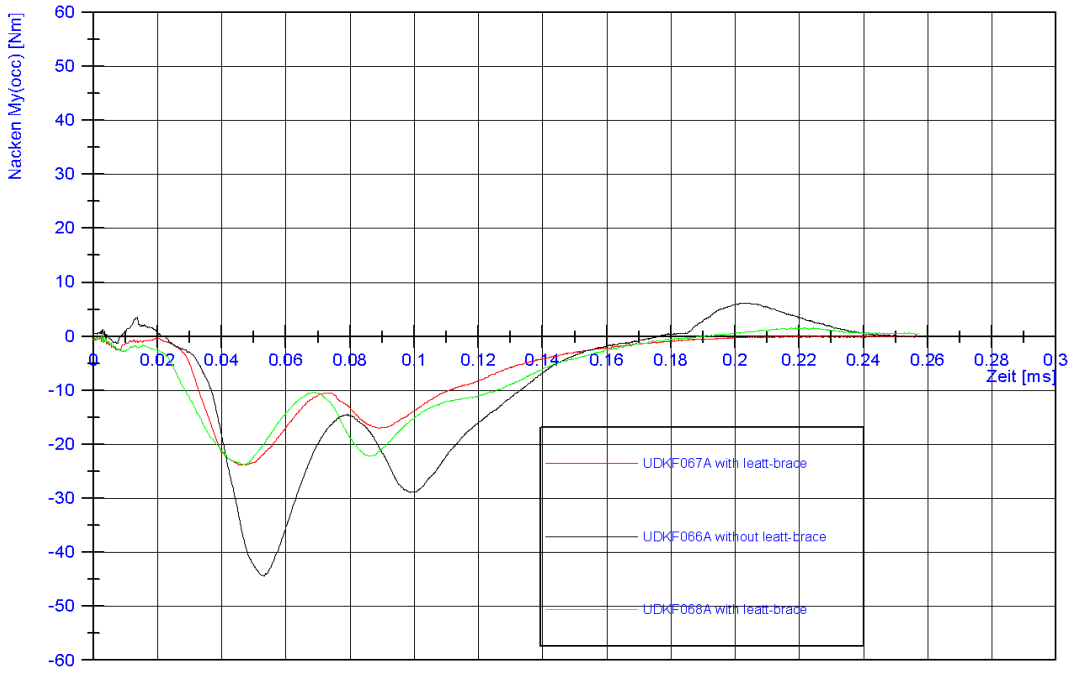

Figure 4-3: Upper neck bending moment obtained from pendulum testing at BMW

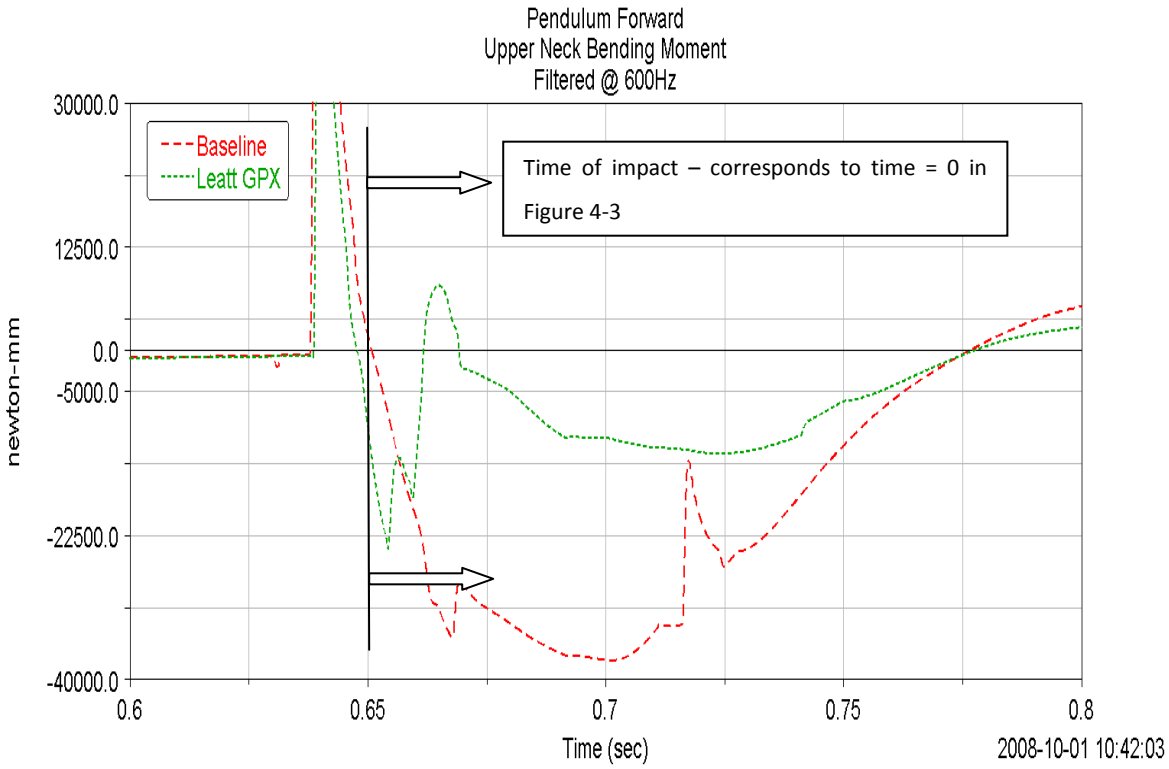

Figure 4-4: Comparable bending moment obtained from LifeMOD™ model

Axial Forces

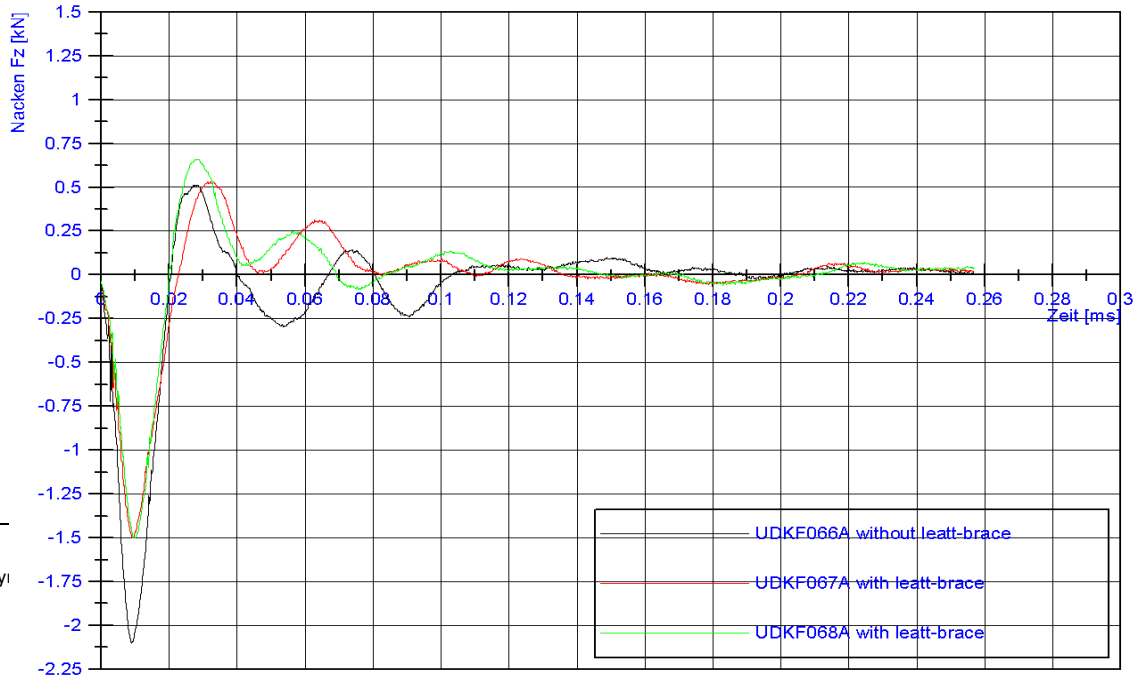

Figure 4-5: Upper neck axial force obtained from pendulum testing at BMW

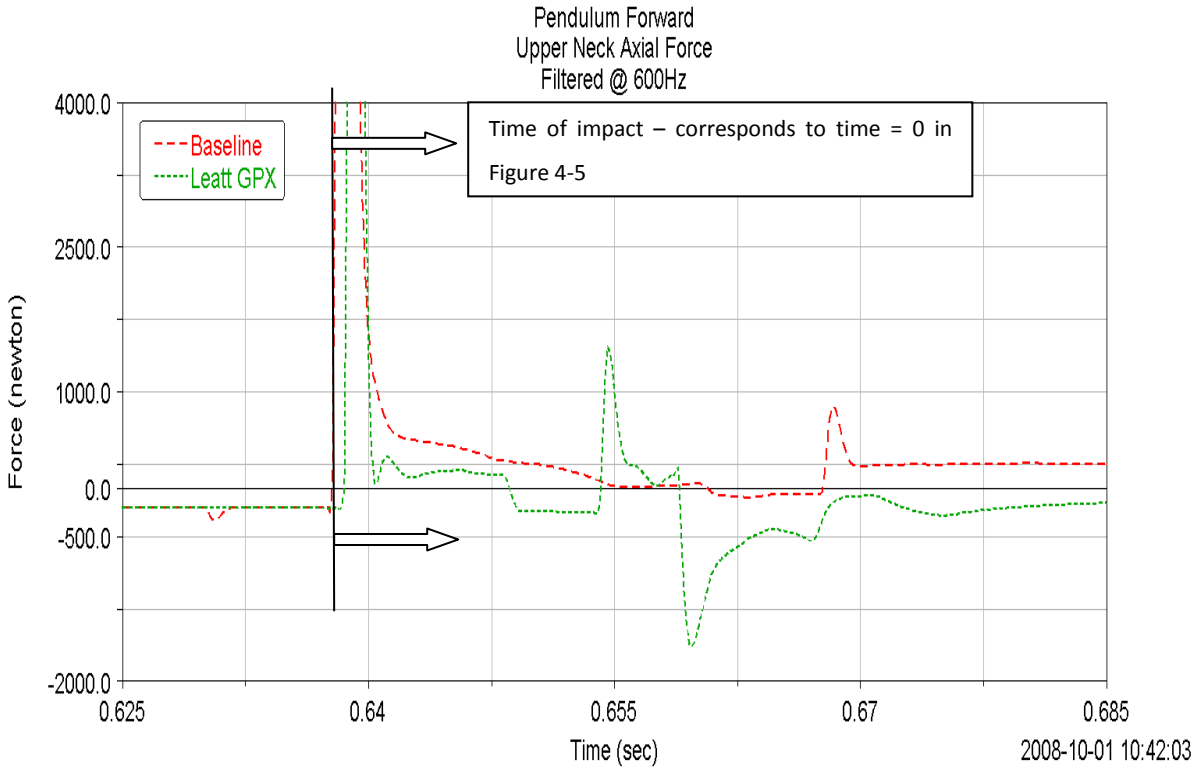

Figure 4-6: Comparable upper neck axial force obtained from LifeMOD™ model

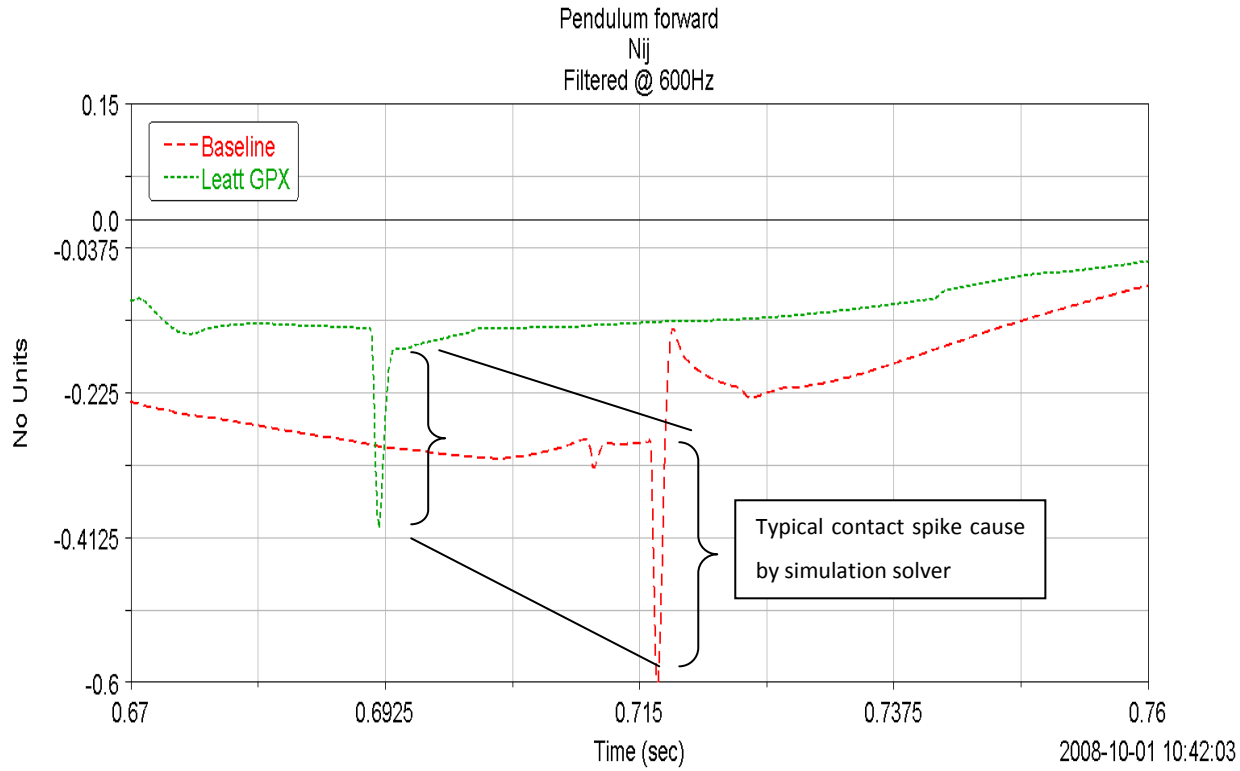

Figure 4-7: Nij subsequent to bending moment, axial force and shear force in LifeMOD™ model

4.2 SFI 38.1 Restrained Torso Frontal Sled Test Used for Further Validation of the Model

4.2.1 Introduction

Testing conducted on a prototype motor vehicle brace (Leatt-Brace® Moto R) was used to further validate the efficiency of the computer simulation model. A 50th percentile male H-III ATD was used in sled testing conducted with Delphi Test Center's frontal sled in Vandalia, Ohio. This was done for 70 G 0° and 30° frontal impacts with and without the neck brace, as well as for impacts at 30 G and 40 G. To illustrate the validation process, the results for the 70 G 0° frontal impact are shown. The results obtained were within the same ranges as those for the sled tests, thereby

adding greater confidence in the computer simulations employed with the Moto-GPX motorcycle brace.

4.2.2 Model Setup

The computer model set up mimicked the SFI 38.1 protocol (Figure 4-8). The dimensions of the buck (car and seat) were adopted from the SFI specification sheet, and a Parasolid (file format) CAD drawing was made and imported into the model. Seatbelt positions and the positioning of the device on the dummy were also set up to mimic those in the test conditions.

4.2.2.1 Limitations and Challenges of the Model

As was the case with computer modeling of the pendulum test, the challenge was to find the correct physical properties. Contact between the dummy and the buck and the physical properties of the seatbelt needed to be added, in addition to the standard properties already determined in the preceding simulation. Seeing that LifeMOD™ automatically inputs the former, only the latter needed to be determined. To achieve this, the high-speed camera footage of the physical tests was used to ensure the seatbelt stiffness and damping reacted in the same manner for the same impulse input. No limitations other than the expected calculation time limitations were observed. All the parameters present in the actual H-III ATD were used in the simulation model setup.

4.2.3 Validation of the Model

By obtaining results in the same order of magnitude as those of the physical SFI 38.1 tests, the computer model could be further validated.

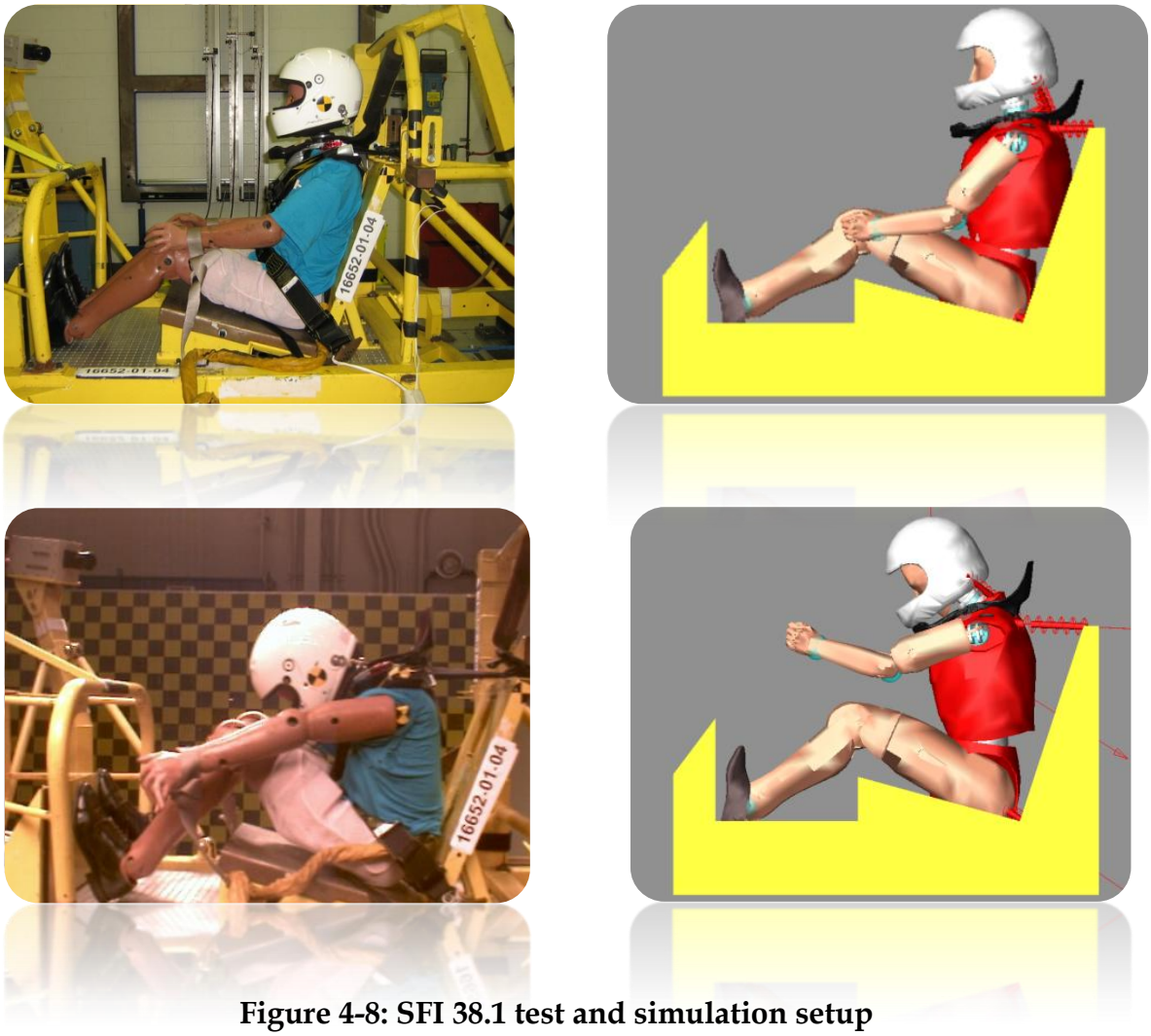

Figure 4-8: SFI 38.1 test and simulation setup

4.2.4 Results

The physical test results provided by the Delphi Test Centre (Vandalia, Ohio) are presented followed by the result of the accompanying simulation for each parameter at the C7/T1 dummy joint or IV disc (Figure 4-9 and Figure 4-10). The bending moments and Nij also were compared. The simulation results were filtered using an analogue Butterworth low-pass filter at 600 Hz.

Baseline results showed less correlation than results generated with the brace in place (110 Nm maximum flexion for the simulation compared to 75 Nm maximum

flexion for the test). This could be attributed to artifactual (uncontrollable) ATD behavior, which is typical during rebound of the ATD in frontal impact sled tests. The device results, however, showed good correlation in flexion (68 Nm maximum flexion for the simulation compared to 78 Nm maximum flexion for the test). Nij values correlated very well (0.6 and 0.63 for the device simulation and test respectively and 1.12 and 1.1 for the baseline simulation and test respectively). The close correlation in this parameter showed overall good correlation in the model, since more than one spinal parameter is evaluated simultaneously in the Nij.

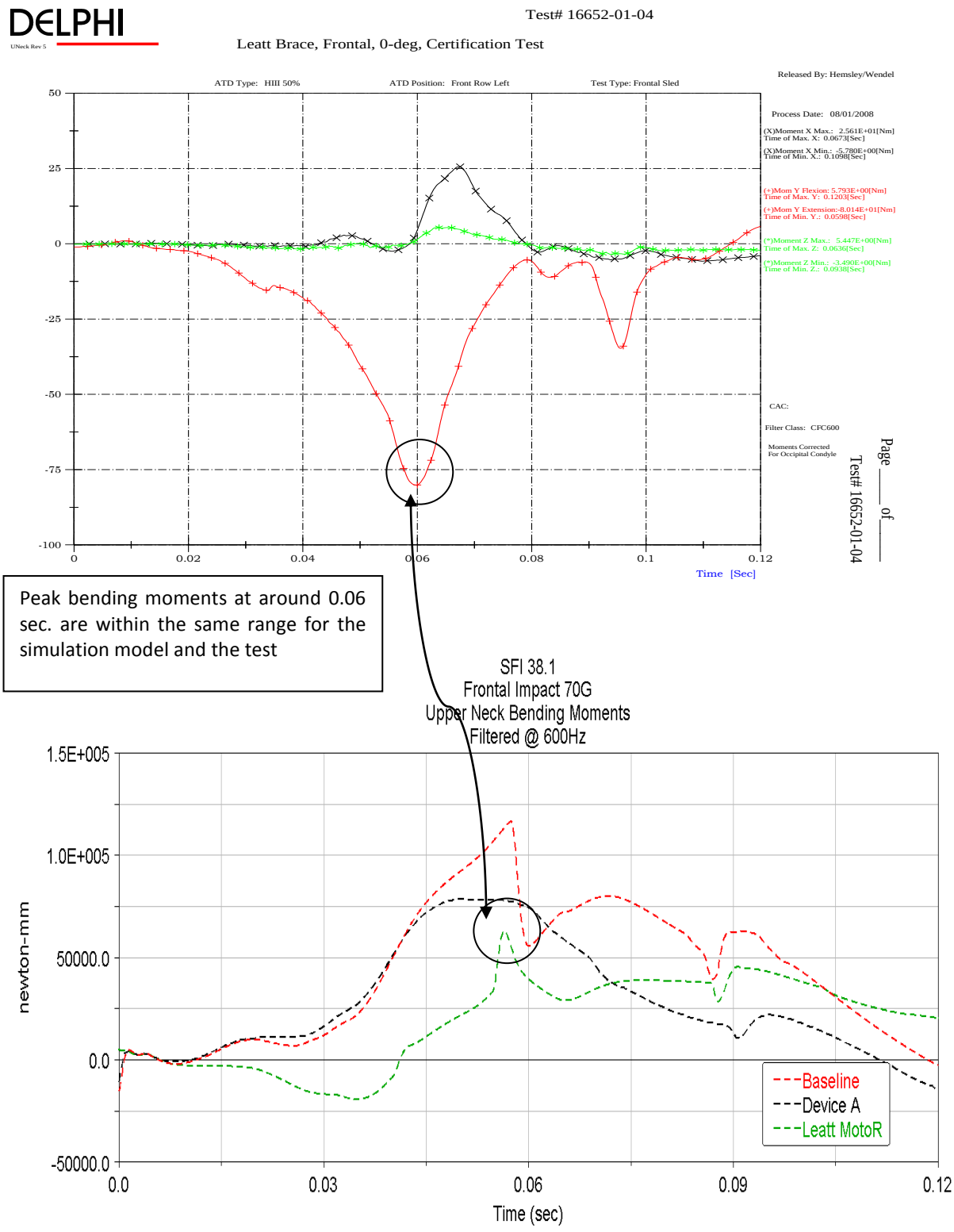

Figure 4-9: Upper neck bending moments obtained through testing and simulation

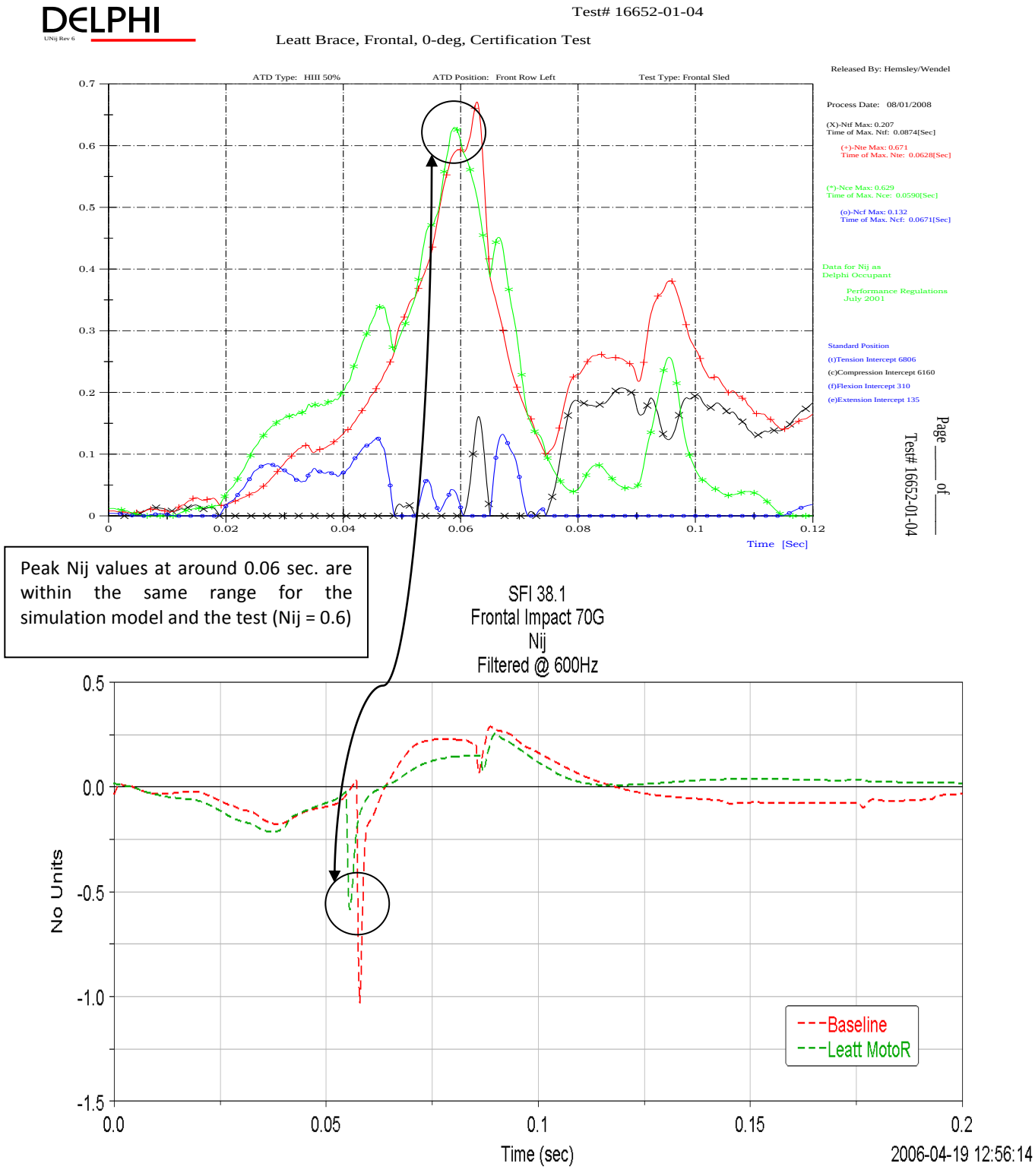

Figure 4-10: Nij obtained through testing and simulation

4.3 Investigation of the James Marshall Crash and Brain Injury Modalities during Whiplash-like Crashes

4.3.1 Introduction

Beyond correlating pendulum test data with computer modeling data, the authors sought to use computer simulation to assess known, real-world events. This cross-check of modeling reliability also offered an opportunity to assess forces and vectors known to produce serious injury in a real crash. Scenarios with and without a brace could be explored. For this simulation, the authors selected the severe crash of Mr. James Marshall

On February 11th, 2006, James Marshall was tragically injured in round 6 of the Amp'd Mobile SuperCross series in San Diego. Running in 5th place in Heat #2, James went over the bars during a tricky step-up, step-down combination. He landed head first in what is generally called a "lawn dart" impact. James sustained a Jefferson fracture (four-part first vertebra fracture), as well as a C5/C6 hyper-extension injury, and broke his pelvis. James was paralyzed instantly and is now a C5 quadriplegic.

Simulations were performed after careful investigation of the crash footage (Figure 4-11). Anthropomorphic sizing and the terrain were also taken into account, and brain dynamics were also considered (Figure 4-12). Since not much data could be found on the modeling of brain dynamics, the authors attempted to model an "apples with apples" comparative scenario. In examining the relative dynamics of the brain and the skull, for one scenario incorporating the Moto GPX and another one without, a good understanding of the absorption properties was needed to achieve the correct acceleration vs. time of the head (as discussed in Section 2.3.5).

4.3.2 Model Setup

The model was set up using the same dummy and contact parameters as in the aforementioned simulations. The computer-simulated dummy was launched head first into a whoops section (a section of track with a row of dirt mounds or moguls) from a motorcycle travelling at 60 km/h. Video analysis and an accident report of the crash were carefully analyzed to ensure confidence in the simulation setup. The subsequent compression and hyper-extension of the cervical spine and head were analyzed to determine the forces and moments present, and whether the Moto GPX would have changed these forces or moments.

The brain dynamics model was set up utilizing rotational stiffnesses to allow for realistic motion (coup/contrecoup effects) within the skull. No applicable stiffness values could be found in the literature, and therefore an "apples with apples" comparison scenario was proposed by the authors, in terms of which simulations with and without the device would be compared. The chosen rotational point of the brain was around the intersection of the brainstem and the cerebellum (Figure 4-13). The mass of an average adult brain was used (1.40 kg). The same ground, helmet, head, brace and chest contact parameters were used as in the previously discussed simulations.

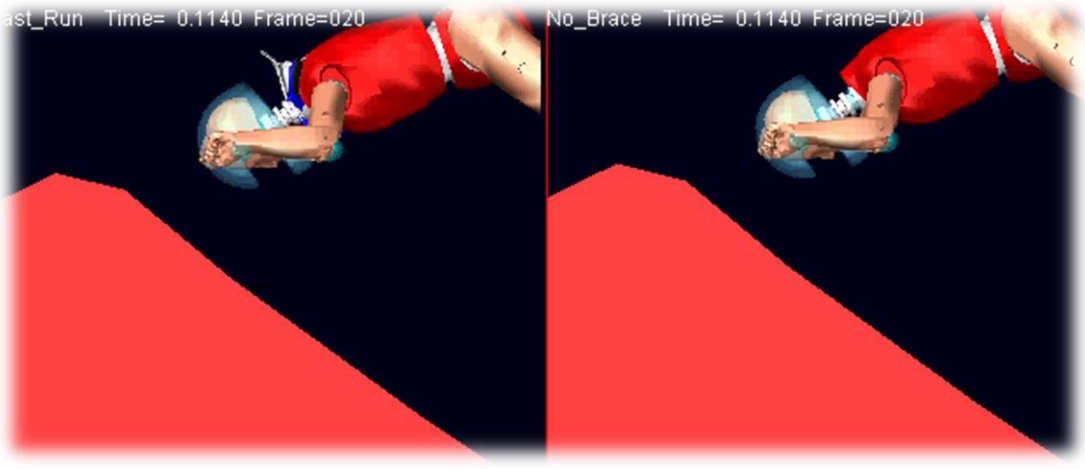

Figure 4-11: James Marshall crash analysis through LifeMOD™ simulation.

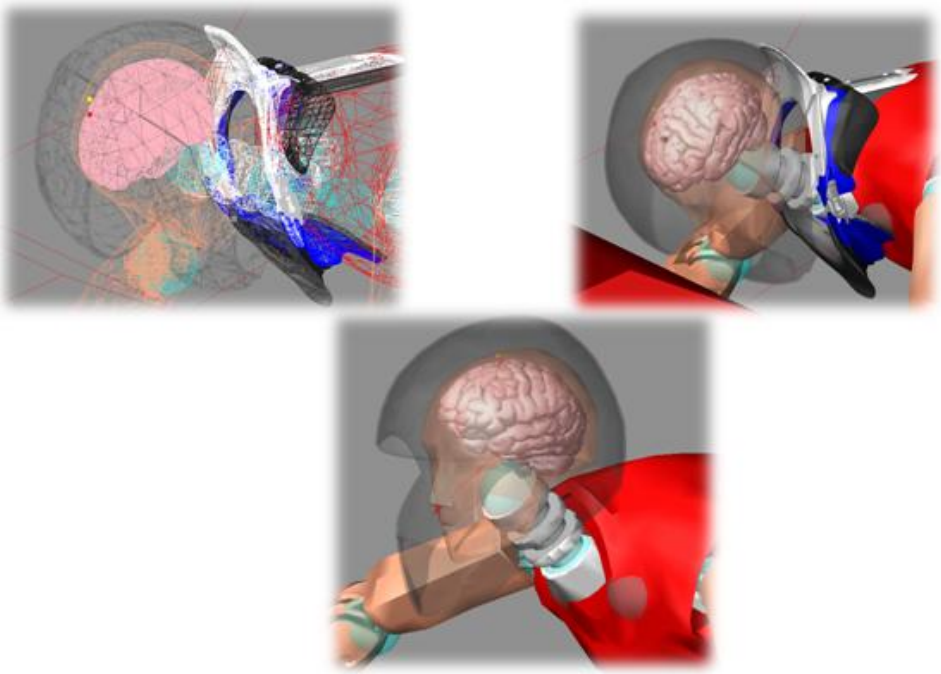

Figure 4-12: Investigation of brain dynamics

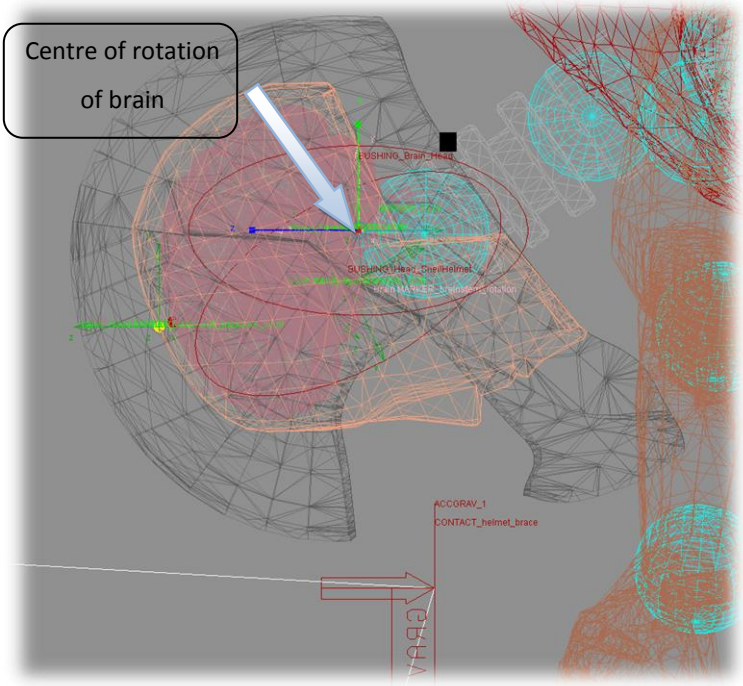

Figure 4-13: Location of rotation point for brain

4.3.3 Limitations and Challenges of the Model

The only challenge was in relation to modeling the reaction of the helmet as it made contact with the ground (contact stiffness parameters). Close examination of the crash footage gave clearer insight into the reaction modality of the helmet to the ground, and parameters were chosen to represent this in the simulation model.

4.3.4 Validation of the Model

Seeing that the model had previously been validated through comparison with two physical test methods, the results of our modeling and the subsequent conclusions drawn from the results can be presented with reasonable engineering certainty.

4.3.5 Results

The simulations showed that using the Leatt GPX would have resulted in a reduction of ± 85% in the upper neck bending moment (in extension) when compared to that obtained without the device (Figure 4-15). Significant reduction also was also observed in upper neck tension, as well as in head and brain accelerations and velocities (Table 4-3).
Figure 4-14 provides a visual demonstration of the reduction in allowable rotation in extension.

In addition to these simulations, the relative components of brain velocity and acceleration were investigated and are presented in the form of linearized accelerations (tangential to the outside radius line of the brain as viewed laterally)and rotational accelerations and velocities for a crash scenario with and without the device (Figure 4-16 through Figure 4-19). The Leatt GPX decreased these relative brain dynamic components. From the point of maximum velocity during whiplash (between 0.39 sec and 0.40 sec in the figures) to the end of the crash, the Moto GPX significantly decreased dynamic brain parameters. The brain

accelerations (relative and absolute), as depicted in Figure 4-18 and Figure 4-19, were well below Kleiven's 0 proposed SDH injury limit of 4 500 rad/s^2 with the Moto GPX.

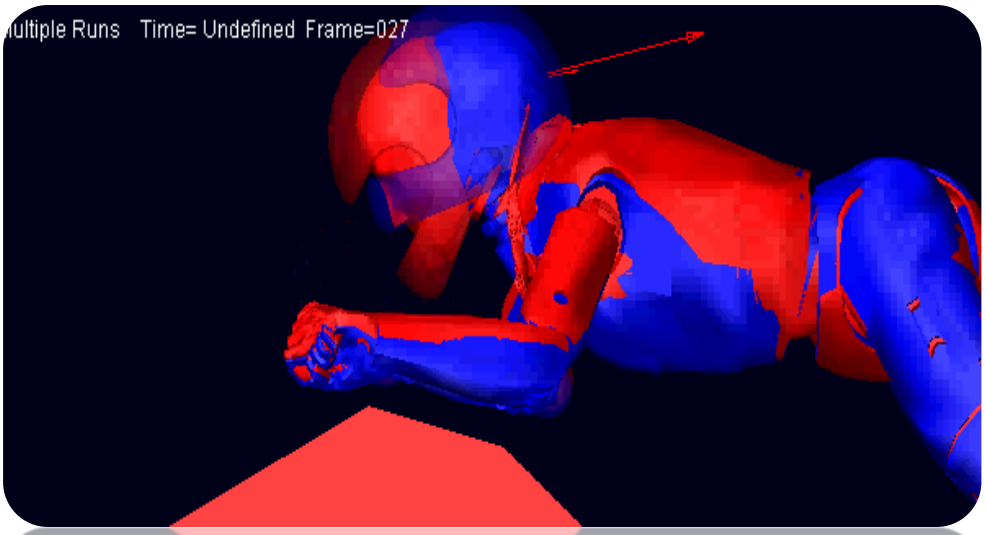

Figure 4-14: Visualization of limitation in allowable ROM with the device

TABLE 4-3: EFFECT OF LEATT MOTO GPX ON BRAIN DYNAMICS

IMPACT FORCE PARAMETERS			
	WITHOUT BRACE	WITH BRACE	REDUCTION PERCENTAGE (AREA UNDER CURVE)
Peak Upper Neck Tension	850	400	*53%*
Peak Relative Rotational Acceleration	1000	250	*75%*
Peak Relative Tangential Acceleration	2.6E06	0.2E06	*92.3%*
Peak Relative Rotational Velocity	200	45	*77.5%*
Displacement	2.9	2.75	*5.2%*

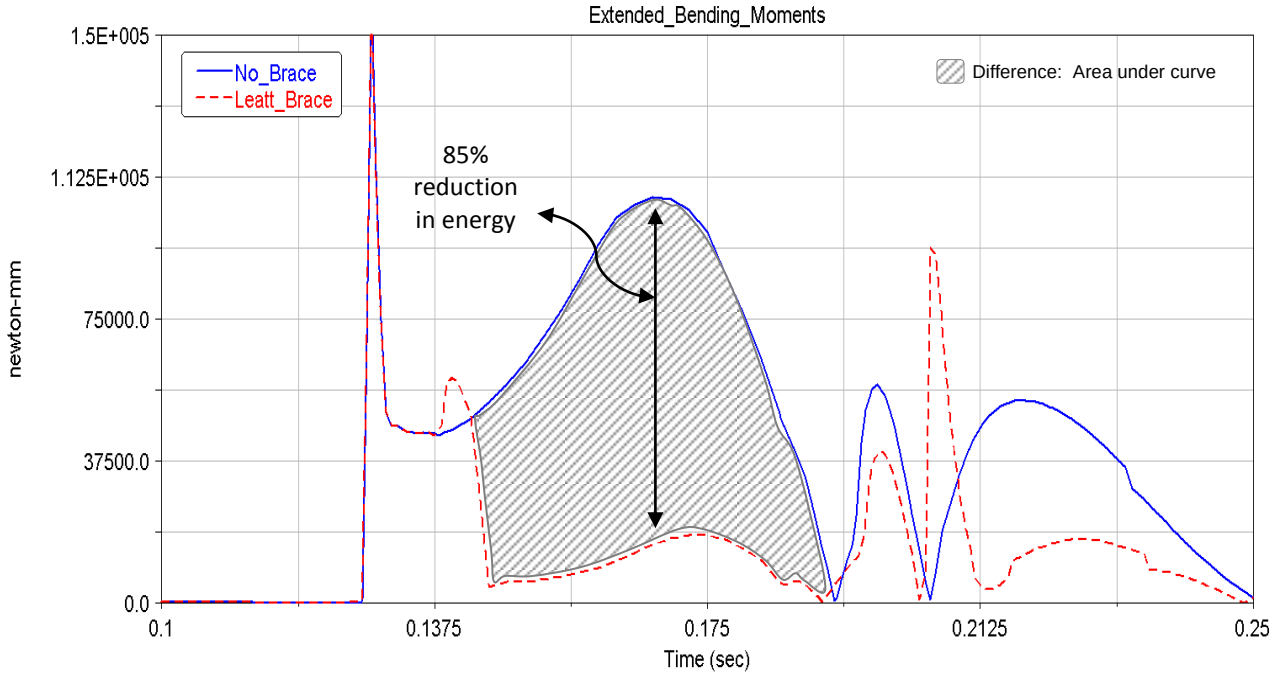

Figure 4-15: Bending moment in extension with and without the device

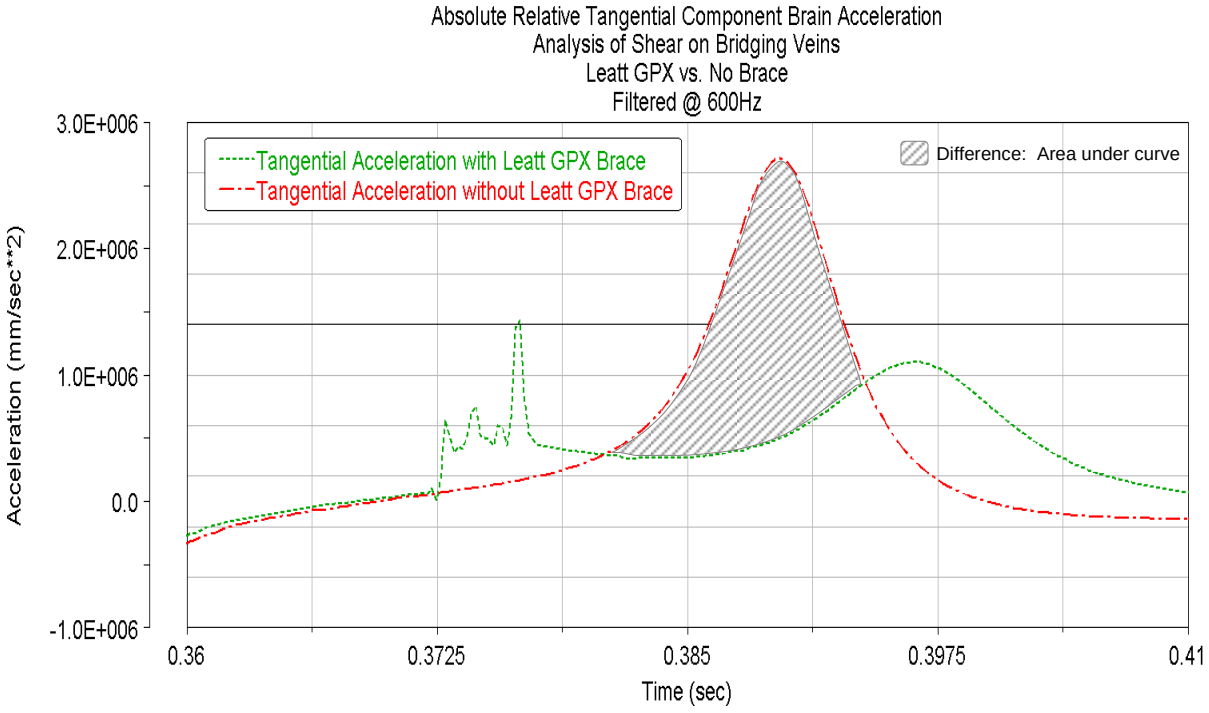

Figure 4-16: Tangential relative brain acceleration

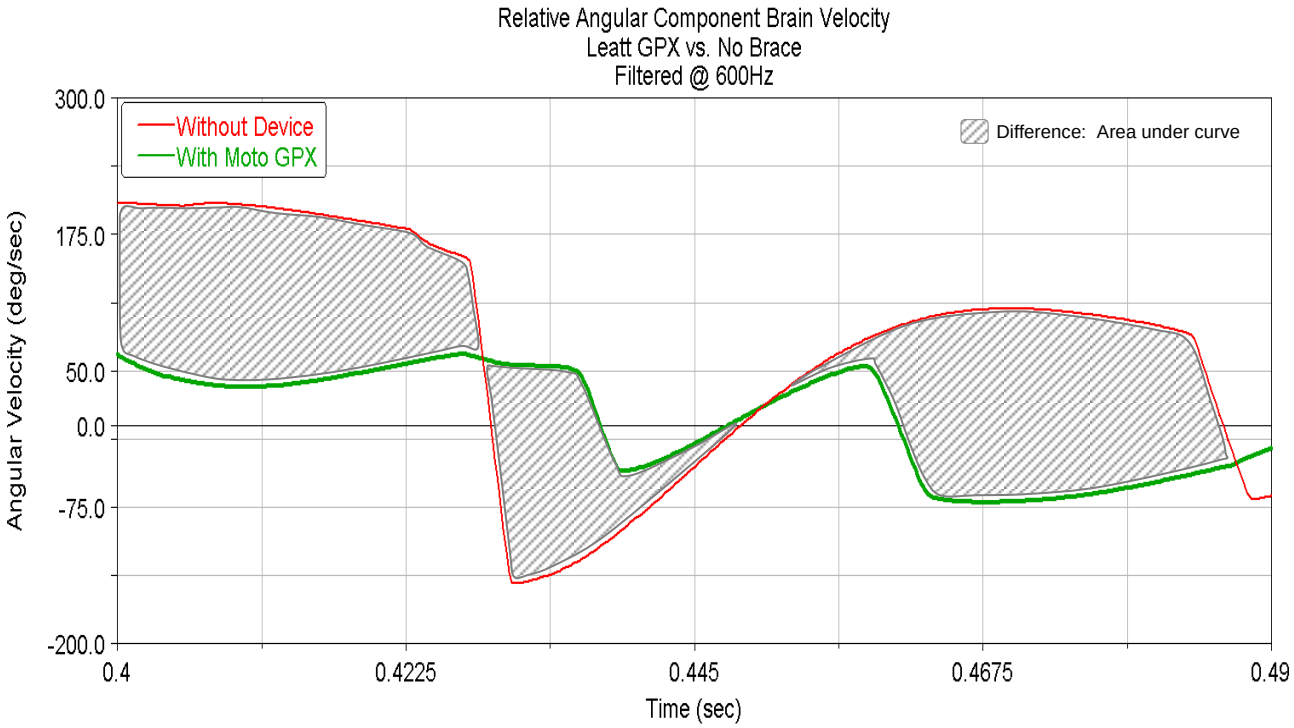

Figure 4-17: Relative angular brain velocity

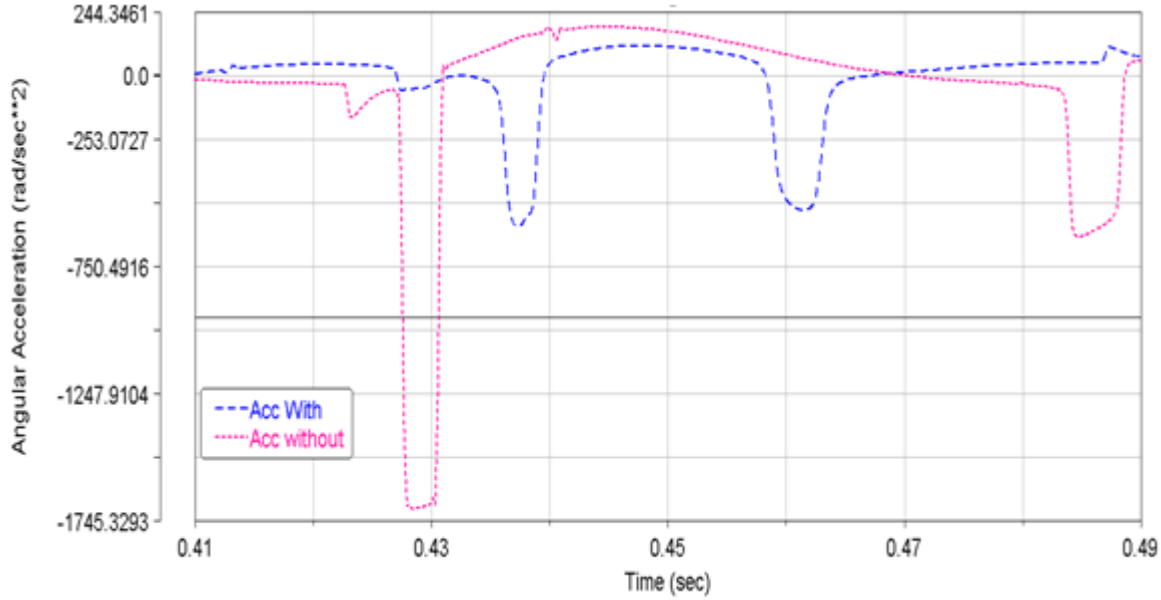

Figure 4-18: Relative angular brain acceleration

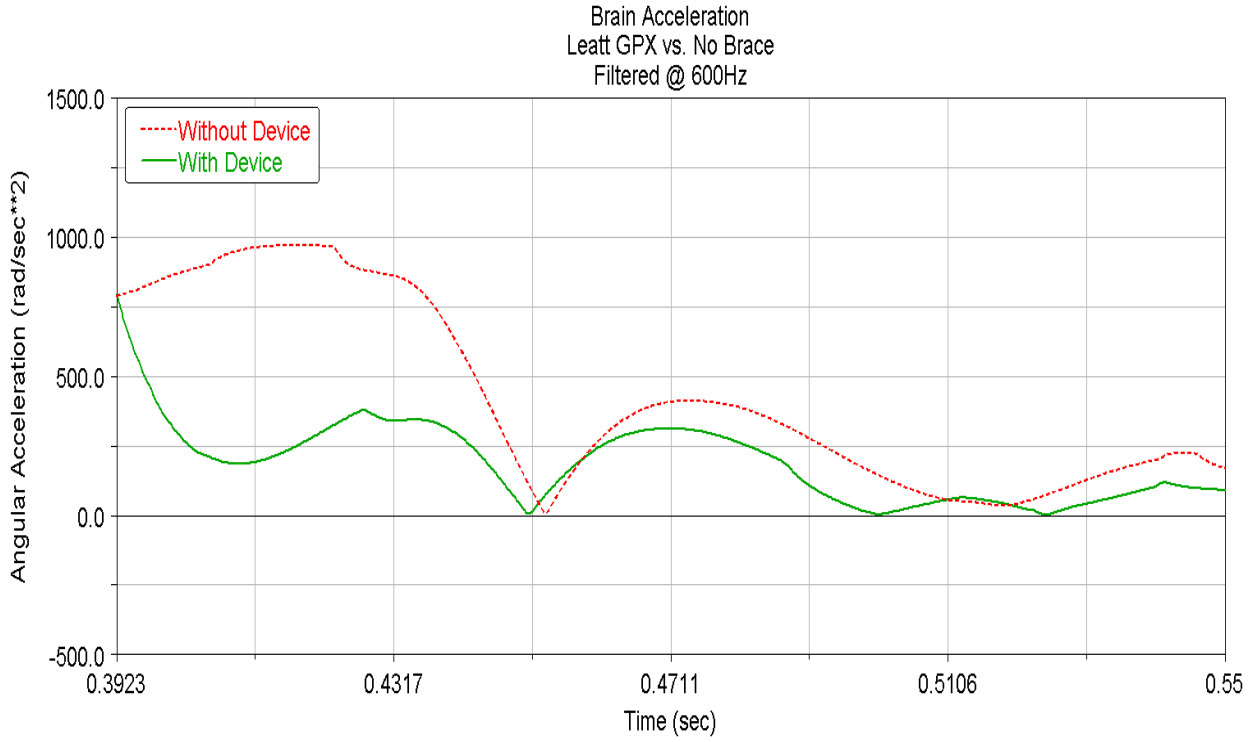

Figure 4-19: Absolute brain acceleration

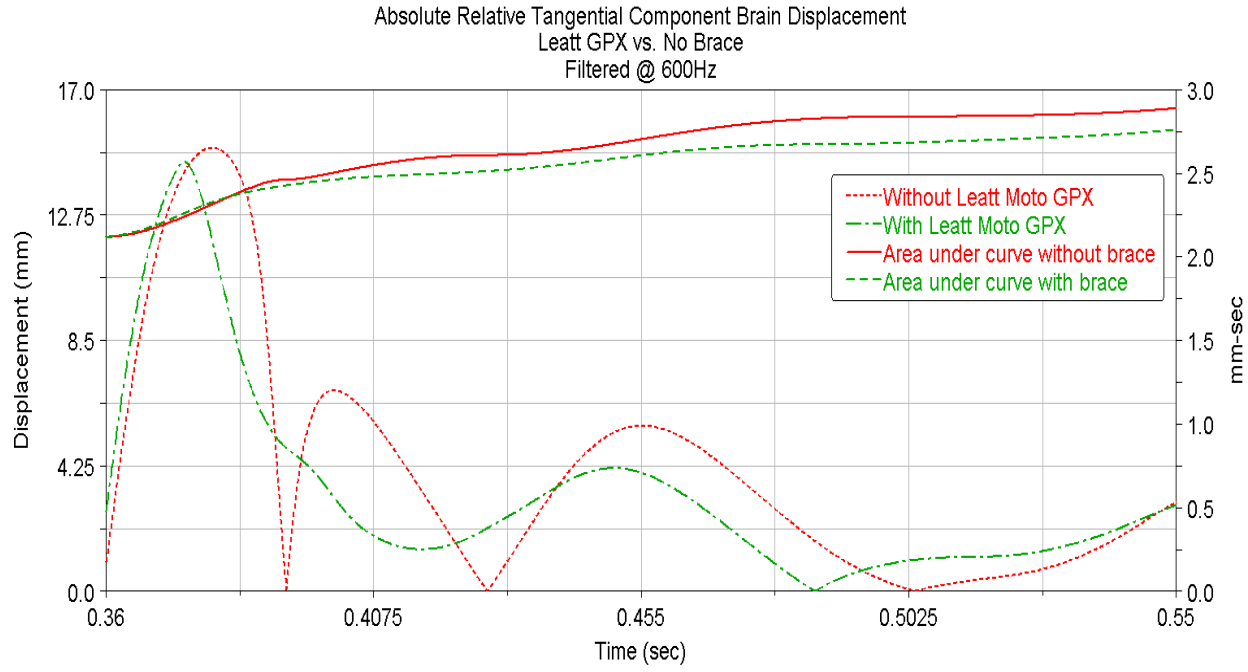

Figure 4-20: Absolute relative brain displacement

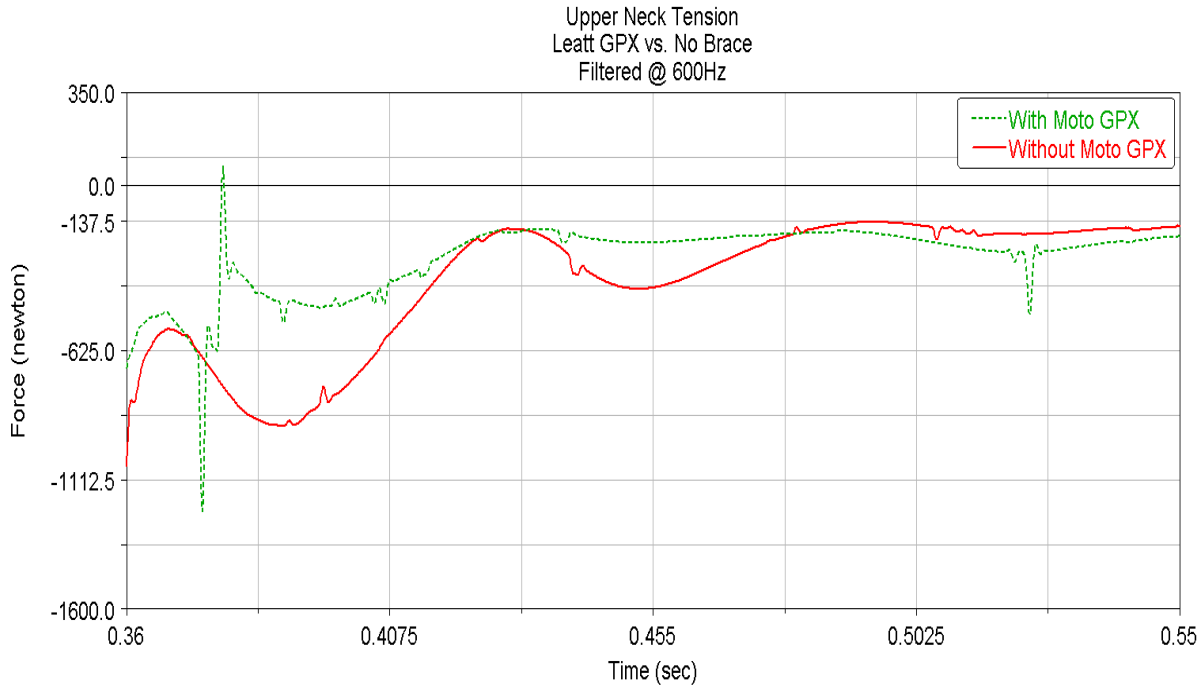

Figure 4-21: Upper neck tension

Upper neck tension was reduced over the majority of the impact time, as can be seen from Figure 4-21.

4.4 Thoracic Injury Assessment using Simulation and Quasi-static Testing with the Leatt-Moto® GPX Neck Brace

4.4.1 Introduction

The ROM of the thoracic spine is significantly lower than that of the cervical and lumbar spine, meaning the thoracic spine is also stiffer. The reasons are explained by the facets connecting the tubercle of the ribs and the demifacets connecting the heads of the ribs, as well as the normal transverse and spinous process constraints. Averaged and linearized initial static stiffness of the thoracic IV discs in pure extension of its two adjacent vertebrae have been reported by Markolf to be 3.8 Nm/deg [30], and by Panjabi *et al.* [31] to be 3.3 Nm/deg. However, as the load on the thoracic spine is increased, as is the case in a crash impact scenario, the IV disc

rotational stiffness increases. Each thoracic IV level thus has more than one stiffness function, depending on the magnitude and coupling of the loads applied to it. The thoracic functional spinal unit therefore can tolerate less extension under combined axial loading and thus will be more prone to hyper-extension injuries under such circumstances.

With the Leatt-Moto® GPX, the posterior helmet platform, in conjunction with the thoracic strut, reduces hyper-extension of the cervical spine. The energy transferred from the helmet onto the platform is transferred through the strut in terms of a bending moment applied onto the upper thoracic spine. In addition to reducing cervical hyper-extension, this bending moment, applied from the strut onto the spine, was hypothesized to prevent excessive force transfer to the mid-thoracic spine through absorption of thoracic energy by the strut because strut fracturing is designed to occur before injury occurs. With the brace, a combination of cervical and thoracic hyper-extension causes a "counter-weighted" combined energy absorption into an almost "arched" C- profile, extending from the back of the helmet to the upper thoracic spine and creates an efficient alternate load path.

In order to evaluate the efficacy of the thoracic strut in terms of mitigating impacts likely to otherwise cause spinal injuries, a detailed spinal model was developed.

4.4.2 Model Setup

First, a toleration band for the failure bending moment of the strut was determined within which the strut would safely bend and disperse hyper-extension energy before failure (Figure 4-22), without failing too early or too late in the absorption process. This was done by using the simulated (pendulum swing setup) device-helmet contact force range (Figure 4-23) during impact, producing the optimum reduction in Nij, and combining it with the appropriate thoracic and posterior platform dimensions of the device to determine the ideal bending moment for the

strut. The device-helmet contact force relates directly to the bending moment transferred through the strut to the thoracic spine. For the Leatt 10° strut, an ideal failure moment to prevent cervical hyper-extension (as is the purpose of the Moto GPX) was determined by this simulation to be between 20 Nm and 35 Nm. To verify that the actual strut failure occurs within this tolerance, physical tests (Figure 4-24) were conducted and the strut broke at an average bending moment of 29 Nm after three consecutive test runs, in the median region for the simulation prediction. Accordingly, the strut as designed and manufactured works to help protect the cervical spine from hyper-extension.

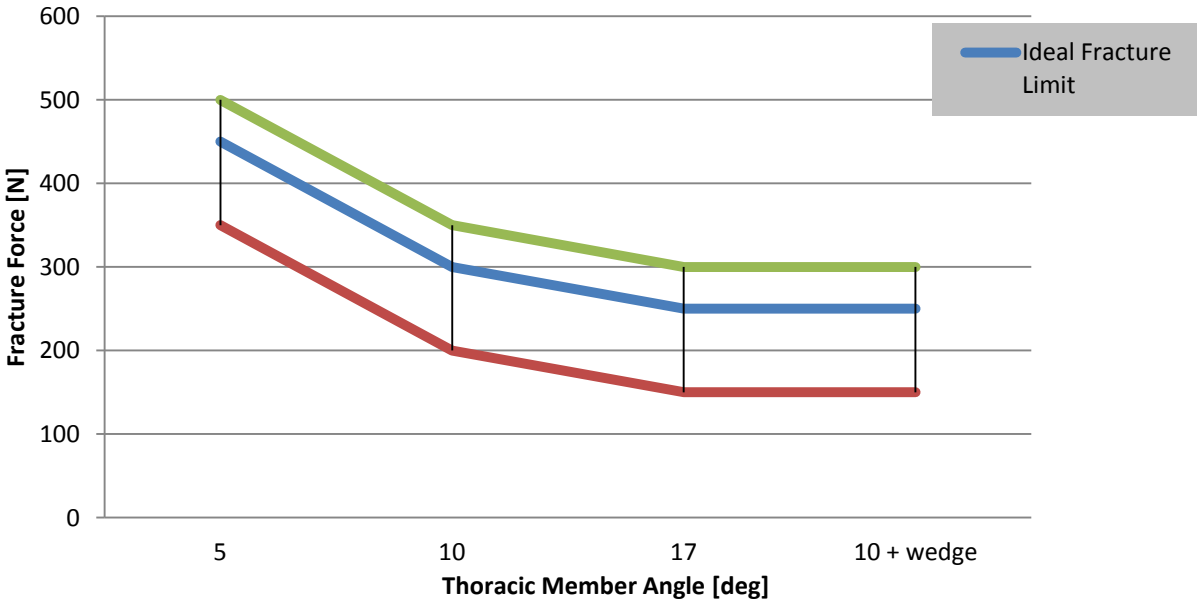

Figure 4-22: Tolerable range of bending moments on the thoracic strut

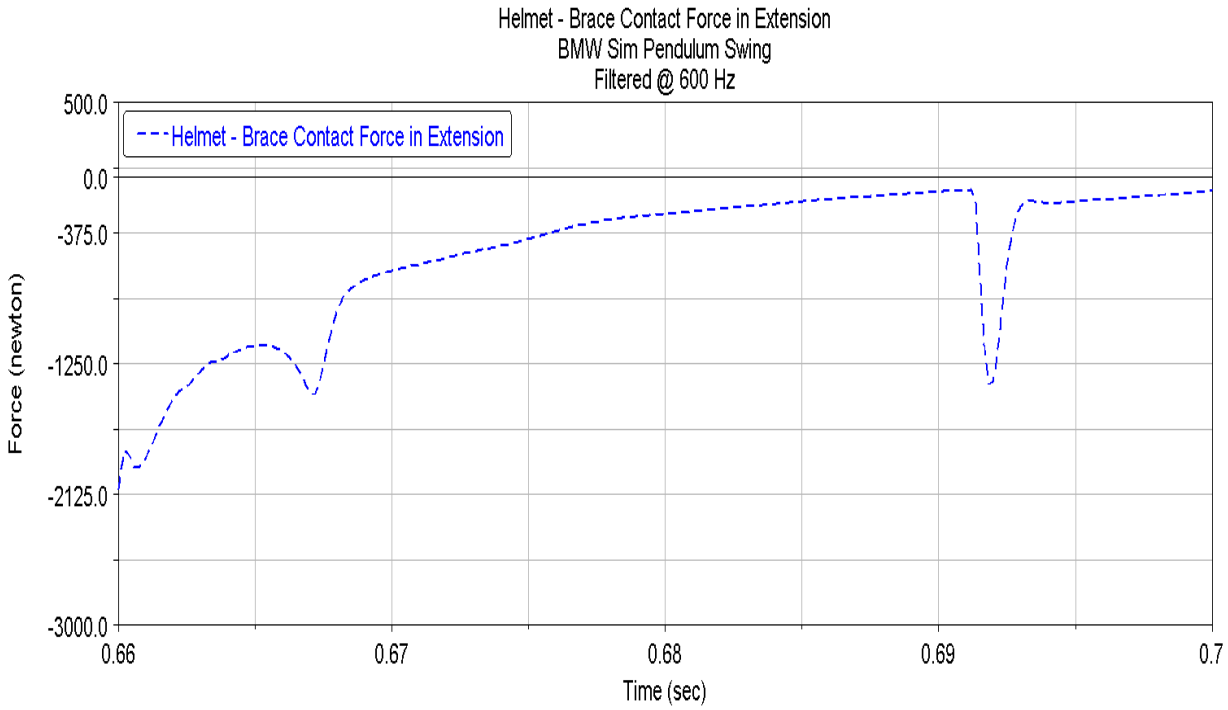

Figure 4-23: Applied force from the helmet to the device in extension

Figure 4-24: Test setup for thoracic strut bending moment

To assess the effect of the strut on the thoracic spine, a detailed spine model was developed. Non-linear IV disc stiffness functions derived from the literature were incorporated at each IV level [32], together with the absolute IV disc failure limits

determined by Yoganandan *et al.* [33]. The typical shape of one of these functions is presented in Figure 4-25. The values obtained were acquired from the physical testing of cadaveric IV disc specimens. In addition, ligament stiffness properties were incorporated into the model, as well as muscle reaction properties, which were created from an anthropomorphic database in LifeMOD™.

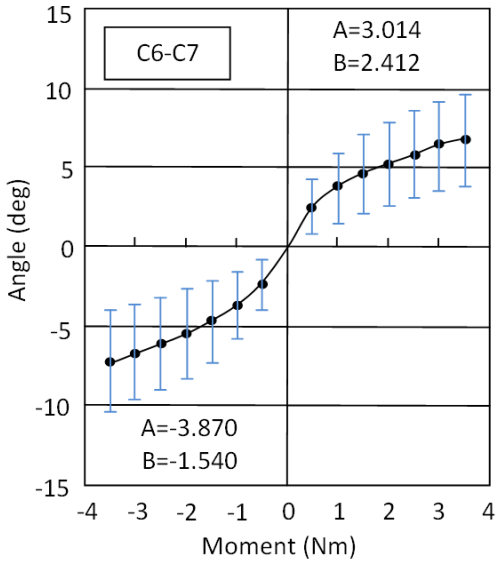

Figure 4-25: Typical IV disc stiffness function [32]

A basic overview of the model setup and properties used is provided below:

Musculature

LifeMOD™ contains a database of muscle tissue properties. These include the physiological cross-sectional area (pCSA) and the maximum allowable stress in each muscle. Each muscle contains a contractile element in series with a spring-damper element, storing the input motion and effectively "training" the muscles to reproduce the necessary force to recreate the desired motion.

Ligaments

Generation of the spinal ligaments was performed manually, since LifeMOD™ does not generate these soft tissues automatically. Yoganandan *et al.* [33] described the biomechanical properties of the relevant cervical ligament tissues, whilst Chazal *et al.* [34] described the ligament properties for cervical, thoracic and lumbar ligaments. The ligament stiffnesses were used as input. Smith *et al.* [35] diagrammed the ligament attachment points from cadaveric analysis (Figure 4-26). This anatomical data was verified by Van de Graaff [3]. The ligaments provide stabilizing forces to the functional spinal unit (FSU), especially when extensive head motions are performed.

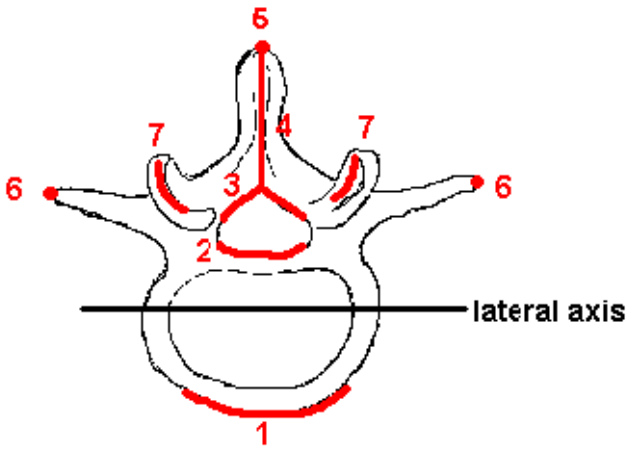

Figure 4-26: Ligament attachment points [35]

IV Disc Generation

The intervertebral disc dynamics are represented by standard, passive six degree-of-freedom bushing elements. Subsequent to extensive studies, rotational stiffness properties were adopted from the literature and assigned to the bushings [32], [33]. The joints were created to act on a line connecting the instantaneous axes of rotation (IAR) of the cervical functional spinal unit (FSU) (indicated in Figure 4-27). Concepts of the IAR are discussed in the literature [36], [37].

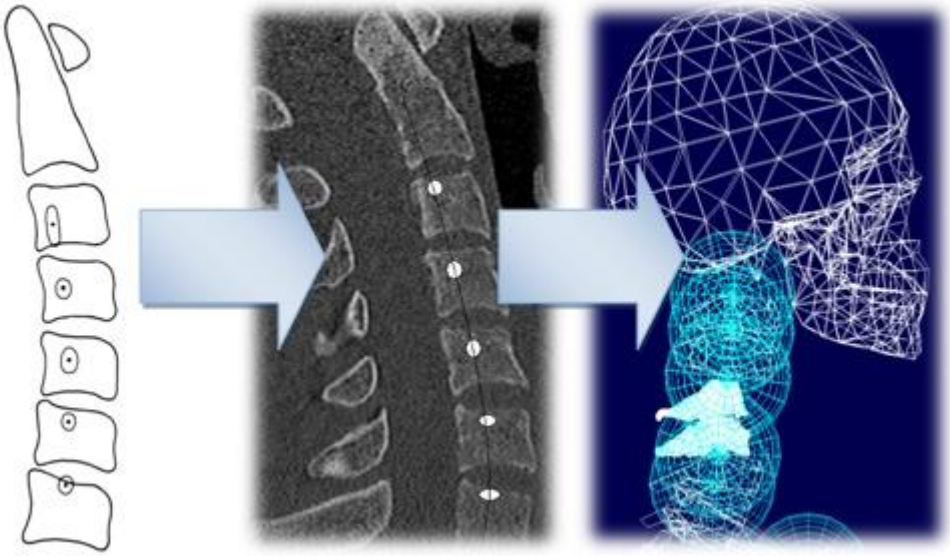

Figure 4-27: Positioning of the IAR in the simulation model

The difficulty with modeling the joints acting on the IAR line is that the IAR moves relative to the FSU as the FSU changes shape. Various studies have been done on this topic, but the exact location of the IAR and how the IAR moves relative to the vertebrae remain unclear [36], [37]. Taking into account the related IAR problem and the available literature, the IAR position was used as indicated by the literature. Since LifeMOD™ allows for six degrees of freedom joint elements, joint translations in the transverse plane (horizontal plane) will account for the positional adaptation of the IAR to any unbalanced forces. The completed model is shown in Figure 4-28.

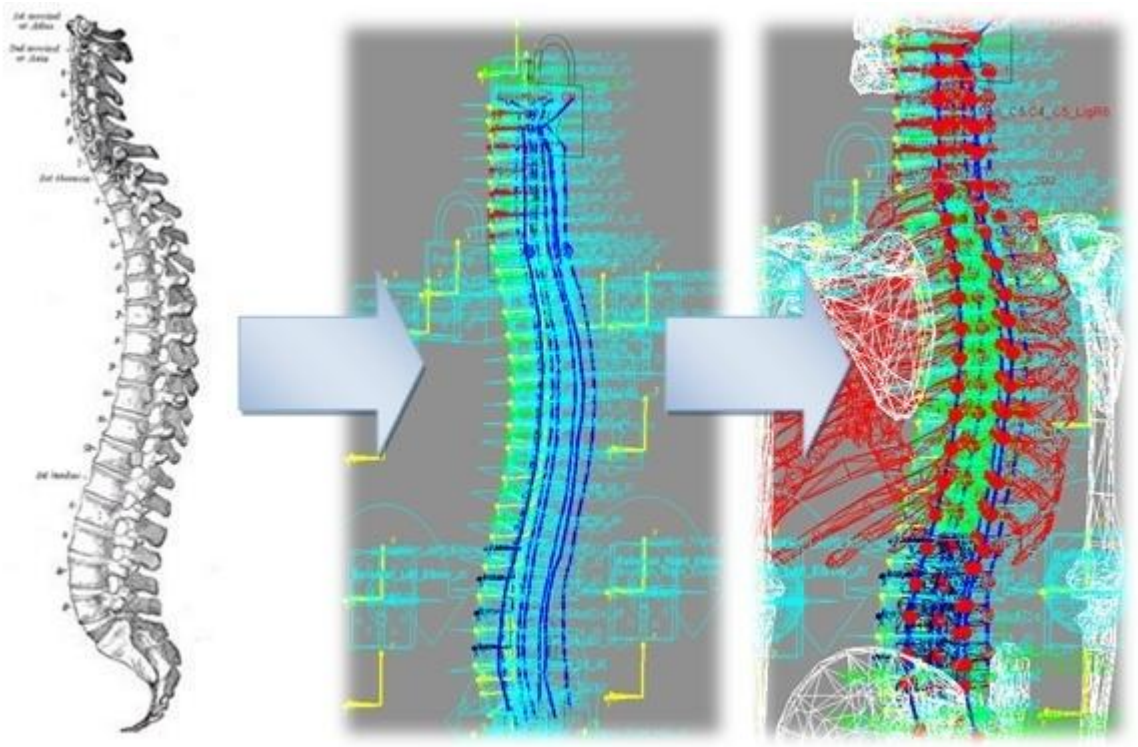

Figure 4-28: Simulation process

4.4.3 Limitations and Challenges of the Model

The simulation model presented here is an approximation of the *in vivo* conditions in the human spine. Inherently, many simplifications and assumptions will be made in such a model. Whilst an attempt was made at modeling all the tissue parameters to resemble *in vivo* conditions as closely as possible, there simply is no way of creating an exact replication of the *in vivo* state of the spine.

Specific limitations were that the IV disc properties used, albeit non-linear, were derived from cadaveric test specimens that would have lost significant stiffness through the loss of nucleus pulposus fluid and annulus fibrosus integrity.

4.4.4 Validation of the Model

Validation of the model was achieved firstly through comparison of the cervical intradiscal pressures derived from the axial forces with those achieved by McGuan and Friedrichs [15]. In their study, intradiscal pressures for a simple but maximum flexion/extension motion of the head were determined through simulation. Values were in the same order of magnitude as the values in this study, ranging from 1.0 MPa (145.10 psi) to 3.06 MPa (444.06 psi). Figure 4-29 shows the ranges obtained by McGuan and Friedrichs [15].

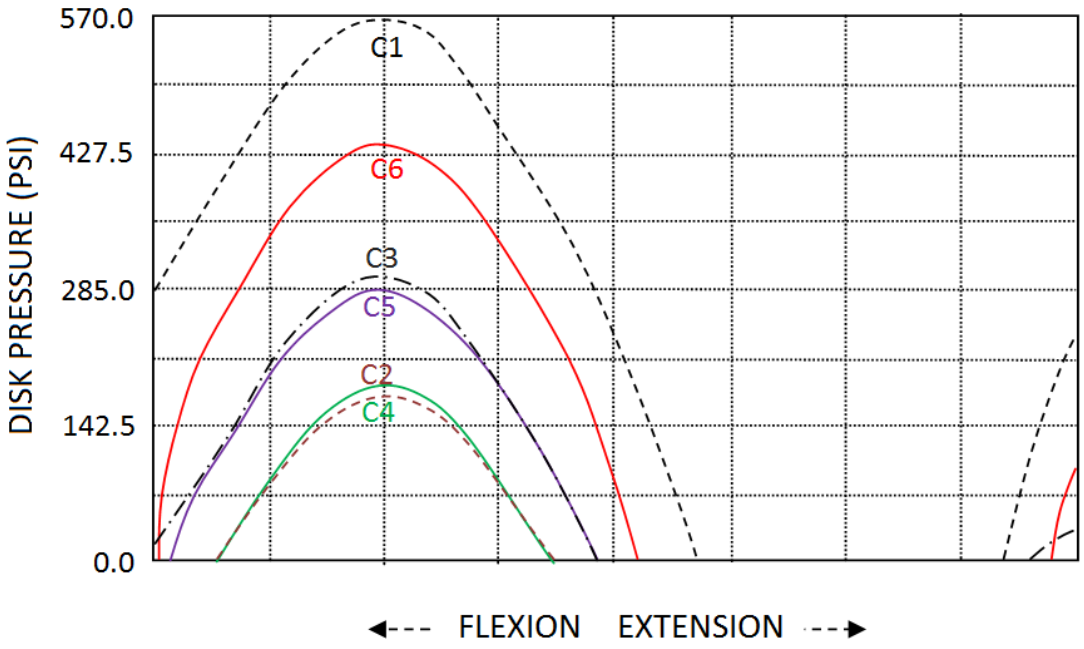

Figure 4-29: Intradiscal pressures modeled by McGuan [15]

A study by Nelson and Cripton [38] (University of British Columbia), in which a detailed surrogate spine model incorporating muscle pre-tension and non-linear IV discs was developed, was used as another form of validation of the model. The IV disc stiffness functions derived from physical testing of the surrogate were comparable to the functions used in the current simulation model (Figure 4-30). The

surrogate spine model (with head), with an equivalent 50th percentile male upper torso mass, was dropped from a height sufficient to generate a contact speed of 3 m/s. The axial forces were recorded for a drop in which the head was forced into hyper-extension by inclining the platform by 15^{o}. Figure 4-31 shows the axial force at C7/T1 with a 104 N muscle pre-tension. The peak axial force was determined at approximately 8 000 N.

The same setup was used as on the previously described H-III ATD model, with recordable motion markers placed on the center of mass of the head, the atlanto-occipital joint (C0/C1) and on the areas representing the C7/T1, T5/T6, T9/T10, T12/L1 and L4/L5 IV disc IARs. The dummy was dropped to a 3 m/s contact and the recorded motions were exported to the detailed spine model. As discussed in Section 2.3.1, models incorporating passive trainable joints cannot react to an input without being "trained" to what the resulting motions of the input are. Therefore the motions from the dummy served as "training" for the detailed model and were used as input to it (Figure 4-32). The axial force resulting from the head drop simulation using the detailed spine was remarkably similar to that obtained using the physical surrogate (Figure 4-33), with the peak force ranging between 6 000 N and 9 000 N.

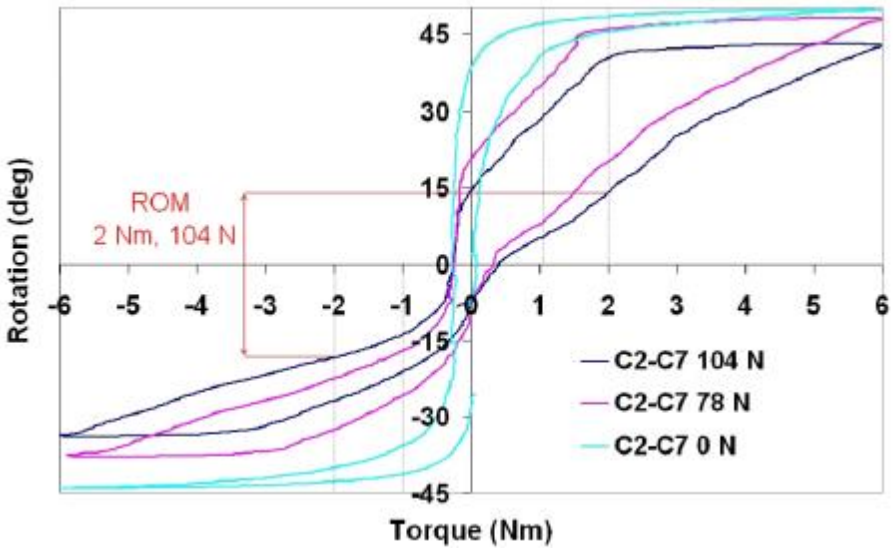

Figure 4-30: Surrogate spine IV disc stiffness functions [38]

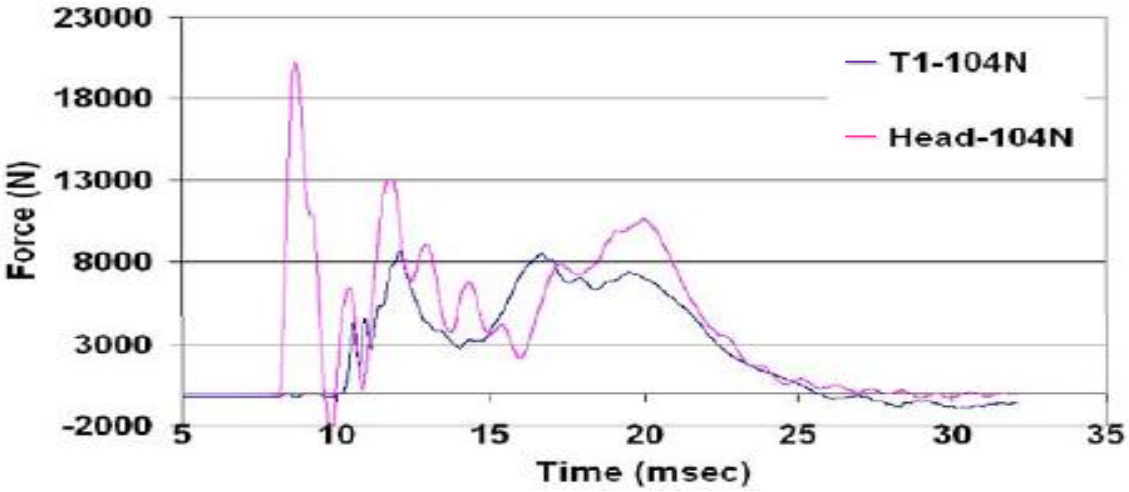

Figure 4-31: Surrogate spine head drop axial force [38]

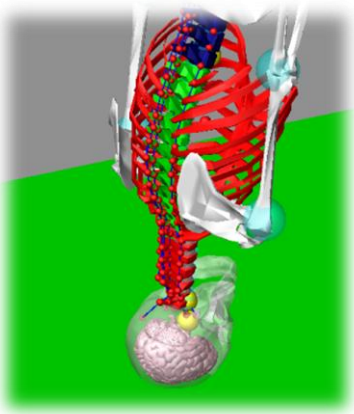

Figure 4-32: Head drop simulation to validate detailed spine model

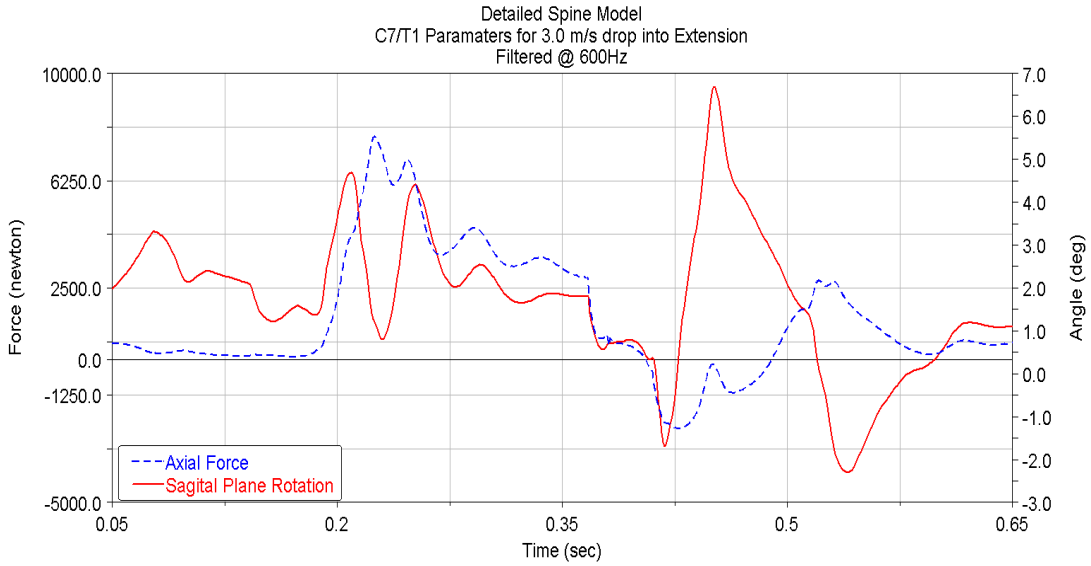

Figure 4-33: C7/T1 axial force through simulation

4.4.5 Results

Through the simulation of a detailed spine in LifeMOD™, it was shown that the individual IV level bending moments on the upper thoracic spine will not be excessive under the applied bending moment tolerance band applied by the strut, as shown in Figure 4-22, since hyper-extension will be limited by the strut and the remaining energy will be dispersed naturally through the IV levels and paraspinal

muscles of the thoracic spine. The IV bending moment in extension at the most affected T6/T7 IV level was shown not to be affected significantly with the strut in place (Figure 4-34 and Figure 4-35). This is attributed to the uptake of energy by the strut.

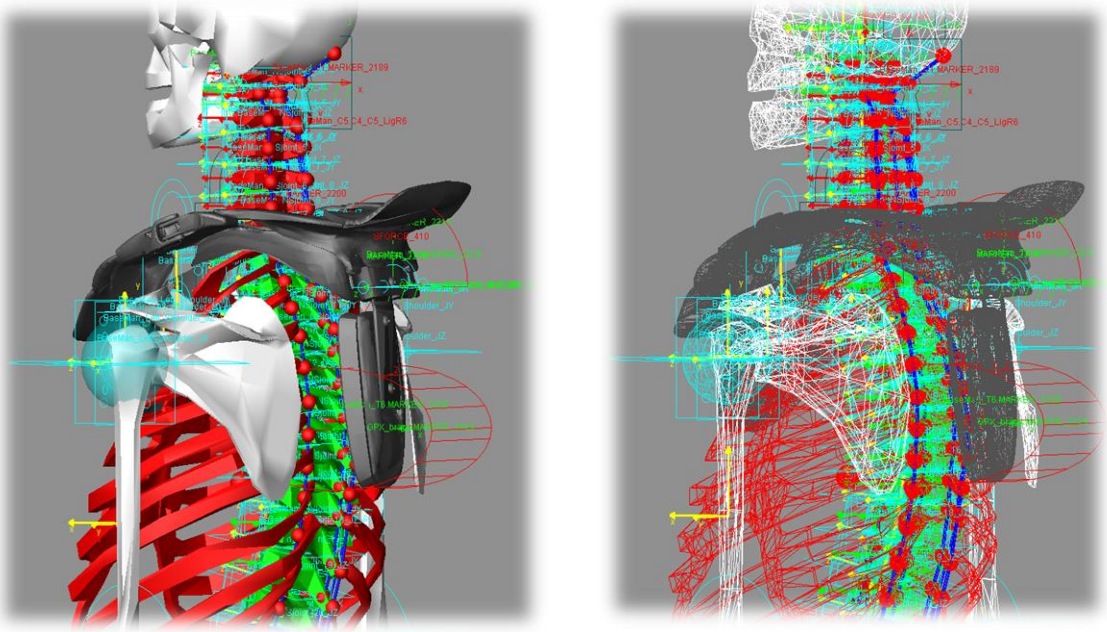

Figure 4-34: Thoracic strut as applied to simulation model

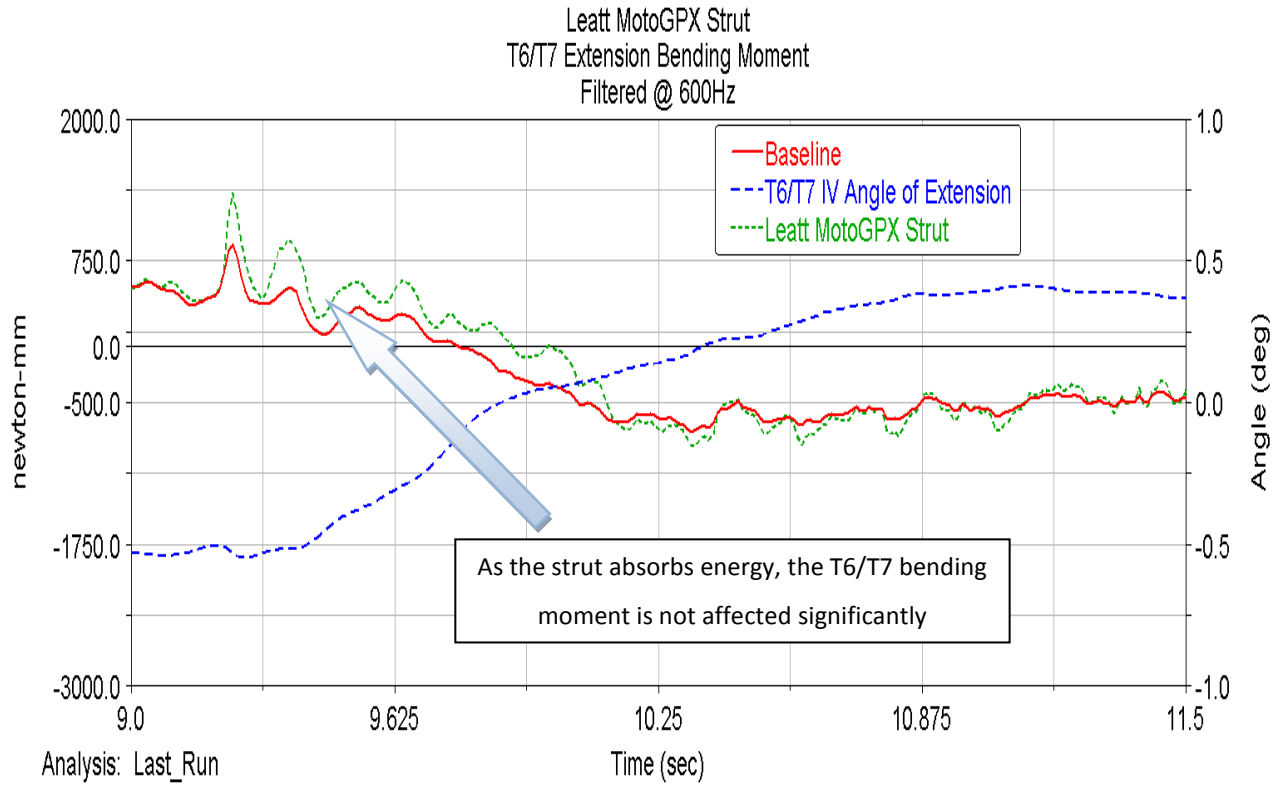

Figure 4-35: T6/T7 bending moment in extension with thoracic strut in place

Other Considerations Regarding the Strut Design

For posterior rib fractures to occur, Kleinman and Schlesinger [39] postulated that excessive posterior levering of the ribs needs to occur during bimanual compression. This requires severe anteroposterior thoracic compression through high-impact collisions (e.g. blunt trauma). From the examination of the simulation model, the maximum anteroposteriorly directed force distributed through the upper thoracic spine by the thoracic strut never exceeds 330 N. Since this force is never directly applied to the posterior region of the ribs, the distributed force to this region should be significantly less than 330 N, which will not be sufficient to damage the ribs.

The thoracic spine is well documented to be the area of the spine that is most frequently injured in motorcycle crashes. In a study by Robertson *et al*. [40],[41], in

which 1 121 motorcycle crashes were reviewed (with no riders using the Leatt-Brace® Moto GPX), 126 of which gave rise to spinal injuries, 54.8% of the injuries were in the areas of the thoracic spine, with T6/T7 being the most commonly injured level (Figure 4-36). Similar findings were made in other studies [42],[43], with an average prevalence of thoracic injury of about 50% to 60%. It was generally concluded in these studies that thoracic injury occurs as a result of hyper-flexion of the spine on impact with objects with axial loading concentrated at the point of maximum kyphosis (being in the area of T4 to T7, Figure 4-37). This can be explained by visualizing a curved twig being bent until it breaks. The twig will naturally snap at its point of maximum curvature.

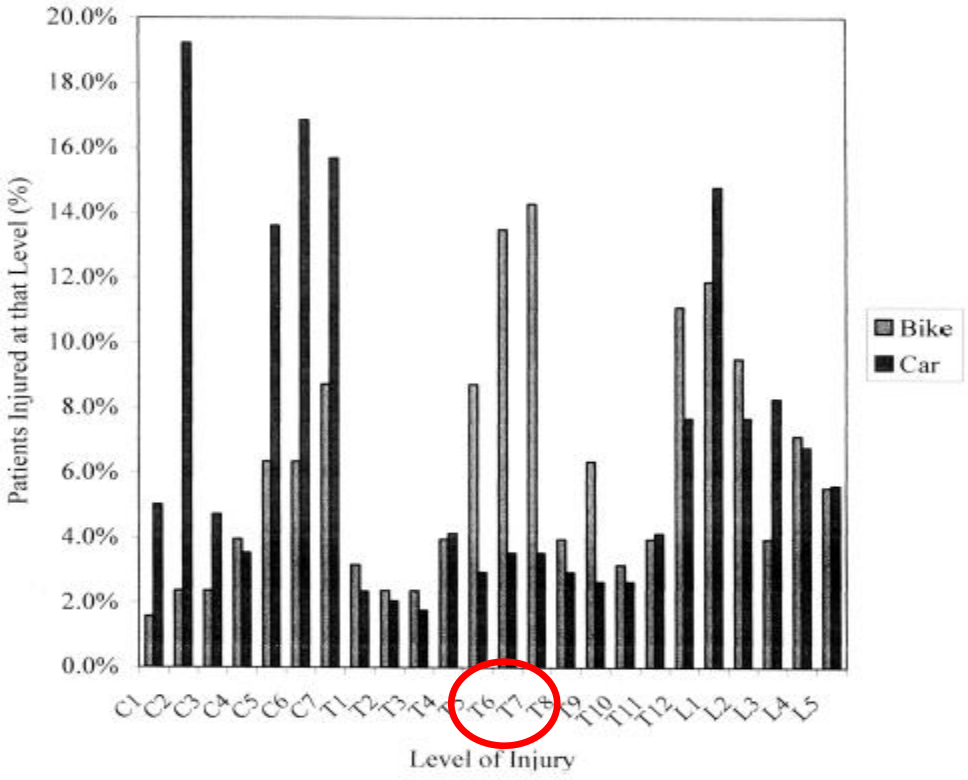

Figure 4-36: Prevalence of thoracic injury [40]

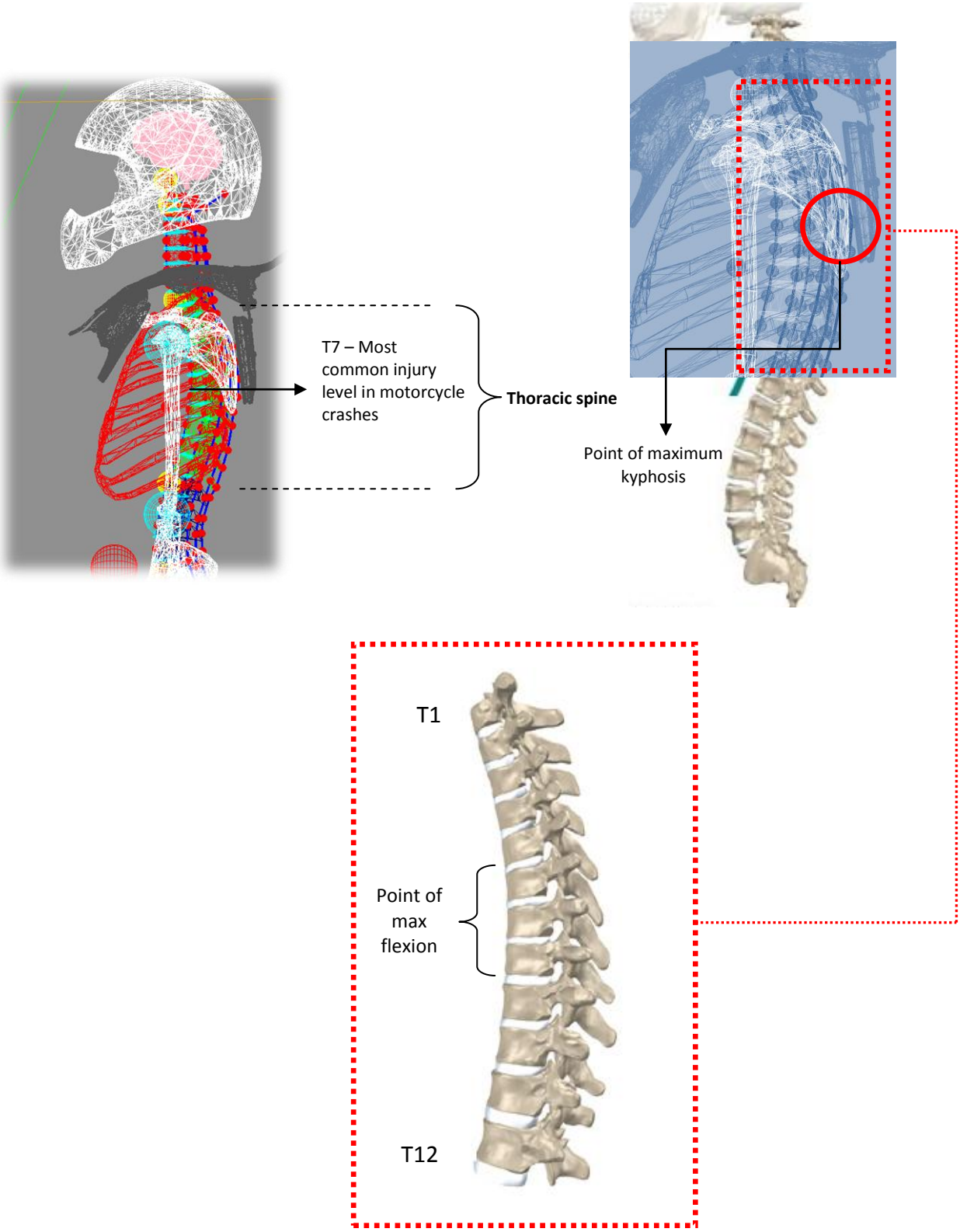

Figure 4-37: Representation of the point of maximum kyphosis

To further examine the effect of the strut on the mid-thoracic spine, another simulation (Figure 4-38 and Figure 4-39) was conducted, in which the detailed spine model was dropped to the ground from a height of 1.5 m with a block impacting the helmet on its anterior side (forehead area) at 36 km/h, resulting in a total impact speed of 46.8 km/h and forcing the head into extreme hyper-extension. This setup was chosen so as to examine a "worst case scenario", where the aim was to initiate a modality for thoracic spine fracture. The force transmitted from the strut (Figure 4-40) to the T7/T8 area (where the strut ends) was plotted over the time of impact and the resulting T7/T8 bending moment was overlaid onto this plot (Figure 4-41). Keeping in mind that LifeMOD™ does not allow the brace to be (with the strut therefore maintaining a rigid state, as seen in Figure 4-39), the strut-to-thoracic spine force was unrealistically high at times (Figure 4-41).What is noticeable from this graph, however, is the out of phase relationship between torque at the T7/T8 level and the strut force, with the peak bending moment occurring at an almost zero transmitted force from the strut to the thoracic spine (Figure 4-41). This finding indicates that the strut will not mediate certain inevitable thoracic spine fractures caused by overwhelming forces. But the fact that thoracic fractures are the injuries that occur most frequently in motorcycle crashes means there is opportunity for at least some thoracic injuries to be reduced in severity. [40],[41],[42],[43].

In order to investigate the effect of the strut in a less severe accident scenario, as in the abovementioned simulation, a head drop was simulated onto a static block, forcing the head into a less extreme hyper-extension. The bending moments on the T6/T7 intervertebral level (most affected level in less severe impacts) were plotted with and without the brace (Figure 4-42). As can be seen from the figure, there is no significant difference in the torque on the thoracic spine with or without the brace, indicating that the strut has no negative effect on thoracic biomechanics.

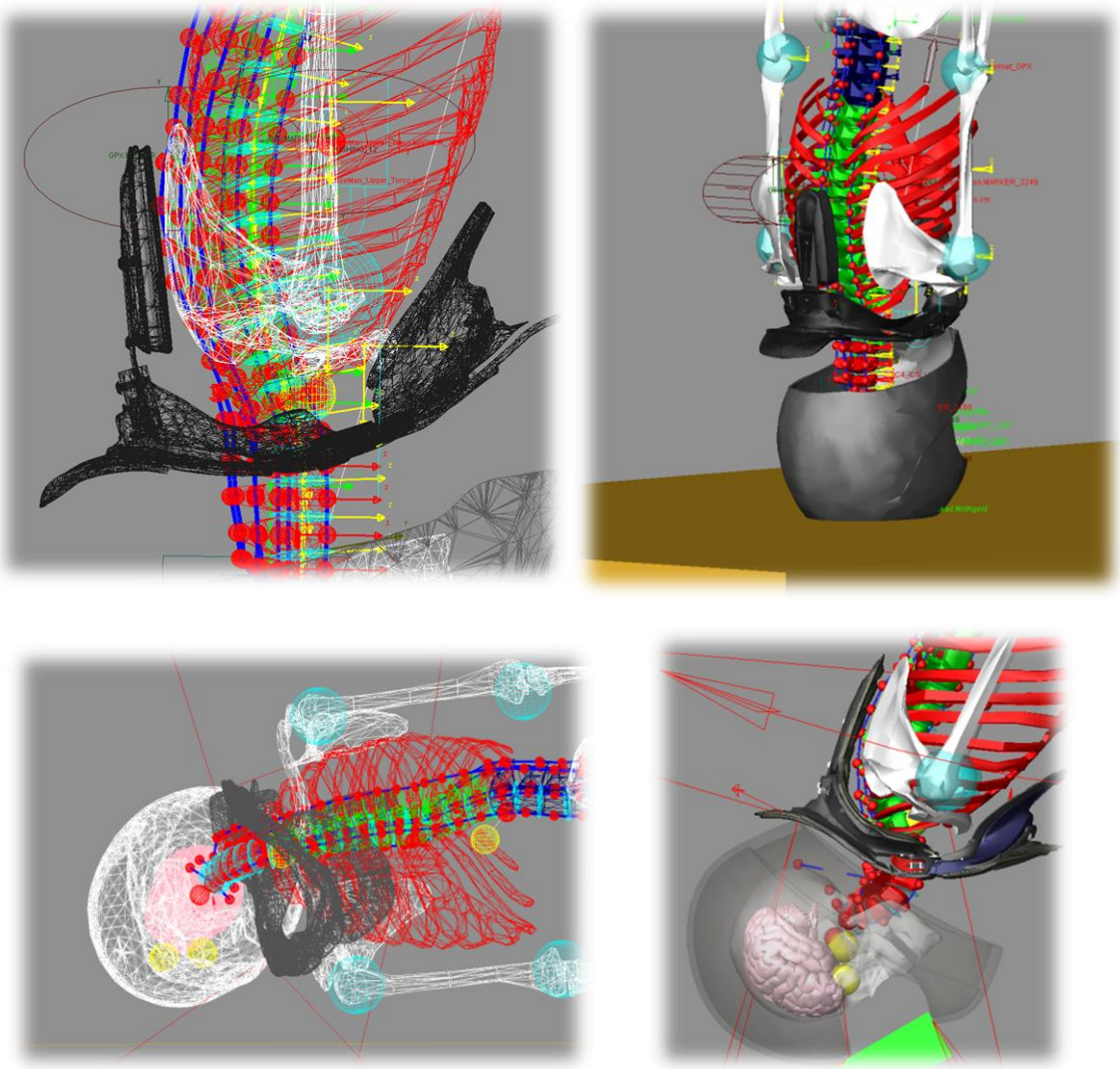

Figure 4-38: Simulation to model effect of strut in extreme hyper-extensive impact

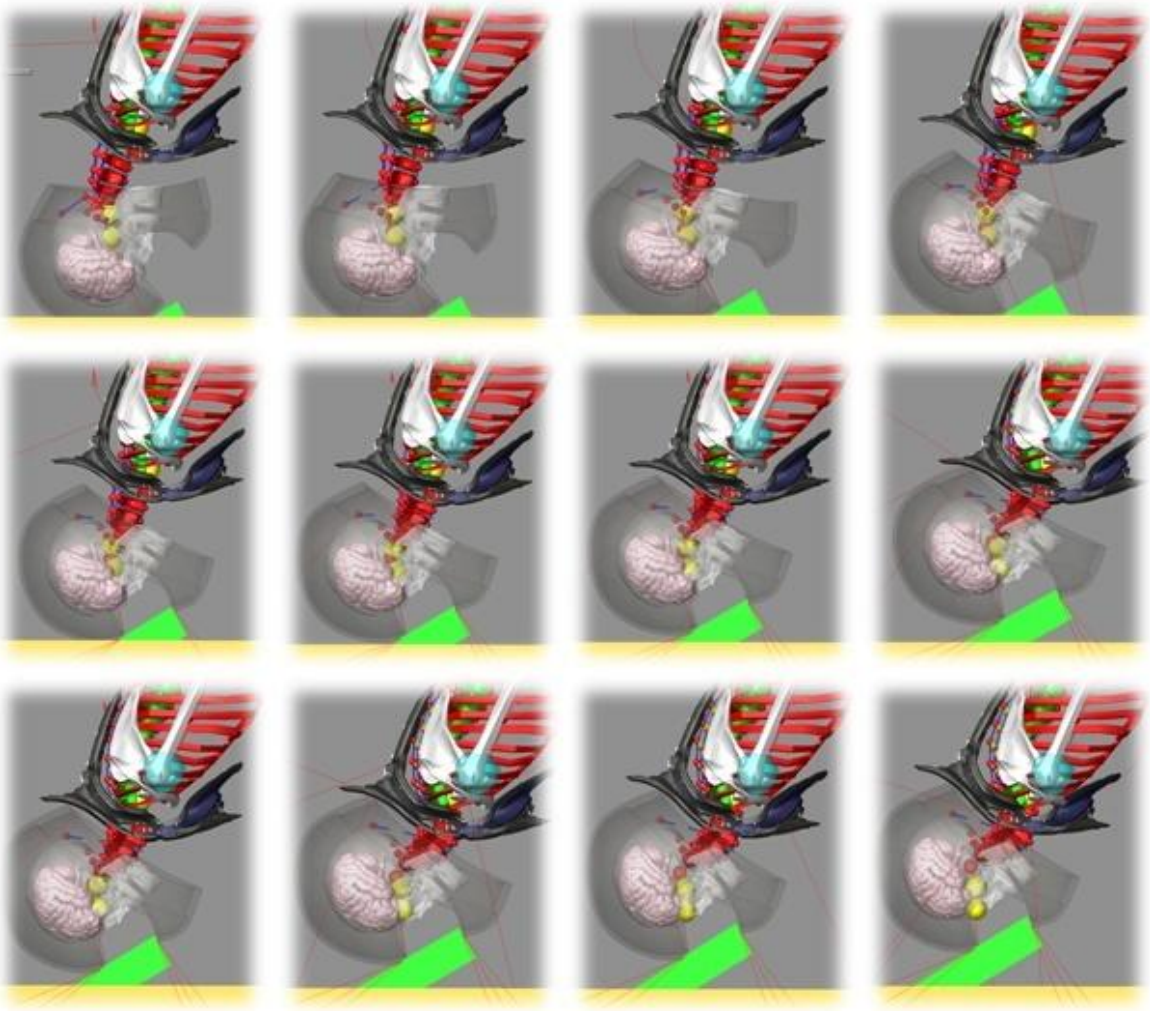

Figure 4-39: Progression of simulation towards extreme hyper-extension

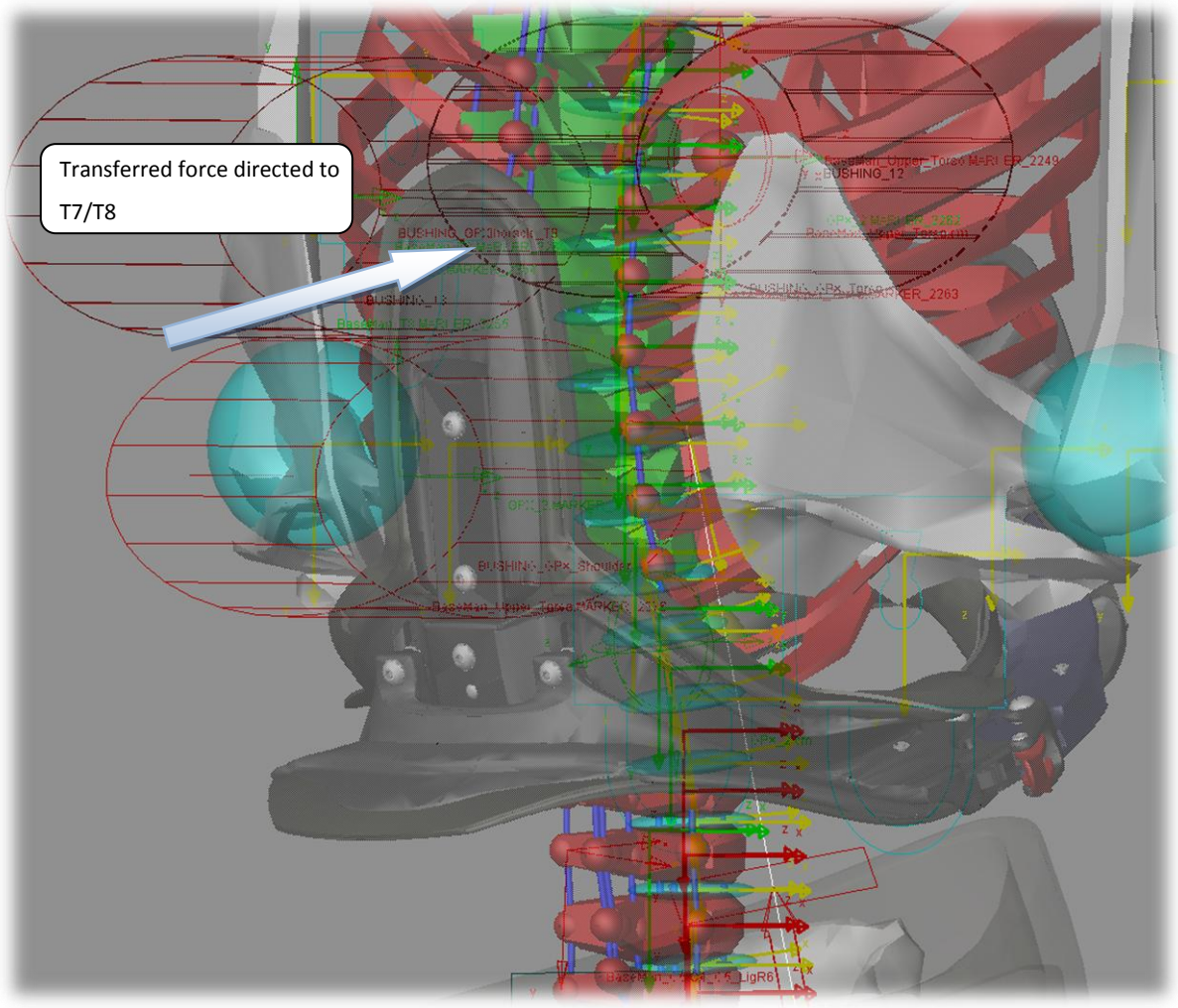

Figure 4-40: Force transmitted from strut to T7/T8

It should also be noted that, in reality, the force transferred from the strut will be distributed from T3 to T8, and not only to T7/T8 or T6/T7. However, in the context of this study, a worst case scenario was assumed, with all of the force transmitted from the strut being focused on T7/T8 and T6/T7 respectively, representing a rigid strut "digging" into the spine. This indicates the existence of a "safety factor" based on the simulations. In this case, it can be seen clearly that the mid-thoracic spine is not adversely affected by the strut.

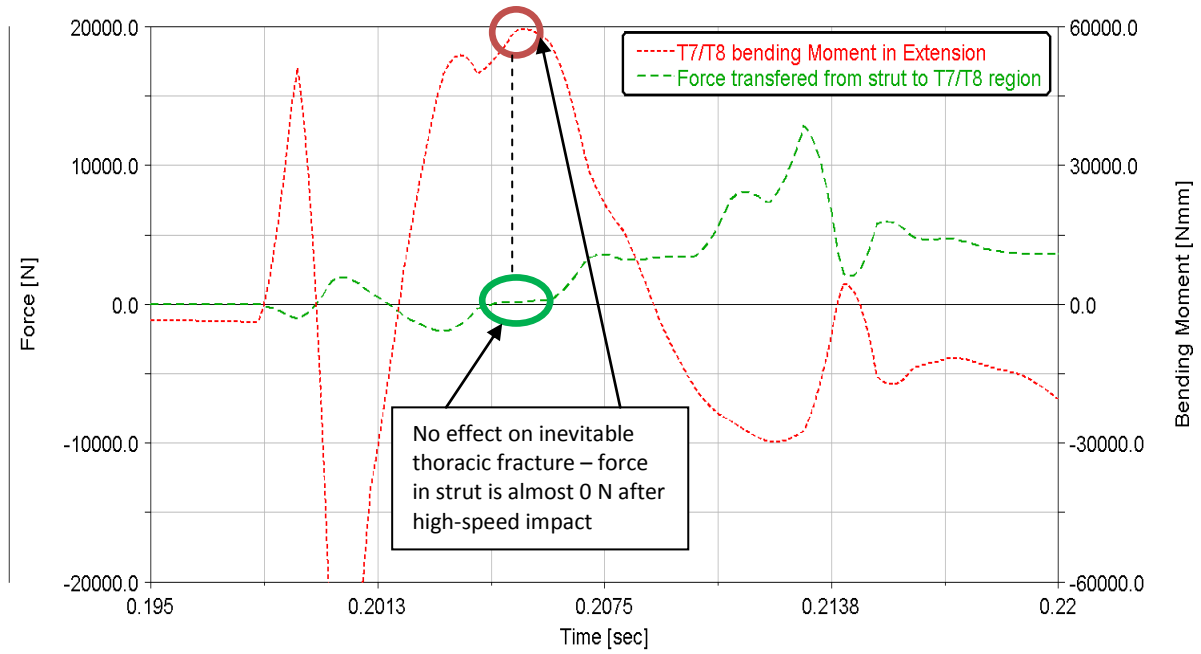

Figure 4-41: Strut force vs. extension bending moment at T7/T8

Figure 4-42: Thoracic bending moment with and without strut (brace)

4.5 FEM Component Failure Analysis

In addition to the dynamic simulations conducted using LifeMOD™ , finite element method (FEM) analysis was conducted using MSC. SimOffice™ (Nastran Solver). Analyses were conducted on components of the Moto GPX to assess the strength and material properties of the designed components. Inputs to the models included material properties such as the moduli of elasticity (E), density (ρ), ultimate tensile strength (UTS in *MPa*) and yield strength (*MPa*). The release clip and frontal lower design of the Moto GPX were subjected to FEM analysis. According to the authors, these components are crucial components when one considers the loading modalities imposed on them during impact. Apart from the FEM analysis, physical tests were also conducted on the rear upper and lower components, as described in Section 4.4.2. It is important that the stresses and strains on these components remain below the allowable material limits for the given force and motion inputs to ensure not only that the components do not shatter or fail at forces below the impact forces but yield at the designed forces. The yield forces are designed to be lower than injury levels for body structures.

Release Clip

The release clip was analyzed using different material types in order to determine its strength in areas with possible stress concentrations (Figure 4-43). Glass-filled nylon, aluminum and polycarbonate were analyzed (see Appendix A for material properties used). A tetrahedral (*Tet 10*) mesh was used. From simulations it was determined that typical forces directed to the clip area (where it was planned to be placed) during various impact scenarios were found to be in the region of 600N. A physical tension test was applied to a glass-filled nylon clip to test its tensile strength and, after three test runs it was found to fracture at an average load of 800 N. The same constraints and quasi-static loading scenario were applied to a glass-filled

nylon FEM model of the clip and the ultimate Von Mises tensile strength was just exceeded. This validated the model.

The Von Mises stresses for the remaining two materials were analyzed subsequently, using the same inputs used in the validation model. The aluminum and polycarbonate showed satisfactory Von Mises stresses and strain for the same loading and constraints. However, due to specific manufacturing and cost considerations, these materials were excluded from consideration as material for the Moto GPX, and the glass-filled nylon was used.

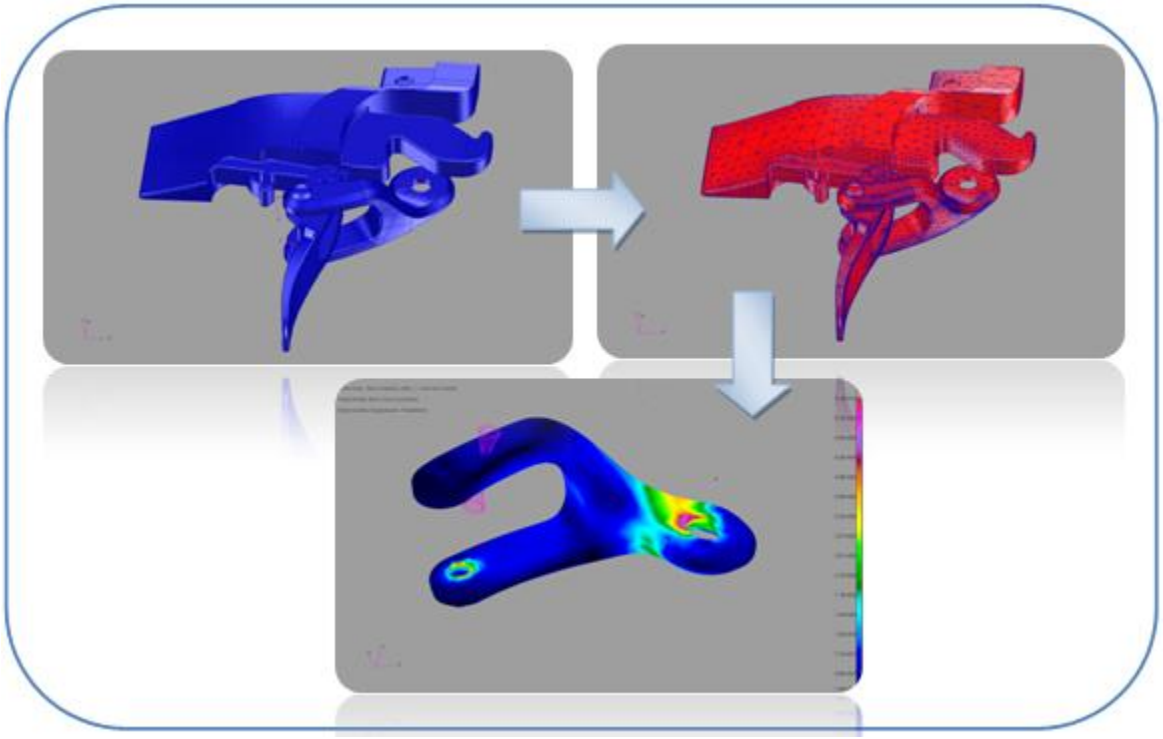

Figure 4-43: FEM of the hinge clip

Frontal Lower

The frontal lower part of the Moto GPX was analyzed using a tetrahedral (*Tet 10*) mesh in order to determine possible stress concentrations and the effect of material choice (Figure 4-44). A physical test was conducted in which the part was subjected

to a quasi-statically applied compression force until failure occurred. After three test runs, the average force was found to be 350 N. This force was never exceeded during the simulations (in LifeMOD™) of contact with the helmet or ground during lateral hyper-flexion of the head in a crash scenario. The same force was applied to an FEM model of the part using the properties of glass-filled nylon and the same force and constraints as applied in the physical test. The ultimate tensile stress was just exceeded, at 350 N, subsequently validating the model for further use with other materials.

The polycarbonate showed satisfactory Von Mises stresses and strain for the same loading and constraints. However, due to specific manufacturing and cost considerations, this material was excluded from consideration as a material for the Moto GPX, and the glass-filled nylon was used.

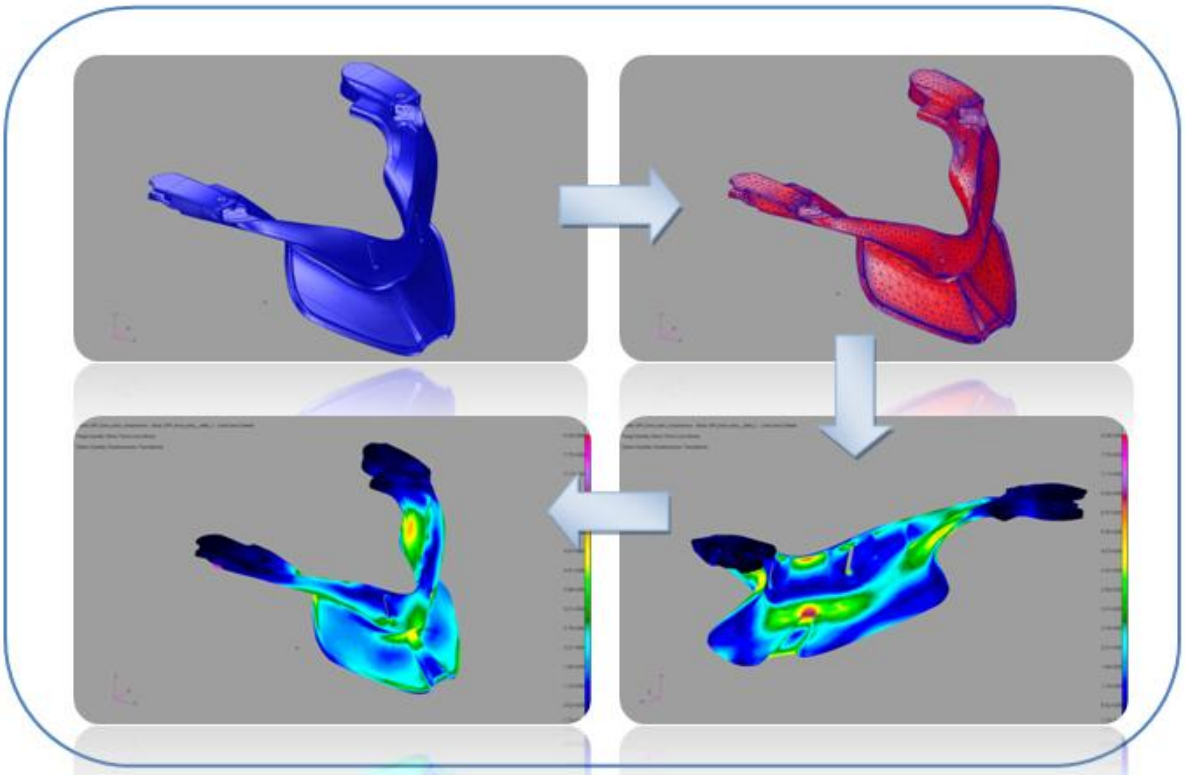

Figure 4-44: FEM of the lower front of the device

Chapter 5

Work in Progress

SFI 57.1 Developments

Leatt Corporation is assisting with developing a specification for the evaluation of an unrestrained torso head and neck safety device in conjunction with the SFI Foundation (SFI 57.1).

The aspects discussed in this study include:

- Physical static tests
- Physical quasi-static tests
- Physical dynamic tests (pendulum swing)
- Extensive simulations with validated models

In addition to this, Leatt Corporation is always looking for new methods of evaluating protective devices, especially with increasingly effective simulation techniques. Simulation models are useable in a wide range of applications, so time spent researching, developing and evaluating new products is also time invested in modeling development.

For example, different material types are currently being investigated and tested for different applications. In addition, the capability of FEM analysis of composite materials has recently been added to the already extensive list of capabilities of the organization.

Proposed Neck Injury Criteria for Motorcycle Riders

It is the belief of the authors that, although it is valid, the formula for the calculation of neck injury criteria (Nij) should consider additional factors. In its present form, the reduction (not prevention) of movement of the head and cervical spine may increase all neck forces (rigid movement reduction device) and increase the Nij result; i.e., if hyper-flexion and hyper-extension are prevented, the Nij may be greater. The range of movement and the forces that occur at a given angle, including bending moments, may well be the most important injury-prediction factors. All classification systems have hyper-flexion and hyper-extension as critical injury factors. In addition to this, it is postulated by the authors that it is important to decelerate the head in a controlled manner. Drop tests are hypothesized by the authors to be more representative of a motorcycle accident, as pendulum tests impart a high upper cervical shear force as a dominant force vector, and not a compression force, which may be a dominant force in motorcycle accidents. Simulation software will allow the torso/head movement interface to be appreciated more adequately as a rider falls from a motorcycle, with a combination of head and bodyweight dynamics acting on the neck. Tests to confirm the efficacy of a neck injury prevention device in a motor vehicle application should include not only frontal impact, but side and rear impact as well, along with measurements of brain deceleration. A new expression is therefore proposed by the authors (yet to be finalized) to accurately predict neck injury risk/benefit. The proposed N_{ij} is given by the following expression:

$$Leatt\ N_{ij} = \frac{ROM}{M_{ROM}} \underbrace{\left\{\frac{F_z}{F_x} + \frac{M_{ocy}}{M_{yc}}\right\}}_{\text{normal } N_{ij}} \times B_f \tag{5-1}$$

where ***ROM*** is the measured test neck range of movement, M_{ROM} is the maximum H-III range of movement, e.g. 180^{o}, ***Bf*** is a brain factor that is related to the peak brain deceleration forces observed divided by the maximum permissible brain forces (included HIC or Gambit). The new Nij pass value will have to be recalculated.

Chapter 6

Conclusions

This document summarizes research and development underlying the design of the Leatt-Moto® GPX.

A detailed discussion of the relevant literature was provided, as well as of the relevant injury mechanisms pertaining to motorcycle crashes.

The design rationale behind the Moto GPX was discussed, and details such as alternative loadpath theory, the thoracic member, clip design and the clavicle relief area were presented.

A presentation of the tests and simulations conducted during the development of the Moto GPX was provided, including the methods of validation of the simulation model used and the quasi-static physical tests performed.

Through this study it was shown that the Moto GPX is an effective neck protection device. It conforms to all applicable test criteria, such as allowable Nij and HIC, through the significant reduction in bending moments and axial forces in the cervical spine. Specific areas in which the device's efficacy is demonstrated are:

- Reduction in cervical spine bending moments, axial and shear forces through energy transfer (alternate loadpath theory), and physical reduction in range of motion.
- Reduction in thoracic spine bending moments in extension through the use of an energy conductive (through absorption) strut that fractures at a pre-determined load.
- Reduction in brain injury-associated dynamics through the correct interaction between deceleration and the time-related control of head impacts.

- No increased likelihood of clavicle fractures, due to its design of a clavicle relief area and the soft padding covering the device.

Finally, this document serves as a reference for interested readers in terms of understanding the research, development and design rationale behind the Leatt-Brace® Moto GPX.

Appendix A

NAN YA FR-PA6 MATERIAL SPECIFICATION

GRADE : 2212G3 ABK1--15% Glass Fiber Reinforced , HIGH IMPACT NYLON 6

PROPERTIES	TEST METHOD	UNIT	REF. VALUE
1.Physical			
Tensile Strength at Yield	ASTM D-638	kg/cm^2	850
Elongation	ASTM D-638	%	4.5
Flexural Strength	ASTM D-790	kg/cm^2	1200
Flexural Modulus	ASTM D-790	kg/cm^2	35000
IZOD Impact (Notched 1/8)	ASTM D-256	kg-cm/cm	19
Rockwell Hardness	ASTM D-785	R-Scale	118
2.Thermal			
Melting Point	DSC	℃	222
H.D.T.(18.6 kg/cm^2)	ASTM D-648	℃	190
Melting Flow Index (MFI)	ASTM D-1238	g/10 min	4.5
3.Electrical			
Volume Resistivity	ASTM D-257	Ω • cm	10^15
Dielectric Strength	ASTM D-149	kv/mm	----
Dielectric Constant(10^6HZ)	ASTM D-150	--	4
Dissipation Factor(10^6HZ)	ASTM D-150	--	0.018
Arc Resistance	ASTM D-495	sec.	85
4.Others			
Specific Gravity	ASTM D-792	--	1.18
Mold Shrinkage (MD)	3 mmt	%	0.8
Mold Shrinkage (TD)	3 mmt	%	1.2
Flammability	UL 94	--	----
Remarks			

REFERENCE MOLDING CONDITIONS		
Drying Time	Hrs	4
Drying Temp.	℃	80
Cylinder Temp.		
Rear	℃	230
Center	℃	240
Front	℃	250
Nozzle Temp.	℃	255
Mold Temp.	℃	90
Injection Pressure	kg/cm^2	600~1400
Screw Rotation speed	rpm	120
Injection Speed	--	fast

Injection M/C : ENGEL ES 50/150 2 oz
Mold : ASTM Test Bar
Gate Size: 5.8mm×1.2mm
Test Bar Thickness : 3.2mm
Test Condition: 23℃ , 50%RH

NAN YA PLASTICS CORPORATION
PLASTICS 4 TH DIVISION
ENGINEERING PLASTICS DEPT.

Melting Flow Index Test Condition: 250℃×2.16Kg

The values in this table are for reference only.

2004/01/25

Property Chart for Polycarbonate

MECHANICAL PROPERTIES:	ASTM	
Specific gravity	D 792	1.20
Tensile strength, Ultimate	D 638	9,000 p.s.i.
Elongation at break	D 638	130%
Tensile modulus	D 638	3.1x10~5 p.s.i.
Rockwell hardness	D 785	R118
Impact strength (73° F) (notched)	D 256	17.0 ft-lb/inch
Flexural strength	D 790	14,200 p.s.i.
Flexural modulus	D 790	3.4x 10~5 p.s.i.
Wear factor against steel 40 psi 50fpm :		2500x10~10
Coefficient of friction 40psi 50fpm :		0.38 Dynamic
THERMAL PROPERTIES:		
Melting point :		310° F
Heat deflection at 66 psi	D 648	285° F
Heat deflection at 264 psi	D 648	270° F
Max serving temperature for short term		275° F
Max serving temperature for long term		240° F
Thermal conductivity	C 177	1.35 Btu-inch/hr-ft~2- ° F
Specific heat		0.30 Btu/lb- ° F
Coefficient of linear thermal expansion	D 696	3.7x10~5
Applicable temp range for thermal expansion		0-200° F
ELECTRICAL PROPERTIES:		
Dielectric constant at 60Hz (73° F, 50% RH)	D 150	3.2
Dissipation factor at 60Hz (73° F)	D 150	0.001
Volume resistivity	D 257	10~17 ohm-cm
Dielectric strength	D 149	380 v/MIL
MISCELLANEOUS:		
Water absorption - 24 hours	D 570	0.15%
Water absorption - saturation	D 570	0.35%
Density	D 792	0.0434 lb/inch~3
Flammability	UL 94	V-2
Weathering Resistance		Limited resistance

These values are representative of those obtained under standard ASTM conditions and should not be used to design parts which function under different conditions

BOHLER UDDEHOLM
AUSTRALIA

7075 - ALUMINIUM ALLOY

Typical Analysis (Ave. values %)	Mg	Mn	Fe	Si	Zn	Cr	Ti	Cu	Zr+Ti	Al
	2.5	0.3	0.5	0.4	5.5	0.23	0.2	1.6	0.25	88.5
NEAREST STANDARD	BS					ISO				
	EN AW-7075					Al Zn5.5MgCu				

DESCRIPTION	Heat treatable, very high strength alloy. Very high fatigue strength.

APPLICATIONS	Machine parts and tools for rubber and plastic.

MECHANICAL PROPERTIES	Temper	Tensile strength MPa	0.2% Proof stress MPa	Elong.A5 %	Elong.A50 %	Hardness Vickers
	O	225	105	-	17	65
	T6	530-570	460-505	7-10	10	160
	T7	505	435	13	12	150

FABRICATION PROPERTIES		
	Machinability	Excellent
	Extruding	Fair
	General	Fair

PHYSICAL PROPERTIES		
	Density	2.81 (kg/dm^3)
	Melting point (Liquidus)	635°C
	Melting point (Solidus, Eutectic)	475°C
	Coefficient of thermal expansion	23.5-µmm^{-1}K^{-1}
	Thermal conductivity	134-W m^{-1}K^{-1}
	Specific heat capacity	862 JKg^{-1} K^{-1}
	Electrical resistivity	52 nΩ m
	Electrical conductivity	33% IACS

Appendix B

SFI SPECIFICATION 38.1 EFFECTIVE: MARCH 24, 2009*

PRODUCT: Head and Neck Restraint Systems

1.0 GENERAL INFORMATION

1.1 This SFI Specification establishes uniform test procedures and minimum standards for evaluating and determining performance capabilities for Head and Neck Restraint Systems used by individuals engaged in competitive motorsports.

1.2 The procedures, test evaluations and standards contained herein, are intended only as minimum guidelines for construction and evaluation of products. Certification that products meet such minimum standards is made by the product manufacturer and products are not certified, endorsed or approved by SFI under this program.

1.3 Use of the "This Manufacturer Certifies That This Product Meets SFI Specification 38.1" logo/designation, the authorized artwork style, or conventional lettering by a manufacturer, on a subject product, is intended only to indicate that the manufacturer of the product has represented that they have submitted the product to the recommended tests, with positive results, in compliance with the standards established herein.

1.4 This SFI Specification requires a demonstration that the product of a manufacturer meets or exceeds the requirements when the manufacturer enters the program, and on a periodic basis thereafter. Any manufacturer may participate in the program by providing Head and Neck Restraint Systems that meet or exceed the SFI Specification 38.1 test standards, by complying with the requirements of the SFI Specification 38.1 program, and by signing a licensing agreement with the SFI Foundation, Inc.

1.5 Compliance with this specification is entirely voluntary. However, when a manufacturer provides Head and Neck Restraint Systems in compliance with all requirements of the SFI Specification 38.1 and enters into the licensing agreement with the SFI Foundation, Inc., they may certify that compliance with such standards is in accordance with the guidelines established herein.

1.6 Manufacturers wishing to participate in the program, in addition to the other requirements of this specification, must label each of their products with the manufacturer's name, trademark or symbol as well as the model number, part number and the date of manufacture of the product.

1.7 No manufacturer may display the SFI logo/designation on their product unless the manufacturer has signed a licensing agreement with SFI and has successfully complied with all the requirements of this specification and the self-certification program.

2.0 DEFINITIONS

2.1 Head and Neck Restraint: An active Head and Neck Restraint System is a protection ensemble providing an alternative load path which decreases both neck stress and head excursion during a vehicle impact without reliance on helmet impact into structures or nets.

2.2 Separate Restraining Devices:

A. Linkages attached to the helmet which transfer restraining loads directly to the helmet from the main device which is secured to the driver's shoulders, torso, etc. Methods for attachment of these linkages to the helmet and main device shall be prescribed by the manufacturer.

B. The main device shall be a mechanism held tightly to the driver's torso by seat belts or other strap systems such that the reactive load carrying components move directly with the torso and controls head, neck, and torso relative positions during forward or off-center impact situations.

2.3 Reaction Linkage: The means by which the head force necessary to limit displacement of the head with respect to the torso is reacted. Acceptable reaction linkages could include load paths to the torso or to the restraint webbing. Direct attachment to react loads to a fixed point or points on a vehicle structure or restraint webbing will not be acceptable because of the potential for torso displacements with respect to these points. Imposed loading by the reaction linkage to other areas of the body should be applied using approaches demonstrated to be practical without imposing risk of serious injury.

2.4 The Head and Neck Restraint System must be designed and manufactured to allow freedom of movement of head, torso, arms, etc., commensurate with operating a race vehicle under all race and associated conditions.

2.5 Adjustment and release mechanism(s) shall be accessible to both the user and to external personnel such that no additional motion is required, other than the release of the seat belts, to disengage the Head and Neck Restraint System during emergency situations.

2.6 All or any portion of the Head and Neck Restraint System pertaining to this specification shall remain as constructed by the original manufacturer and not modified.

3.0 CONSTRUCTION

3.1 MATERIALS

The materials used in the construction of the Head and Neck Restraint System shall be resistant to the elements to which they are exposed in normal service. Besides environmental considerations such as heat and UV light, these elements include fluids used in and around motor vehicles that may come in contact with the restraint system. All metal rivets, bolts, buckles, adjusters, etc. shall be corrosion resistant and have sharp edges and burrs removed. The materials and design shall not promote combustion as defined by flame resistance testing herein.

4.0 MODEL CLASSIFICATION

Any variation of the original design, i.e. construction methods, materials, size and quantity of straps or links shall be considered a model change. Any change which affects the kinematic response of the user of the device, must be tested at the judgment of SFI. SFI will assemble a review panel through which manufacturers can present items of modification that they feel do not constitute additional testing.

5.0 TESTING

5.1 IMPACT PERFORMANCE

5.1.1 SAMPLES

Test samples shall be fully processed new Head and Neck Restraint Systems that are representative of devices currently being produced or to be produced. All necessary attachment and adjustment hardware along with instructions shall be supplied by the certifying manufacturer.

5.1.2 APPARATUS

A. The system shall be tested using a 50th percentile male Hybrid III anthropomorphic test device (ATD) seated and restrained in a pan type seat assembly per Figure 1 and with a Nylon SFI Specification 16.1 six-point driver restraint system (to be supplied by SFI) mounted to a conventional race car style mounting frame without steering wheel and steering column. The driver restraint system shall be installed so that each shoulder belt is horizontal from the top of the Head and Neck Restraint Device system to the belt attachment point. The attachment points for the lap belts and anti-submarine belt (crotch strap) may not be altered in any way. Head side supports and supplemental head nets for the seat shall not be included. A full-face racing helmet weighing 3.0 lbs. (1.36 kg) minimum without face shield shall be fitted to the Hybrid III ATD to achieve a typical fit per the helmet manufacturer's instructions. If attachment of tethers or other devices to the helmet are required, drilling and attachment location, methods and hardware shall be per manufacturer's instructions.

Figure 1
Test Sled Seat Assembly

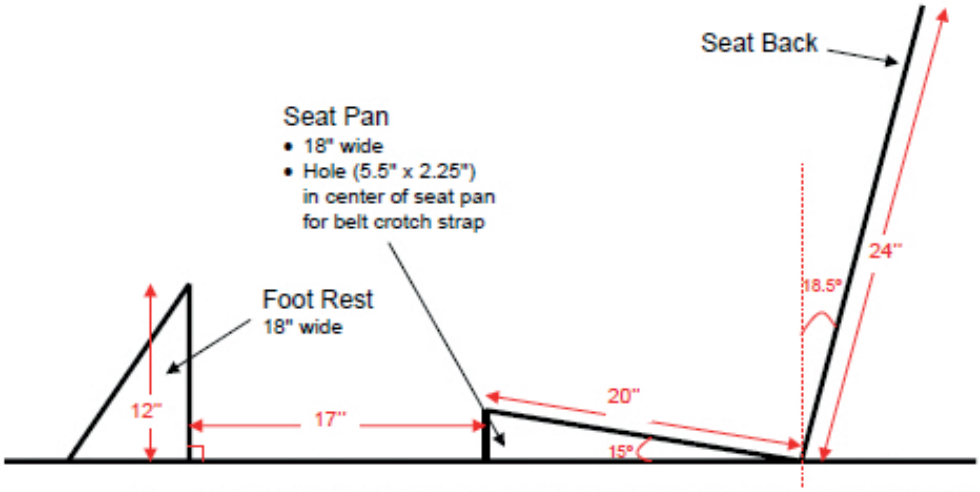

B. Instrumentation in the Hybrid III ATD will be set up to read Upper Neck Tension and Compression Forces, and all data acquisitions necessary for calculating Nij (per FMVSS 208.) The data from the upper neck transducers will be collected and filtered at SAE J211/1 Rev. March 95 channel frequency Class 600.

C. A test sled (hydraulic or other) shall be capable of propelling the entire assembly in paragraph 5.1.2.A above in a manner to achieve a pulse contour per Figures 2A and 2B, producing a nominal 68G peak, 63 KPH (39.1 mph) velocity change.

Figure 2A

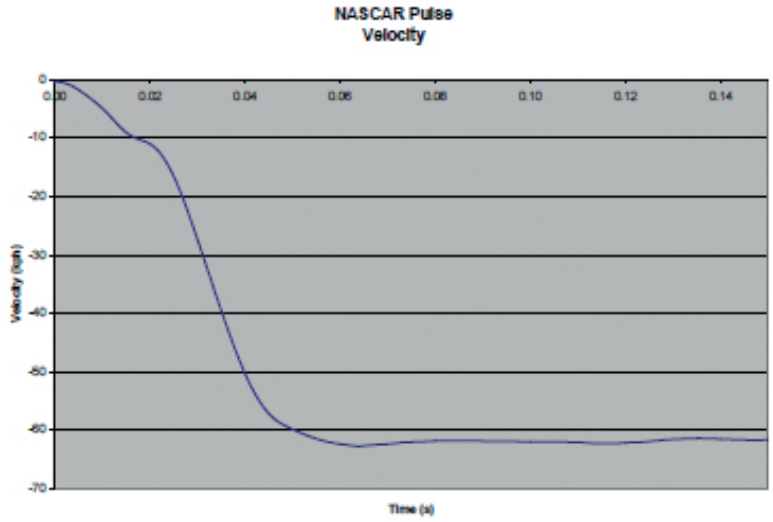

Figure 2B

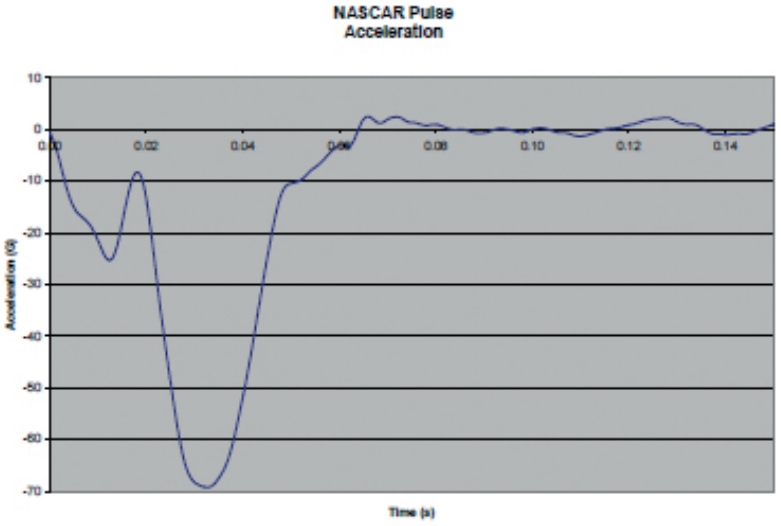

D. If it becomes desirable to utilize an alternative lab rather than DELPHI or to employ a different ATD than the Hybrid III, then test procedures and requirements may need to be reevaluated at the discretion of SFI.

5.1.3 PROCEDURE

A. The Head and Neck Restraint System shall be assembled per the manufacturer's instructions to the 50th percentile male Hybrid III test device (ATD) and the ATD then shall be seated and restrained in the seat and mounting frame with the full face helmet fitted, all as described in paragraph 5.1.2.A of this specification. This complete assembly shall be mounted on the test sled.

B. The test sled shall be propelled to produce the racing acceleration pulse (Figures 2A and 2B) at a nominal 68G peak, 63 KPH (39.1 mph) velocity change. Two (2) frontal tests and one (1) 30° right frontal test will be required. The results of both frontal tests and the 30° right frontal test must meet the requirements of paragraph 6.1.1.

C. The data recorded in the test shall be analyzed for the first 80 milliseconds of the test and then analyzed at 120 milliseconds of the test.

5.2 FLAME RESISTANCE

The test shall be conducted at an ambient temperature between 10oC (50oF) and 30oC (86oF).

5.2.1 SAMPLES

One Head and Neck Restraint System sample at ambient temperature shall be tested.

5.2.2 APPARATUS

A. THERMAL LOAD

The thermal load shall be applied by a gas Bunsen burner, with an inside diameter of 0.4 inch (9.5mm).

B. TIMING DEVICE

A timing device with an accuracy of ±0.5 seconds shall be used to measure combustion rates.

C. FIXTURE

A fixture shall be used to support the Head and Neck Restraint System sample.

5.2.3 PROCEDURE

The Bunsen burner flame height shall be adjusted to 1.5 inches (38mm) and positioned perpendicular to each component surface in each area where different materials exist including tethers, etc. The component surfaces and tether shall be subjected to the thermal load at a distance of 0.75 inch (19mm) from the surface of the component to the center of Bunsen burner nozzle for a period of 15 ±1 seconds and immediately removed. Measurement of the speed of combustion shall start simultaneously with the removal of the flame.

6.0 PROOF OF COMPLIANCE

Head and Neck Restraint System certifying manufacturers are required to provide the following information to enroll in this program:

6.1 TEST RESULTS

Test results shall be documented in a test report.

6.1.1 IMPACT PERFORMANCE FOR EACH TEST (procured from Hybrid III test device).

At 80 milliseconds:

Maximum Upper Neck Tension	2,500N (562 lbs)
Maximum Upper Neck Compression	2,500N (562 lbs)
Maximum Value of NIJ	1.0

At 120 milliseconds:

Maximum Upper Neck Tension	3,200N (719 lbs)
Maximum Upper Neck Compression	3,200N (719 lbs)
Maximum Value of NIJ	1.0

6.1.2 FLAME RESISTANCE

A. Tether Test

The speed of combustion of tether material per paragraph 5.2.3 shall be less than or equal to 3 inches/minute (77mm/minute).

B. Head and Neck Restraint System Surface Material Test

When the surface materials are tested per paragraph 5.2.3, the flame shall self extinguish within 10 seconds.

C. No flaming debris, molten debris or holes may form in the components.

7.0 TEST REPORTS

A separate test report, or set of test reports if required, shall be submitted for each product model. If more than one test facility is required to complete all necessary tests, then a separate test report shall be submitted from each one. A test report shall be submitted for each component, if tested separately. The test facility shall assign a unique number to each test report. This number along with the report date and page number shall appear on each page. Each test report shall include:

7.1 RELEVANT INFORMATION

7.1.1 Manufacturer's name, contact name, address and telephone number.

7.1.2 Name, address and telephone number of the test facility.

7.1.3 Name and signature of the responsible test supervisor.

7.1.4 Actual date of the test.

7.1.5 Specification number and effective date.

7.1.6 Product name, description, model designation and part number.

7.1.7 Component name and description.

7.2 TESTS

Each test conducted shall be listed showing the test name, apparatus used, procedure used and test results obtained along with any other appropriate information.

7.3 AUTHENTICATION

Test reports shall be authenticated and stamped by a Professional Engineer who is registered in the state in which the testing is conducted. If necessary, SFI may allow an equivalent entity to provide authentication.

8.0 INITIAL DESIGN VALIDATION

To receive initial recognition from SFI as a participant in the SFI Specification 38.1 Program, the manufacturer must submit to SFI all information delineated in the Proof of Compliance section. This information shall be provided for each Head and Neck Restraint System model offered by the applicant that is to be included in the program. Any change in design, materials and/or methods of manufacturing not specifically excluded is considered a model change and, therefore, requires initial design validation.

9.0 PERIODIC REVALIDATION

Test reports with successful test results must be submitted to SFI at least once every 24 month period following the date of the initial design validation test for each model of Head and Neck Restraint System manufactured by the participant. If multiple test reports are required to obtain all test results, then the earliest test date shall be used to determine when the periodic revalidation reports are due. Also, SFI shall retain the option to conduct random audit reviews. SFI shall purchase the product on a commercial basis and test for compliance to the specification. The submitting manufacturer shall reimburse SFI for all audit costs.

10.0 CERTIFICATION OF COMPLIANCE

Upon demonstration of successful compliance with all the requirements of the specification and the self-certification program and upon entering the licensing agreement with SFI, the manufacturer may advertise, present and offer the Head and Neck Restraint System for sale with the representation that their product meets the SFI Specification 38.1. Continuing certification is contingent upon the following additional considerations: (1) the product shall be resubmitted for testing following any change in design, materials and/or methods of manufacturing not specifically excluded, and (2) periodic revalidation test reports are submitted when due to SFI.

11.0 CONFORMANCE LABELS

The conformance label is a "punch-out" sticker or label for the Head and Neck Restraint System. The label shall be punched with the month and year of manufacture and be placed on the outside surface. The month and year of manufacture shall be punched in each label with a 1/8" hole punch.

12.0 DECERTIFICATION

Participating manufacturers are subject to decertification when not in compliance with the requirements of this program or when their products are not in compliance with the requirements of this specification. Decertification will provide SFI the right to effect any and all remedies, which are available to SFI in the licensing agreement.

13.0 APPEAL PROCEDURE

In the event of decertification, the manufacturer is entitled to an appeal of the decision of SFI. Requests for appeal must be received by SFI no later than thirty days following receipt of the notice of decertification. Appeals of such decisions will be heard at the next meeting of the Board of Directors of SFI.

14.0 STATEMENT OF LIMITATIONS

Testing procedures and/or standards contained in this specification are intended for use only as a guide in determining compliance with the minimum performance requirements as defined herein. The granting and assignment of the "This Manufacturer Certifies That This Product Meets SFI Specification 38.1" logo/designation is in no way an endorsement or certification of product performance or reliability by SFI. SFI, its officers, directors and/or members assume no responsibility, legal or otherwise, for failure or malfunctions of a product under this program.

15.0 COSTS

All costs involved in this program will be absorbed by the submitting manufacturer.

16.0 COMPLIANCE PERIOD

As this specification is revised to reflect changes in technology and/or field conditions, to remain current, participating manufacturers in the SFI Specification 38.1 Head and Neck Restraint System must demonstrate full compliance with the requirements of this specification within ninety (90) days of the latest effective date.

---

*	Original Issue:	October 25, 2004
	Reviewed:	December 11, 2004
	Revised:	July 19, 2007
	Revised:	August 26, 2008
	Reviewed:	December 11, 2008
	Revised:	March 24, 2009